# The Interpretation of Low Energy Proton-Proton Scattering*†

J. DAVID JACKSON‡ AND JOHN M. BLATT¶
*Department of Physics and Laboratory for Nuclear Science and Engineering, Massachusetts Institute of Technology, Cambridge, Massachusetts*

TABLE OF CONTENTS



## I. INTRODUCTION

THE scattering of protons by protons is one of the important sources of quantitative information about nuclear forces. It gives the best (until quite recently the only) estimate of the range of the forces between two nucleons. The accuracy of the experiments is comparatively high, due to the fact that the energy control and the detection of charged particles is easier than for neutral particles (such as the neutron in neutron-proton scattering).

The theoretical interpretation of proton-proton scattering experiments has been given in the classic papers of Breit and collaborators[1] which not only constitute the pioneer work in this field, but also contain an exhaustive treatment of the subject. For both neutron-proton and proton-proton scattering at low energies (below 4 Mev) the de Broglie wave-length of the nuclear motion is large compared to the range of nuclear forces. Hence the nuclear interaction is effective only in the $S$-states (zero-orbital angular momentum) of the two-particle system. (Experimentally, the observed scattering can be attributed almost entirely to $S$-wave scattering up to appreciably higher energies, of the order of 10 Mev.) The protons are identical particles which obey the Pauli exclusion principle. The exclusion principle limits the possible states of the proton-proton system. Two protons in an $S$-state, in particular, have to have antiparallel spins (be in the singlet spin state). The triplet spin state is forbidden. The $S$-wave proton-proton scattering thus involves only one nuclear "phase shift," the one for the $^1S$-state. In contrast to this, neutron-proton $S$-wave scattering involves two phase shifts, for the $^1S$- and $^3S$-states respectively.

While the analysis of proton-proton scattering is thus simpler in principle, it is complicated somewhat by the Coulomb scattering which is present in addition to the nuclear effects. The Coulomb scattering is coherent with the nuclear scattering, so that interference terms between the two effects appear in the cross section. Since the nuclear forces are attractive while the Coulomb forces are repulsive, the interference will be mostly destructive, leading to characteristic minima in the differential cross section at certain angles. In spite of the complicated appearance of the differential cross section as a function of angle, one should nevertheless be able to fit it completely at any one energy $E$ with *only one adjustable parameter*, the nuclear phase shift $\delta_0(E)$ for the nuclear scattering in the $^1S$-state.

The work of Breit and his collaborators has shown that this is indeed the case. In particular, the excellent data of Herb *et al.*[2] give very good agreement (well within the claimed experimental error) with a unique $^1S$-wave phase shift $\delta_0(E)$ at every energy $E$.

Having obtained the nuclear phase shift from the experiments, one wants to draw conclusions regarding the nuclear forces between two protons in the $^1S$-state. One way, the one followed by Breit *et al.*, is to make certain very explicit assumptions about the nuclear interaction (e.g., that it be a square well potential of a definite range and depth) and compute the theoretically expected

* Assisted by the Joint Program of the ONR and the AEC.

† Based on a Ph.D. thesis submitted by one of us (J.D.J.) to M.I.T. The thesis was issued as Technical Report No. 29, Laboratory for Nuclear Science and Engineering, M.I.T., Cambridge, Massachusetts (July 15, 1949).

‡ Present address: Department of Mathematics, McGill University, Montreal, Canada.

¶ Present address: Department of Physics, University of Illinois, Urbana, Illinois.

[1] Breit, Condon, and Present, Phys. Rev. **50**, 825 (1936), referred to as BCP; Breit, Thaxton, and Eisenbud, Phys. Rev. **55**, 1018 (1939), referred to as BTE. Other works in this series will be cited in context.

[2] Herb, Kerst, Parkinson, and Plain, Phys. Rev. **55**, 247 (1939), referred to as HKPP.

phase shifts $\delta_0(E)$ at the same energies at which the experiments were performed. These values are then compared with the phase shifts found from the experiments. If the experimental and theoretical phase shifts agree within the experimental errors, the assumed potential provides an acceptable representation of the proton-proton force, at least as far as these experiments are concerned. If the theoretical phase shifts differ appreciably from the experimental ones, one has to try again with a different choice of theoretical potential. This new choice can be different in various ways: The potential shape (e.g., square well) may be retained, but new values used for the potential parameters (range and depth of the well); or else a new well shape may be tried (e.g., the Yukawa well shape); or else one may assume that the nuclear forces are "velocity-dependent" and cannot be represented by a static potential.

It has been conventional to restrict the number of possible potential well shapes to four:[1] the square well (potential hole), Gaussian well, exponential well, and Yukawa well. It was found that any one of these shapes would give satisfactory agreement with the data, provided only that the range and depth of the well were suitably chosen. Thus the data do not delimit the potential shape to any great extent. In effect, only two parameters (such as a range and a depth) of the potential are determined with reasonable accuracy.

There has long been a feeling, therefore, that the low energy data really do not merit such a detailed approach. This feeling was expressed by Landau and Smorodinsky,[3] among others. They pointed out that under the assumption of an interaction of zero range, a certain function (which we shall call $\mathbf{K}$) of the nuclear phase shift and the velocity $v$ of the protons should be independent of energy. This function, closely analogous to the quantity $f$ of BCP (reference 1), is defined as follows:

$$\mathbf{K}=\frac{\pi\cot\delta_0}{\exp(2\pi\eta)-1}+h(\eta), \tag{1.1}$$

where $\delta_0$ = phase shift for the $^1S$-wave nuclear scattering (the $K_0$ of BCP); $\eta=e^2/hv=0.158(06)E^{-\frac{1}{2}}$ ($E$ in Mev), and $h(\eta)$ = a slowly varying function, defined in Section VII.

The insufficiency of the zero-range approximation (equivalent to $\mathbf{K}$ = constant) had already been pointed out previously.[1] In agreement with this, Landau and Smorodinsky found that a plot of the experimental values of $\mathbf{K}$ *vs.* energy did not yield a constant value of $\mathbf{K}$, but rather showed a systematic increase of $\mathbf{K}$ with energy. To a very good approximation, the points could be fitted by a straight line. The fact that $\mathbf{K}$ is not constant was correctly interpreted as a range correction, the slope of the straight line being related to a kind of "effective range" of the proton-proton force. One should note that the approximate linearity of $\mathbf{K}$ as a function of energy is implicit in Eqs. (7.5), (7.6) and (7.7) of BCP. The work of Landau and Smorodinsky served to focus attention on the use of $\mathbf{K}$, (1.1), as the basic quantity in an analysis of the scattering data.

In this paper we shall base the analysis of the proton-proton scattering data upon the use of this function $\mathbf{K}$, rather than upon a direct comparison of phase shifts.

The general variational approach to scattering problems developed by Schwinger[4] was used by him to give a formal mathematical derivation of a power series for $\mathbf{K}$ in powers of the energy $E=2\hbar^2k^2/M$ ($M$ = proton mass, $k$ = wave number of relative motion, $E$ = energy in the laboratory system, $k^2=1.20(5)E$ where $k^2$ is in $10^{24}$ cm$^{-2}$ and $E$ is in Mev) including explicit expressions for the coefficients of the series in terms of the wave function of the system at zero energy.

$$\mathbf{K}=R(-a^{-1}+\tfrac{1}{2}r_0k^2-Pr_0^3k^4+Qr_0^5k^6-\cdots). \tag{1.2}$$

Here $R=\hbar^2/Me^2=2.88(15)\times10^{-12}$ cm is a characteristic length for proton-proton scattering ($R$ is the Bohr radius of a proton bound to a fixed unit charge) and $a$, $r_0$, $P$, $Q$, $\cdots$ are constants which are related to the range, depth and detailed shape of the nuclear potential responsible for the deviations from pure Mott scattering.

The Schwinger expansion (1.2) shows immediately why the plot of $\mathbf{K}$ *vs.* energy (or *vs.* $k^2$) should be a straight line at low energies. One can also give an interpretation for the coefficients $a$ and $r_0$: $a$ is the proton-proton analog of the scattering length of Fermi and Marshall[5] evaluated at zero energy, while $r_0$ is an "effective range" of the nuclear interaction between the two protons. The fact that Landau and Smorodinsky found a very good straight line fit to their plot of $\mathbf{K}$ *vs.* energy can be interpreted to mean that the higher terms in (1.2) have sufficiently small coefficients so that they are negligible in the energy range in question (below 2.5 Mev). The data then determine closely only two constants related to the nuclear potential, namely $a$ and $r_0$, put (rather wide) limits on $P$, and leave the higher coefficients in (1.2) completely open.

Given any well *shape* (square well, Yukawa well, etc.) one has two adjustable constants at one's disposal: the well depth and the width (range) of the well. One can therefore adjust a well of any shape to fit the experimental values of the two variational parameters $a$ and $r_0$, provided only that the "shape-parameter" $P$ of this well is within the bounds prescribed by experiment (a rather weak requirement at the present time).

The quantity $\mathbf{K}$ and the series (1.2) are closely related to a similar expansion for low energy neutron-proton scattering[6] (also due to Schwinger) which can be used to simplify the analysis of the low energy data on the neutron-proton system.[7] Indeed, in the limit of very

[3] L. Landau and J. Smorodinsky, J. Phys. U.S.S.R. 8, 154 1944).

[4] J. Schwinger, "Hectographed notes on nuclear physics," Harvard (1947); Phys. Rev. 72, 742A (1947).

[5] E. Fermi and L. Marshall, Phys. Rev. 71, 66 (1947).

[6] J. M. Blatt and J. D. Jackson, Phys. 76, 18 (1949).

[7] J. M. Blatt, Phys. Rev. 74, 92 (1948).

high energies ($\eta$ very small compared to unity) the first term in the definition of **K**, (1.1), approaches $Rk\cot(\delta)$; if the second term, $h(\eta)$ were absent, we would get directly the neutron-proton expansion:

$$k\cot(\delta)=-a^{-1}+\tfrac{1}{2}r_0k^2-Pr_0^3k^4+\cdots. \qquad (1.3)$$

However, $h(\eta)$ does not vanish as $\eta$ approaches zero, rather it behaves like $\log(\eta^{-1})$. This failure of the proton-proton expansion (1.2) to reduce completely to the neutron-proton expansion (1.3) even at high energies is related to the fact that the Coulomb force has an "infinite range," i.e., the wave function does not approach a plane wave plus a spherical scattered wave even at very large distances from the scattering center. Nevertheless, recent work[8] has shown that the proton-proton coefficients $r_0$, $P$, $Q$, etc., are very closely equal to the corresponding coefficients of (1.3) in the absence of Coulomb forces, provided the same nuclear potential is assumed to act in both cases. The scattering length $a$ changes appreciably when the Coulomb field is switched off, but one can give good estimates for the amount of this change (see reference 8 and Section VIII of this paper).

Before proceeding with the discussion of the analysis based on (1.1) and (1.2) we should mention a slightly different approach recently discussed by Breit and Bouricius.[9] They have shown that the data can also be fitted quite well by a "boundary condition" on the logarithmic derivative of the wave function at a definite (small) distance. They point out that this is closely related to the possibility of getting an adequate fit to the data using only the first two terms of the series (1.2). We shall not use the boundary condition approach here.

The analysis of proton-proton scattering data by the variational method involves four steps, the first two being common to all methods of analyzing the data:

(1) The experimental measurements must be reduced to differential cross sections in the center-of-mass system. This involves intricate corrections for various geometrical effects, multiple scattering of the beam, etc. None of these corrections will be discussed here; they are treated in detail in BTE.

(2) The differential cross section at any one energy as a function of scattering angle is then used to determine the phase shifts $\delta_0$, $\delta_1$, $\delta_2\cdots$ of the $S$-wave, $P$-wave, $D$-wave$\cdots$nuclear contributions to the scattering. At low energies the $S$-wave contribution is by far the most important. Section IV of this paper is devoted to a simplified method (based upon the work of BTE) for finding the $S$-wave phase shifts from the data (including their probable errors); in Section V we give a straightforward method for determining the higher phase shifts $\delta_1$, $\delta_2$ etc., under the assumption that they constitute small corrections to the observed scattering. While these simplified procedures are based directly upon the work of BTE and BCP, we feel that they lead to a sufficient saving in labor of computation to merit separate discussion. In particular, it is now a matter of perhaps an hour's work to determine whether an experimental run is consistent with pure $S$-wave scattering, whether the $S$-wave phase shift is consistent with previous data, and, if contributions of higher angular momenta are indicated, to find a good estimate for these higher phase shifts. Section V also includes a discussion of the experimental accuracies necessary to determine the presence of higher phase shifts, and to distinguish between $P$-wave and $D$-wave contributions to the deviation from pure $S$-wave scattering. A complete discussion of all the experimental data to date is contained in Appendix II and Section VI.

(3) The next step in the analysis is peculiar to the variational method: the experimental $S$-wave phase shifts $\delta_0$ at the various energies are used to compute **K**, (1.1), at those energies, and a plot of **K** *vs.* $k^2$ is made. This plot is used to find the experimental values of the scattering length $a$ and the effective range $r_0$ and to delimit the possible values of $P$. Because of the fact that there are no accurate data near zero energy, the best values of $a$ and $r_0$ will depend somewhat upon the choice of $P$. Section VII of the paper is devoted to this part of the analysis, giving the best values implied by all the available data. We should perhaps emphasize once more that we are restricting ourselves here to plotting the data for the $S$-wave nuclear scattering only (even though higher phase shifts are estimated for some of the data in Section VI). At higher energies, waves of higher angular momentum will in general enter the observed scattering to an appreciable extent. The phase shifts for those waves must be evaluated and put on different plots. A curvature of the plot of **K** *vs.* $k^2$ discussed here has nothing to do with the presence or absence of higher phase shifts in the scattering; rather it is related to the detailed shape of the nuclear potential in the $^1S$-state of the proton-proton system.

(4) The final step in this analysis is the fitting of theoretical potential wells to the observed values of the variational parameters. In general, the more the variational parameters are determined accurately or delimited appreciably by experiment, the better will one be able to narrow down the possible theoretical well shapes which can be used to give agreement with experiment. Section IX of this paper contains a derivation of the expressions for the variational parameters $a$, $r_0$, $P$, $Q$, in terms of the wave function of the proton-proton system at and near zero energy;[10] Section X is devoted to the effect of small

[8] G. F. Chew and M. L. Goldberger, Phys. Rev. **75**, 1637 (1949); H. A. Bethe, Phys. Rev. **76**, 38 (1949).

[9] G. Breit and W. G. Bouricius, Phys. Rev. **75**, 1029 (1949).

[10] This derivation is based upon a variational principle due to Schwinger (see reference 4). A much simpler derivation using the basic properties of the differential equation involved has been given recently by Chew and Goldberger and Bethe (see reference 8) as well as F. C. Barker and R. E. Peierls (Phys. Rev. **75**, 312 (1949). On the basis of simplicity, the non-variational method should appear in Section IX. However, it does not; rather, it is presented in Appendix IV. The reasons for the retention of the somewhat more involved Schwinger formulation in the text are several: The variational principle has certain useful properties

changes in the potential on the variational parameters; finally, Section XI gives the numerical results obtained for the four conventional well shapes (square well, Gaussian well, exponential well, and Yukawa well) in a form appropriate for direct comparison with the data summarized in Section VI. The present best values for the "intrinsic range" and "well depth parameter"[6] for each of those four wells are also stated, with their probable errors. They are in substantial agreement with the values found by BTE.

We are restricting ourselves throughout this paper to experiments below about 10 Mev. The obvious reason is that no higher energy experiments of adequate accuracy are available at present. However, we feel that even when experiments at higher energies do become available, it will be very hard to interpret them intelligently without a rather accurate knowledge of the implications of the lower energy work. In the course of this analysis, we have come to the conclusion that *four different types of experiments are highly desirable in the low energy region:*

(1) An accurate determination of the cross section at 90° (45° in the laboratory system) near 400 kev. The same recommendation has been made, on slightly different grounds, by Breit, Broyles, and Hull.[11] This experiment and the differences between our approach and that of reference 11 are discussed in Section VII (these differences have no influence upon the ultimate recommendation to experimenters, however.)

(2) A repetition, with comparable accuracy, of the work of Dearnley, Oxley, and Perry[12] with cyclotron sources at 7 Mev. This point seems to be rather out of line at present, and an independent determination is highly desirable, in view of the radical implications if it should be confirmed: we show in Sections VII and XI that *none* of the conventional well shapes can give an adequate fit to the data if the DOP point is included, indeed that no reasonable potential well can do so; rather the DOP point would probably demand the introduction of "velocity-dependent" forces.[13] We hesitate to take such a step without further experimental confirmation.

(3) A careful determination of *relative* cross sections (as a function of scattering angle) with moderate absolute accuracy in the 5–10-Mev region, for scattering angles in the "central region" around 90° in the center-of-mass system. We show in Section V that such measurements which we believe are feasible with cyclotrons can determine the presence or absence of appreciable contributions of other than $S$-waves to the nuclear scattering. The measurements cannot distinguish whether these deviations from pure $S$-wave scattering, if found, are due to $P$-wave effects or $D$-wave effects or to a mixture of both. The angular region over which such relative measurements are useful is discussed in Section V. As an aid to planning such experiments, theoretical estimates of the higher phase shifts are given in Section XII over this energy range, for the four conventional well shapes.

(4) If the cyclotron relative cross-section measurements should prove the existence of higher phase shifts at energies below 10 Mev, absolute cross-section measurements over a somewhat wider range of scattering angles would then discriminate between $P$-wave and $D$-wave contributions to the scattering. Van de Graaff generators with good voltage control should be used for this work. Reasons are given in section $V$ why it pays to set a much higher standard of accuracy for the beam energy determination than for the determination of the absolute yield.

The results obtained here are in essential agreement with earlier results of Breit and collaborators wherever a comparison can be made; also, some of the recommendations for future experiments have been made before.[1]

## II. THE DIFFERENTIAL CROSS SECTION FOR PROTON-PROTON SCATTERING— FORMAL WORK

The pure, unscreened Coulomb field has an infinite range; that is, the wave function cannot be written as a superposition of a plane wave $\exp(ikz)$ and a scattered spherical wave $f(\theta)\exp(ikr)/r$, even at very large distances from the scattering center. We shall assume that the electrostatic potential is screened out at some distance $\rho$, of the order of the Bohr radius of an atom. The asymptotic wave function for the Coulomb scattering of two *non-identical* particles can then be written in the center of gravity system as:

$$\psi\sim\exp(ikz)+f_{\text{Coul}}(\theta)\exp(ikr)/r, \qquad (2.1)$$

where $\theta$ is the angle between the direction of the incident beam and the direction in which the scattered particles are observed. The pure Coulomb scattering amplitude $f_{\text{Coul}}(\theta)$ is, for angles $\theta$ sufficiently large so that the impact parameters in the scattering are smaller than the screening radius (Bohr radius),[14]

$$f_{\text{Coul}}(\theta)=-(e^2/2mv^2)\operatorname{cosec}^2(\theta/2)\times\exp[-2i\eta\log\sin(\theta/2)+2i\sigma_0]^{**} \qquad (2.2)$$

(just because it is a variational principle); the precedent had been established in the authors' earlier paper on neutron-proton scattering (see reference 6), the extension to proton-proton scattering is simple. However, the main reason is that the present paper was originally written as a research report, rather than a review paper. In the process of revision into its present form, the authors found that the viewpoint and results of the variational principle were sufficiently woven into the text that it would have been a prohibitive amount of work in the time available to make the necessary changes concomitant with the reversing of the roles of Section IX and Appendix IV. The indulgence of the reader is asked on this point. It is suggested that one read Section VIII (the Landau-Smorodinsky result), Appendix IV, then Section IX for the clearest understanding of the theoretical formulation of the expansion (1.2).

[11] Breit, Broyles, and Hull, Phys. Rev. **73**, 869 (1948).

[12] Dearnley, Oxley, and Perry, Phys. Rev. **73**, 1290 (1948), referred to as DOP.

[13] J. A. Wheeler, Phys. Rev. **50**, 643 (1936).

[14] N. F. Mott and H. S. W. Massey, *Theory of Atomic Collisions* (Oxford University Press, New York, 1933).

** This equation differs in one respect from Eq. (16), Chapter III of Mott and Massey. We have written the radial de-

where $m$=reduced mass=$(\frac{1}{2})(M_{\text{Proton}})$, $v$=relative velocity of the two particles, $\theta$=angle of scattering in the center of gravity system, $\eta=e^2/\hbar v$, and $\exp(2i\sigma_0)=(i\eta)!/(-i\eta)!$

This Coulomb scattering amplitude can be written also as a sum over contributions of the separate orbital angular momenta:

$$f_{\text{Coul}}(\theta)=(2ik)^{-1}\times\sum_{l=0}^{\infty}(2l+1)[\exp(2i\sigma_l)-1]P_l(\cos\theta) \quad (2.3)$$

where $\exp(2i\sigma_l)=(l+i\eta)!/(l-i\eta)!$, and $P_l(\cos\theta)$=Legendre polynomial of order $l$, not normalized.

Equations (2.2) and (2.3) are not quite correct for a screened Coulomb field, for two reasons: The joining of the screened to the unscreened region will produce a common phase factor in all the relevant terms of the sum (2.3), which has no influence on the result. Second, the screening will produce important changes in the terms of (2.3) corresponding to very high orbital angular momenta $l$. This in turn means that (2.2) is incorrect for very small angles. The critical value of $l$ is given by the condition

$$l_{\text{crit}}\cong\rho/\lambda\!\!\!^{-} \quad (2.4)$$

where $\rho$ is the screening radius and $\lambda\!\!\!^{-}$ is the de Broglie wave-length of the relative motion, divided by $2\pi$. For proton-proton scattering around 1 Mev, this value of $l$ (beyond which (2.3) breaks down) is of order $10^4$. The critical angle $\theta_{\text{crit}}$ below which the screening becomes important, and (2.2) is no longer valid, is given by (for $\eta\ll1$):

$$\theta_{\text{crit}}\cong\lambda\!\!\!^{-}/\rho. \quad (2.5)$$

For proton-proton scattering around 1 Mev, this angle is of order $10^{-4}$ radians. For angles larger than that, formulas (2.2) and (2.3) are applicable.

Equations (2.2) and (2.3) must still be corrected for the fact that protons are identical particles which have spin $\frac{1}{2}$ and obey the Pauli exclusion principle. The wave function (2.1) is not in agreement with the exclusion principle. Rather, the correct space wave function must be symmetric under the interchange of the particles ($z\rightarrow-z$, $\theta\rightarrow\pi-\theta$) for two protons in the singlet spin state, while it must be antisymmetric under this exchange if the two protons are in the triplet spin state. Thus (2.1) has to be replaced by

$$\psi\sim[\exp(ikz)\pm\exp(-ikz)]+[f_{\text{Coul}}(\theta)\pm f_{\text{Coul}}(\pi-\theta)]\exp(ikr)/r, \quad (2.6)$$

where the upper (plus) sign refers to protons in the singlet spin state, the lower (minus) sign to protons in the triplet spin state.

The identity of the colliding particles makes the two collisions pictured in Fig. 1 indistinguishable from each other. Classically, one would add up the cross sections for the two collisions, in order to get at the cross section for a collision in which either one of the particles is found moving at an angle $\theta$ to the direction of the incident beam, after the collision. This classical differential cross section is therefore

$$d\sigma_{\text{classical}}=(|f_{\text{Coul}}(\theta)|^2+|f_{\text{Coul}}(\pi-\theta)|^2)d\Omega. \quad (2.7)$$

Formula (2.6) shows that the quantum mechanical treatment gives additional, interference, terms between the two scattered waves. These interference terms are different for scattering in the singlet and triplet states. The quantum mechanical differential cross sections are therefore given by

$$d\sigma_{\text{quant}}=(|f(\theta)|^2+|f(\pi-\theta)|^2\pm[f^*(\theta)f(\pi-\theta)+f(\theta)f^*(\pi-\theta)])d\Omega, \quad (2.8)$$

where the upper and lower sign again refers to scattering in the singlet and triplet spin states, respectively. For pure Coulomb scattering, the Coulomb scattering amplitude $f_{\text{Coul}}$, (2.2), has to be substituted into (2.8).

The experiments so far have been conducted with unpolarized beams of protons scattered from unpolarized targets. We must average the cross sections (2.8) over the relative spin orientations in a random assembly of protons. The singlet state will occur one-quarter of the time, the triplet state, three-quarters of the time. The *observed cross section* is therefore the following function of the scattering amplitude $f(\theta)$:

$$d\sigma=(\tfrac{1}{4})d\sigma_{\text{singlet}}+(\tfrac{3}{4})d\sigma_{\text{triplet}}=(|f(\theta)|^2+|f(\pi-\theta)|^2-(\tfrac{1}{2})[f^*(\theta)f(\pi-\theta)+f(\theta)f^*(\pi-\theta)])d\Omega. \quad (2.9)$$

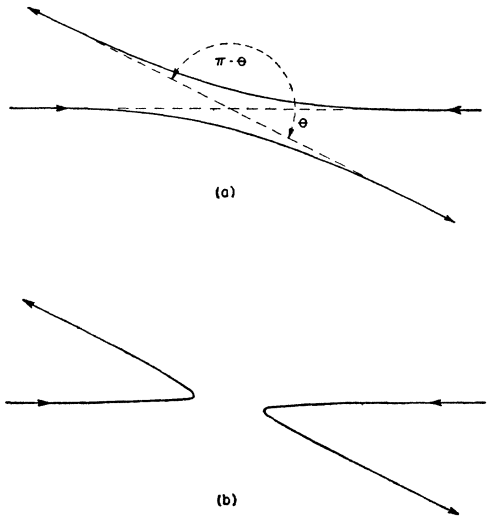


FIG. 1. Two seemingly different identical particle collisions that are experimentally indistinguishable.

pendence of the outgoing wave in the unscreened region as $S'=r^{-1}\exp(ikr-i\eta\log2kr)$ rather than the $S$ of Mott and Massey. The compensating change in $f(\theta)$ produces $\log\sin^2(\theta/2)$ in the exponential phase factor. A study of the Coulomb wave functions shows that $S'$, rather than $S$, is the quantity which is analogous to the $\exp(ikr)/r$ of (2.1).

This result is due to Mott.[15] If one substitutes in (2.9) the amplitude for pure Coulomb scattering, (2.2), one gets the *Mott cross section* for proton-proton scattering without nuclear effects:

$$d\sigma_{\text{Mott}}=(e^2/2mv^2)^2[\text{cosec.}^4(\theta/2)+\sec^4(\theta/2)-\\ -\text{cosec.}^2(\theta/2)\sec^2(\theta/2)\\ \times\cos[2\eta\log\tan(\theta/2)]]d\Omega. \quad (2.10)$$

It is apparent from (2.9) or (2.10) that the scattering cross section is the same for the angles $\theta$ and $\pi-\theta$. This is merely an expression of the indistinguishability of the two collisions pictured in Fig. 1.

We now consider the modifications introduced into this cross section by the nuclear forces between two protons. The radial wave function for pure Coulomb scattering with orbital angular momentum $l$ has the following behavior for values of $r\gg l\lambda$ but still $r\ll\rho$, the screening radius:

$$F_l(r)\sim\sin(kr-l\pi/2-\log(2kr)+\sigma_l) \quad (2.11)$$

where $\sigma_l$ is the pure Coulomb phase shift defined in connection with Eq. (2.3). The nuclear forces†† will lead to a change in this phase shift. It is customary to write this modified phase shift as a sum of two terms, i.e., the asymptotic behavior of the radial function $u_l(r)$ for $l\lambda\ll r\ll\rho$ is written as

$$u_l(r)\sim\sin(kr-l\pi/2-\log(2kr)+\sigma_l+\delta_l). \quad (2.12)$$

The quantity $\delta_l$ (called $K_l$ in the papers by Breit *et al.*) is commonly referred to as the "nuclear phase shift." One should point out that $\delta_l$ is by no means equal to the phase shift which would be obtained if the Coulomb field between the protons were suddenly switched off. Rather, the combined phase shift $\sigma_l+\delta_l$ is due to the action of the nuclear forces and the Coulomb force both, and the separation into $\sigma_l$ and $\delta_l$ is merely a matter of convenience.

The modified scattering amplitude $f(\theta)$ in the presence of nuclear and Coulomb forces is given by

$$f(\theta)=(2ik)^{-1}\sum_{l=0}^{\infty}(2l+1)\\ \times[\exp[2i(\sigma_l+\delta_l)]-1]P_l(\cos\theta). \quad (2.13)$$

The expansion (2.13) is completely analogous to the expansion (2.3) for the scattering amplitude due to the Coulomb field alone. We have merely replaced the Coulomb phase shift $\sigma_l$ by the modified phase shift $\sigma_l+\delta_l$ throughout.

[15] N. F. Mott, Proc. Roy. Soc. **A126**, 259 (1930).

†† We shall assume throughout this paper that the nuclear forces are central forces. This is certainly true in singlet states, hence in particular in the $^1S$-state which is the only important state for low energy proton proton scattering. The modifications introduced by tensor forces into the analysis of triplet state scattering (in particular, scattering in the $^3P$-states) have been discussed by Breit, Kittel, and Thaxton (see reference 16). At present, there is so little conclusive evidence of any $P$-wave scattering whatsoever that we do not feel it is worth while to complicate the exposition given here by the inclusion of tensor forces.

Equation (2.13) will converge extremely slowly. For values of $l$ sufficiently high so that the combined Coulomb and angular momentum "barrier" keeps the protons apart beyond the range of the nuclear forces, the modifications in the pure Coulomb scattering will be negligible, i.e., $\delta_l$ will become very small as $l$ increases. It is convenient, therefore, to write the scattering amplitude $f(\theta)$, (2.13), as a sum of two terms: the amplitude $f_{\text{Coul}}(\theta)$ for pure Coulomb scattering, and an additional term which we shall call $f_{\text{nuc}}(\theta)$:

$$f(\theta)=f_{\text{Coul}}(\theta)+f_{\text{nuc}}(\theta). \quad (2.14)$$

Comparison of (2.3) and (2.13) shows that $f_{\text{nuc}}(\theta)$ is given by the sum

$$f_{\text{nuc}}(\theta)=(2ik)^{-1}\sum_{l=0}^{\infty}(2l+1)\\ \times\exp(2i\sigma_l)[\exp(2i\delta_l)-1]P_l(\cos\theta). \quad (2.15)$$

Since $\delta_l$ is in practice negligible compared to unity already for $l=1$, the series (2.15) converges very rapidly indeed. We shall refer to $f_{\text{nuc}}(\theta)$ as the "nuclear scattering amplitude." The same caution applies to this, however, as to the phase shift $\delta_l$. If the Coulomb field did not exist, the scattering amplitude due to the sole action of the nuclear forces would be quite different from (2.15). Indeed, this difference is a great complicating factor in the comparison of neutron-proton and proton-proton scattering.

The cross section for proton-proton scattering is obtained by combining Eqs. (2.9), (2.14), (2.15), and (2.2). The result has been written down explicitly for the case where only the first three terms of (2.15) are significant, by Breit, Condon, and Present. The formulas are fairly lengthy and will not be given here. We will content ourselves with writing down the complete formula for the case in which only the $S$-wave phase shift $\delta_0$ is appreciable. This formula for the differential scattering cross section in the center-of-mass system is:

$$\sigma(\theta)=(e^2/2mv^2)^2[\{\text{cosec}^4(\theta/2)+\sec^4(\theta/2)\\ -\text{cosec}^2(\theta/2)\sec^2(\theta/2)\cos(2\eta\ln\tan\theta/2)\}\\ -(2/\eta)\sin\delta_0\{\text{cosec}^2(\theta/2)\\ \times\cos(\delta_0+2\eta\ln\sin\theta/2)\\ +\sec^2(\theta/2)\cos(\delta_0+2\eta\ln\cos\theta/2)\}\\ +(4/\eta^2)\sin^2\delta_0]. \quad (2.16)$$

The first term of (2.16) is just the Coulomb scattering given by the Mott formula (2.10); the second term is the interference term between the $S$-wave nuclear interaction and the Coulomb force; the third is the specifically nuclear scattering (although, as is mentioned, it is not the same as neutron-proton scattering). The only unknown in (2.16) is the nuclear phase shift $\delta_0$.

The formula (2.16) for the scattering cross section is given in the center-of-mass coordinates. In practice one observes the scattering in the laboratory, corrects the data for various effects (see BTE), and then transforms to the center-of-mass system. If $\Theta$ is the scattering angle in the laboratory, then for particles of equal mass $\Theta=\theta/2$, $\theta$ being the center-of-mass angle. The cross sections

are related through:

$$\sigma_{\text{lab}}(\Theta)=4\cos(\Theta)\sigma(2\Theta). \tag{2.17}$$

Note that because of the recoil of the struck proton no scattering is observed at laboratory angles greater than 90 degrees.

While formula (2.9) is perfectly adequate, it somewhat obscures the detailed influence of the Pauli exclusion principle. Let us split the scattering amplitude $f(\theta)$ into two parts, even and odd under the exchange of the space coordinates of the two particles:

$$\begin{aligned} f(\theta)&=f_{\text{even}}(\theta)+f_{\text{odd}}(\theta),\\ f_{\text{even}}(\theta)&=(\tfrac{1}{2})[f(\theta)+f(\pi-\theta)],\\ f_{\text{odd}}(\theta)&=(\tfrac{1}{2})[f(\theta)-f(\pi-\theta)]. \end{aligned} \tag{2.18}$$

Clearly this split can be made for $f_{\text{Coul}}$ and $f_{\text{nuc}}$ separately. The cross section then becomes:

$$d\sigma=(|f_{\text{even}}(\theta)|^2+3|f_{\text{odd}}(\theta)|^2)d\Omega. \tag{2.19}$$

This equation shows that the contributions of the even and odd parts of $f(\theta)$, (2.15), are incoherent. In particular, there are no interference terms between $S$-wave and $P$-wave scattering, even in the differential cross section. The even parts of $f(\theta)$ are associated with scattering in the singlet spin state, the odd parts with scattering in the triplet spin state. It is well known that the Legendre polynomials $P_l(\cos\theta)$ are even for even values of $l$, odd for odd values of $l$. Hence the separation (2.18) is equivalent to separating the terms with even and odd $l$, respectively, in the sums (2.3) and (2.15).

As far as the nuclear interactions are concerned, the Pauli principle demands that two protons in a state of even $l$ must have opposite spins; hence we can deduce information about the nuclear force between two protons in the singlet spin state from the observed nuclear phase shifts $\delta_l$ with even values of $l$. Conversely, the nuclear force between two protons in the triplet spin state can only be found from the nuclear phase shifts $\delta_l$ with odd values of $l$. In practice, we have rather detailed information about $\delta_0$, so that the force in the $^1S$-state is fairly well known (much of the rest of the paper will be devoted to making this statement more precise). Only indications, but no reliable values, are available as yet for any of the other phase shifts. Furthermore, we shall show in Section V that very high accuracy is necessary before one can determine whether a given deviation from pure $S$-wave nuclear scattering is due to a $P$-wave or a $D$-wave nuclear interaction. In view of the great interest in the $P$-state interaction as far as general nuclear physics is concerned, in particular in connection with the observed saturation of nuclear binding energies, the authors feel that an attempt should be made to ascertain the precise nature of the deviations from pure $S$-wave nuclear scattering (if any), in spite of the great experimental difficulties.

Of course, the states of higher angular momentum will give rise to more and more scattering as the energy is increased. Nevertheless, we feel that very careful measurements should be made below 10 Mev, to detect the small discrepancies there, in addition to measurements at higher energies. The reasons for this recommendation are:

(1) At low energies, one can be fairly sure that nuclear interactions in states with $l\geqslant 3$ can be neglected. Hence one has to determine at most five parameters from the data (the phase shifts for the $^1S$- and $^1D$-state nuclear scattering, and three phase shifts for scattering in the $^3P$-state, in case a tensor force should exist in that state).

(2) Furthermore, there is good reason to believe that the number of unknown parameters in the scattering can be reduced to three: As long as the phase shifts in the $^3P$-states are small enough so that one can neglect their squares and products, the $P$-wave nuclear scattering can be described by one (mean) phase shift, even in the presence of a tensor force. (See Section V.)

(3) Some of the experimental corrections which have to be applied to the scattering data (e.g., corrections for penetration of the slits in the collimating system) are less serious at lower energies.

Thus it appears reasonable that careful low energy experiments should be performed, as well as experiments at higher energies (e.g., 32 Mev, and higher). With good low energy measurements (where the effects of waves of higher angular momentum are presumably small, but should be relatively simple to understand), the interpretation of the higher energy data will be made more secure and freer from ambiguities than without such data. Considering the time it takes to make careful experiments in this field, it is very desirable that both low energy and high energy experiments should be conducted simultaneously.

## III. THE DIFFERENTIAL CROSS SECTION FOR PROTON-PROTON SCATTERING—QUALITATIVE DISCUSSION

The quantitative formulation given in the preceding section leads to formulas which are sufficiently complex so that a more qualitative discussion may be helpful. We shall start out by considering the pure Coulomb (Mott) scattering only. It differs from the Rutherford scattering in two ways: symmetry around $\theta=90°$ (in the center-of-mass system), and the presence of interference terms between the two contributions $f_{\text{Coul}}(\theta)$ and $f_{\text{Coul}}(\pi-\theta)$. For reasonably high energies (above 0.5 Mev) $\eta=e^2/\hbar v$ will be small compared to unity, and the cosine in the interference (third) term of the Mott formula (2.10) can be replaced by unity, provided $\theta$ is around 90°. The behavior of the cross section as a function of angle will be smooth. The interference term is negative, decreasing the cross section below its "classical" value (2.7). As the angle $\theta$ is decreased (or increased beyond 90°) the interference term will start fluctuating more and more rapidly. However, for $\theta\ll 1$, the first term of (2.10) is entirely dominant, so that the rapid fluctuations in the interference term as a function of angle do not induce appreciable fluctuations into the cross section as a whole.

Formula (2.10) breaks down at very small angles ($\theta \lesssim \theta_{\text{crit}}$, (2.5)) where screening becomes important. If one replaces the pure Coulomb field by the screened field: $V(r)=(e^2/r)\exp(-r/\rho)$, and uses the Born approximation to estimate the scattering cross section, the result is that the cross section levels off for $\theta<\theta_{\text{crit}}$ and approaches a constant value as $\theta$ approaches zero. A simple order of magnitude estimate shows that most of the total (transmission) cross section for proton-proton scattering comes from this region of angles. Hence the transmission cross section, even with a very thin target, cannot be used to find information about the nuclear interaction between two protons. In that respect proton-proton scattering is appreciably more difficult than neutron-proton scattering; differential cross-section measurements are necessary.

We shall now assume that the nuclear forces affect the scattering in the $^1S$-state only. We must then compare the nuclear scattering amplitude (from (2.15)):

$$f_{\text{nuc}}(\theta)=\exp(2i\sigma_0)k^{-1}\exp(i\delta_0)\sin(\delta_0) \qquad (3.1)$$

with the *even* part of the Coulomb scattering amplitude; from (2.2) and (2.16) this latter is given by:

$$[f_{\text{Coul}}(\theta)]_{\text{even}}=-\exp(2i\sigma_0)$$
$$\times(e^2/2mv^2)\tfrac{1}{2}[(\sin^2(\theta/2))^{-i\eta-1}+(\cos^2(\theta/2))^{-i\eta-1}]. \qquad (3.2)$$

We can disregard the phase factor $\exp(2i\sigma_0)$ since it occurs in both scattering amplitudes. At low energies (below $\frac{1}{2}$ Mev) the nuclear $S$-wave phase shift $\delta_0$ is much less than a radian. The nuclear scattering amplitude (3.1) is therefore almost real. It is positive for an attractive nuclear potential, negative for a repulsive potential. At higher energies, $\delta_0$ becomes comparable to unity, so that $\exp(-2i\sigma_0)f_{\text{nuc}}$ ceases to be even approximately a real number.

Again apart from the phase factor $\exp(2i\sigma_0)$, the even part of the Coulomb scattering amplitude (3.2) will be approximately real at *high* energies, where $\eta$ becomes very small (we recall that $\eta=0.158E^{-\frac{1}{2}}$ where $E$ is the energy in the laboratory system measured in Mev). Even at energies as low as $\frac{1}{2}$ Mev, however, the square bracket in (3.2) will be approximately real at angles around 90°. The negative sign in front of (3.2) comes from the fact that the Coulomb force between two protons is repulsive.

There is thus a region of energies, somewhere between $\frac{1}{4}$ and 1 Mev, in which both the nuclear scattering amplitude (3.1) and the even part of the Coulomb scattering amplitude (3.2) are approximately real (apart from the $\exp(2i\sigma_0)$) and have opposite signs. Appreciable destructive interference can be expected between these two contributions. At energies below some critical value, $E_{\text{crit}}$, the magnitude of (3.1) will be less than even the minimum magnitude of (3.2) (which occurs at 90°). Thus the interference, though it exists, will not be complete at any angle.

At energies above $E_{\text{crit}}$, the magnitude of (3.1) will exceed the minimum magnitude of (3.2). There will therefore exist an angle,¶¶ call it $\theta_m$, at which the magnitudes of (3.1) and (3.2) will be equal. Since the relevant quantities are still approximately real and of opposite sign, the singlet state scattering cross section (due to the even parts of the scattering amplitudes) will become very small due to the destructive interference. The region of angles in which the destructive interference is important is rather limited: The nuclear scattering amplitude for pure $S$-wave scattering is independent of angle, while the even part of the Coulomb scattering amplitude is a very rapidly varying function of $\theta$. Thus the interval of angles in which both are of approximately equal magnitude will be rather narrow.

Of course, the cross section will not vanish even at $\theta=\theta_m$, for two reasons: (1) The interference is not complete since the phases of (3.1) and (3.2) on the complex plane will not be exactly opposite to each other, and (2) there will still be the contribution from the odd part of the Coulomb scattering amplitude (the triplet state scattering) which suffers no interference at all (see Eq. (2.19)).

The most favorable case for interference obtains when the destructive interference in the singlet scattering occurs at 90°; the triplet scattering (the second term of (2.19)) is zero at that angle. Since the magnitude of (3.2) has its minimum at this angle, also, the cross section will be extremely small (actually of the order of $\sim 10^{-27}$ cm$^2$ per steradian). This situation will occur right at the critical energy $E_{\text{crit}}$. At higher energies than that, the

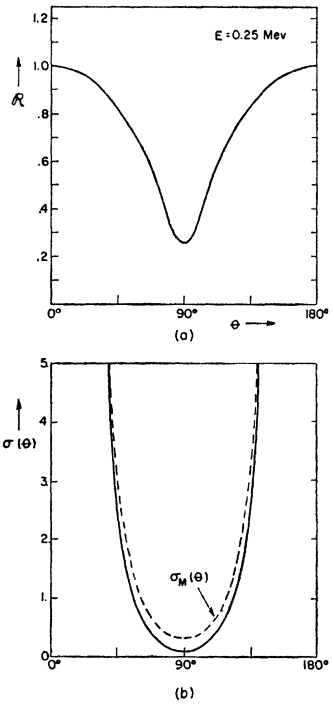


FIG. 2. Differential scattering cross section in the center-of-mass system, solid line-nuclear plus Coulomb, dotted line-Coulomb alone; and $\mathfrak{R}$, the ratio of total to Mott scattering at an energy of 250 kev (less than $E_{\text{crit}}$) in the laboratory. The destructive interference effects are apparent near 90 degrees.

¶¶ There will be two such angles, of course: $\theta_m$ and $\pi-\theta_m$, since the cross section is symmetric about 90°. We shall consider angles below 90° only from now on; the symmetry about 90° will be understood.

interference angle $\theta_m$ will move away from 90°, and the interference will be less pronounced, mostly because of the contribution of the triplet state Coulomb scattering.

In Figs. 2 and 3 we have plotted typical cross section *vs.* angle curves at an energy $E<E_{crit}$ and $E>E_{crit}$ respectively. The Mott cross section is shown dashed. We have also plotted the ratio of observed cross section to Mott cross section at these two energies. It is seen that for $E>E_{crit}$ there is an appreciable central region of angles around 90° where the scattering is mostly due to the nuclear forces. There is then a shallow interference minimum at $\theta=\theta_m$. For smaller angles the Coulomb cross section takes over completely. The figures do not show the leveling off of the Coulomb cross section due to the screening, because of the limitations of the scale.

We still have to estimate the value of the critical energy $E_{crit}$. We can get a rough upper limit for $E_{crit}$ as follows: The nuclear force is known to have a short range. Hence it acts only when the protons are essentially at the same place. We can compare the probability of finding two protons close together with the probability of finding two uncharged particles together, other things being equal. The ratio of these two probabilities is determined by the "Coulomb penetration factor" $C^2$:

$$C^2=\frac{2\pi\eta}{\exp(2\pi\eta)-1}. \tag{3.3}$$

This factor is always less than unity due to the Coulomb repulsion between the protons. However, when $C^2$ is close to unity this means that the Coulomb force is ineffective in keeping the protons apart. Consequently the nuclear scattering will be important. The energy above which $C^2$ is greater than one-half is approximately 800 kev (in the laboratory system). This can serve as a rough upper limit for the critical energy $E_{crit}$ for proton-proton scattering, since at higher energies the nuclear scattering will be predominant (at least at large scattering angles), while at lower energies the nuclear and Coulomb scatterings are expected to compete.

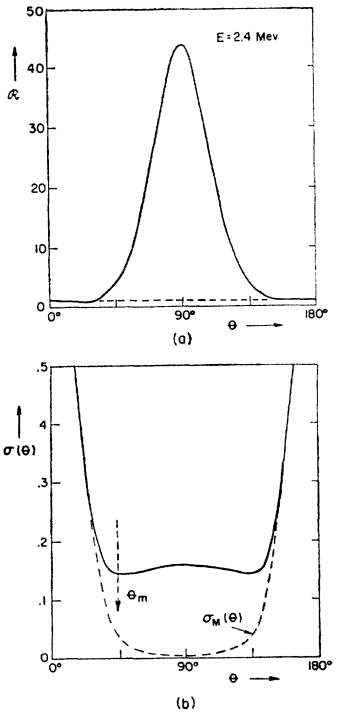


FIG. 3. Differential scattering cross section in the center-of-mass system, solid line-nuclear plus Coulomb, dotted line-Coulomb alone; and ℜ, the ratio of total scattering to Mott scattering at an energy of 2.4 Mev (greater than $E_{crit}$) in the laboratory. The scattering is predominantly nuclear except at small (and large) angles.

We have not used any information about the nuclear force in this estimate except its short range. Clearly the precise magnitude of the critical energy $E_{crit}$ must depend upon the strength of the force as well as its short range (actually, it will depend upon the product $V_0b^2$, $V_0$ being the depth and $b$ the range of the well).

The more detailed analysis of the data shows that empirically the critical energy $E_{crit}$ is close to 400 kev in the laboratory system. At this energy $\eta=0.25$ and the Coulomb penetration factor is $C^2=0.41$.

Experiments at energies around 400 kev are highly recommended and discussed in some detail in Section VII of this paper. While a differential cross-section measurement near 90° is necessary, one might be able to use the fact that the Coulomb cross section (which is presumably well known) is predominant at other angles in order to obviate the necessity of an absolute yield measurement. One could measure the relative yield at two angles, 90° and some smaller angle (such as 40°) where the scattering is predominantly Coulomb. The ratio of the two yields is sufficient to determine the nuclear phase shift $\delta_0$ uniquely. While this technique avoids the necessity for calibrating the beam current and the pressure in the chamber, it is suggested for use only at rather low energies. For energies in excess of about 1 Mev, the angles for which the Coulomb scattering is dominant become so small that accurate measurements (even of relative yields) are very difficult. The determination of the nuclear phase shift from the relative yield measurement suggested above amounts to a calibration of the strength of the (unknown) nuclear forces in terms of the (known) electrostatic forces between two protons.

Finally we wish to mention the multiple Coulomb scattering. The scattering cross section for small angle single scattering is so large (even with the correction for screening) that the observed small angle scattering through any physically realizable layer of matter is due to many successive scattering events. While this does not matter greatly in itself (we are not interested in the small angle scattering) it acts as a disturbing influence in the measurement of the large angle scattering cross section. One cannot assume that a proton enters the scattering chamber, proceeds in a straight line to the scattering volume selected by the collimating and detector slits, gets scattered there and proceeds from there in a straight line to the detector. Rather the paths before and after the main scattering event will show small random curvatures due to multiple Coulomb scattering.

TABLE I. Mott cross section $\sigma_M$ and quantities $q$ and $\sin\omega$ for larger scattering angles. $E$ is in Mev in the laboratory system. $\theta$ is in the center-of-mass system. $\sigma_M$ is in $10^{-24}$ cm² per steradian in the center-of-mass system.

| Scattering angle $\theta$ | Quantity | Leading term | Corrections $(1+c_1E^{-1}+c_2E^{-2}+\cdots)$ $c_1$ | $c_2$ |
|---|---|---|---|---|
| 40° | $\sin\omega$ | 1 | −0.29269 | 0.02308 |
| | $q$ | $0.80796E^{-1}$ | −0.05415 | 0.00388 |
| | $\sigma_M$ | $0.33520E^{-2}$ | 0.00764 | −0.000065 |
| 50° | $\sin\omega$ | 1 | −0.14510 | 0.00461 |
| | $q$ | $0.32495E^{-1}$ | −0.01401 | 0.000249 |
| | $\sigma_M$ | $0.13481E^{-2}$ | 0.00762 | −0.000037 |
| 60° | $\sin\omega$ | 1 | −0.08883 | 0.00192 |
| | $q$ | $0.15545E^{-1}$ | −0.00831 | 0.000162 |
| | $\sigma_M$ | $0.06449E^{-2}$ | 0.00646 | −0.000016 |
| 70° | $\sin\omega$ | 1 | −0.06408 | 0.00121 |
| | $q$ | $0.086570E^{-1}$ | −0.010295 | 0.000207 |
| | $\sigma_M$ | $0.035916E^{-2}$ | 0.004148 | −0.000004 |
| 80° | $\sin\omega$ | 1 | −0.05312 | 0.000953 |
| | $q$ | $0.057927E^{-1}$ | −0.013685 | 0.000258 |
| | $\sigma_M$ | $0.024032E^{-2}$ | 0.001368 | −0.0000004 |
| 85° | $\sin\omega$ | 1 | −0.050734 | 0.000900 |
| | $q$ | $0.051890E^{-1}$ | −0.014889 | 0.000277 |
| | $\sigma_M$ | $0.021528E^{-2}$ | 0.000370 | 0 |
| 90° | $\sin\omega$ | 1 | −0.049966 | 0.000884 |
| | $q$ | $0.049966E^{-1}$ | −0.015332 | 0.000283 |
| | $\sigma_M$ | $0.020730E^{-2}$ | 0 | 0 |

This effect tends to smooth out the cross section as a function of angle, and is particularly disturbing when the variation of cross section with angle is rapid (as in the Coulomb scattering itself). While no discussion of these and similar corrections to the raw data will be given in this paper, we mention this because it is the one correction which one can never quite get rid of: If one tries to eliminate the multiple Coulomb scattering, say by decreasing the thickness of the scatterer, one also eliminates the effect one is trying to observe.

## IV. DETERMINATION OF THE S-WAVE PHASE SHIFTS FROM THE EXPERIMENTAL CROSS SECTIONS—THEORY

The techniques of determining phase shifts from the experimental data have been described in detail by BTE, and in other papers by Breit and collaborators. It will suffice to describe a somewhat simpler formula for the phase shift than has been given previously, and to tabulate the few auxiliary quantities necessary for its use.

For energies below 10 Mev, the scattering is almost entirely made up of $S$-wave nuclear scattering and Coulomb scattering. With the assumption that the nuclear scattering is only $S$-wave scattering, the differential cross section in the center-of-mass system (2.16) can be written in the form:

$$\sigma(\theta)=\sigma_M(\theta)[1+9^{-1}(\sin\omega-\sin(2\delta_0+\omega))], \quad (4.1)$$

where $\theta$ is the scattering angle in the center-of-mass system; $\sigma_M(\theta)$ is the Mott cross section (2.10). $\delta_0$ is the nuclear $S$-wave phase shift. The quantities $q$ and $\omega$ are functions of the energy and scattering angle only, and are defined by:

$$\tan\omega\equiv\frac{2/\eta+\mathcal{Y}}{\mathbf{X}}, \quad (4.2)$$

$$q\equiv\frac{\eta\mathfrak{M}}{\mathbf{X}}\cos\omega, \quad (4.3)$$

where, in the notation of BTE,

$$\mathbf{X}=\frac{\cos(\eta\ln\sin^2\theta/2)}{\sin^2\theta/2}+\frac{\cos(\eta\ln\cos^2\theta/2)}{\cos^2\theta/2},$$

$$\mathcal{Y}=\frac{\sin(\eta\ln\sin^2\theta/2)}{\sin^2\theta/2}+\frac{\sin(\eta\ln\cos^2\theta/2)}{\cos^2\theta/2}, \quad (4.4)$$

$$\mathfrak{M}=\left(\frac{Mv^2}{e^2}\right)^2\sigma_M.$$

The formula (4.1) can be solved for $2\delta_0$ to yield:

$$2\delta_0=\sin^{-1}\left[\sin\omega-q\left(\frac{\sigma(\theta)}{\sigma_M(\theta)}-1\right)\right]-\omega. \quad (4.5)$$

Rapidly convergent expansions for $\sigma_M$, $q$ and $\sin\omega$ in inverse powers of the energy can be obtained from their analytic forms. Such expansions are collected in Table I for center-of-mass scattering angles of 40 to 90 degrees. The leading term given in column 3 is to be multiplied by the corresponding correction term involving $c_1$ and $c_2$. For example, the value of $\sigma_M$ in barns per steradian at $\theta=40°$ is given by

$$\sigma_M(40°)=0.3352E^{-2}\left(1+\frac{0.00764}{E}-\frac{0.000065}{E^2}+\cdots\right),$$

where $E$ is the energy in the laboratory system. By means of these expansions and trigonometric tables the phase shifts can be found from the experimental data with a minimum of effort.

At small scattering angles the expansions for $\sin\omega$ and $q$ are inconvenient due to slow convergence even at energies above 1 Mev. It has been found that the quantity $Q$ defined by

$$Q=q\sec\omega \quad (4.6)$$

and $\tan\omega$ yield useful expansions for small angles. With this definition of $Q$, formula (4.5) is replaced by:

$$2\delta_0=\sin^{-1}\left[\sin\omega-Q\cos\omega\left(\frac{\sigma(\theta)}{\sigma_M(\theta)}-1\right)\right]-\omega. \quad (4.7)$$

In Table II we give expansions for $\sigma_M$, $Q$, and $\tan\omega$ for center of mass scattering angles from 16 to 40 degrees

for use with formula (4.7). It is seen that the convergence of the expansions of $Q$ and $\tan\omega$ is rather poor for the two smallest angles (8 and 10 degrees in the laboratory). At the larger angles, however, the correction terms given are seen to be adequate except for low energies.

For energies considerably below 1 Mev the expansions in Tables I and II are not correct, and use must be made of the exact expressions (4.2) and (4.3) for $\tan\omega$ and $q$, or the numerical tables of BTE. In this connection it is useful to note that $\tan\omega$ is just the ratio of the quantity $(4/\eta^2\mathfrak{M}+2\mathfrak{Y}/\eta\mathfrak{M})$ given by Table II of BTE to the quantity $2\mathbf{X}/\eta\mathfrak{M}$ given by Table I of BTE. Similarly, $Q$ is just $\eta$ times the ratio of $\mathfrak{M}$ (Table V of BTE) to $\mathbf{X}$ (Table III of BTE) by definition. Once $\tan\omega$ and $Q$ are known, formula (4.7) can be applied in the usual way.

It should be remarked that (4.5) or (4.7) leads to certain ambiguities as to the sign and magnitude of $2\delta_0+\omega$. The correct value of $\delta_0$ cannot be determined from the value of the cross section at one angle and one energy. It is necessary to know the magnitude and angular distribution of the scattering in order to determine the correct sign and magnitude of the phase shift, from the interference of the nuclear scattering with the Coulomb scattering. For example, suppose the correct value of $\delta_0$ is $\alpha$. For $S$-wave scattering alone, $\alpha$ would be independent of scattering angle. Now (4.5) or (4.7) allows another solution, $\delta_0'=\pi/2-\omega-\alpha$. However, $\omega=\omega(\theta)$ so that $\delta_0'$ would have the dependence on scattering angle characteristic of $\omega$; hence this solution can be excluded provided the scattering is known at more than one angle. Physically, the phase shift can be seen to approach zero very rapidly at zero energy ($\delta\sim e^{-2\pi\eta}$ for small $k$ (large $\eta$), from (1.1) and (1.2)) because the Coulomb repulsion keeps the protons apart, far outside the range of the nuclear force.

In order to establish the uncertainty in a value of the phase shift implied by an experimental measurement with certain experimental uncertainties in cross section and energy, it is convenient to have tables of the quantities $\sigma(\partial\delta_0/\partial\sigma)_E$ and $E(\partial\delta_0/\partial E)_\sigma$, that is, the variation in $\delta_0$ due to a change in the cross section with energy kept constant, and the variation in $\delta_0$ due to a change in the energy keeping the cross section fixed. These quantities, when multiplied by the relative uncertainties in cross section and energy respectively, give directly the uncertainty in the phase shift $\delta_0$. $\sigma(\partial\delta_0/\partial\sigma)_E$ and $E(\partial\delta_0/\partial E)_\sigma$ are, of course, dependent upon the scattering angle and energy, and upon the actual value of the scattering cross section at that angle and energy. In order to tabulate these functions, one must assume, effectively, the functional dependence of $\delta_0$ on energy, since that is the only unknown in the formula for the scattering cross section (4.1). BTE give tables (Tables VI and VIII in their paper) of $0.01\sigma(\partial\delta_0/\partial\sigma)_E$ and $0.01E(\partial\delta_0/\partial E)_\sigma$ for energies from 0.175 Mev to 2.4 Mev and angles from $\theta=30°$ to 90°, under a reasonable assumption as to the dependence of $\delta_0$ on energy. These tables have been extended to smaller angles and to energies up to 10 Mev assuming the energy dependence of $\delta_0$ implied by the linear fit of $\mathbf{K}$ (1.1) *vs.* $k^2$ to the Van de Graaff data (see Section VII).

TABLE II. Mott cross section $\sigma_M$ and quantities $Q$ and $\tan\omega$ for smaller scattering angles. $E$ is in Mev in the laboratory system. $\theta$ is in the center-of-mass system. $\sigma_M$ is in $10^{-24}$ cm² per steradian in the center-of-mass system.

| Scattering angle $\theta$ | Quantity | Leading term | Corrections $(1+c_1E^{-1}+c_2E^{-2}+\cdots)$ $c_1$ | $c_2$ |
|---|---|---|---|---|
| 16° | $\tan\omega$ | $0.24034E^{\frac{1}{2}}$ | −2.3533 | −0.28984 |
| | $Q$ | $7.8474E^{-\frac{1}{2}}$ | 0.19443 | 0.03075 |
| | $\sigma_M$ | $13.546E^{-2}$ | 0.003875 | −0.000124 |
| 20° | $\tan\omega$ | $0.37004E^{\frac{1}{2}}$ | −1.3024 | −0.12319 |
| | $Q$ | $4.9306E^{-\frac{1}{2}}$ | 0.15335 | 0.01887 |
| | $\sigma_M$ | $5.5280E^{-2}$ | 0.004824 | −0.000121 |
| 25° | $\tan\omega$ | $0.56499E^{\frac{1}{2}}$ | −0.70526 | −0.049009 |
| | $Q$ | $3.0657E^{-\frac{1}{2}}$ | 0.11740 | 0.01081 |
| | $\sigma_M$ | $2.2511E^{-2}$ | 0.005846 | −0.000110 |
| 30° | $\tan\omega$ | $0.79084E^{\frac{1}{2}}$ | −0.41985 | −0.021717 |
| | $Q$ | $2.0616E^{-\frac{1}{2}}$ | 0.091816 | 0.006428 |
| | $\sigma_M$ | $1.08153E^{-2}$ | 0.006644 | −0.000096 |
| 35° | $\tan\omega$ | $1.04071E^{\frac{1}{2}}$ | −0.26766 | −0.010372 |
| | $Q$ | $1.44758E^{-\frac{1}{2}}$ | 0.072901 | 0.003915 |
| | $\sigma_M$ | $0.57707E^{-2}$ | 0.007268 | −0.000081 |
| 40° | $\tan\omega$ | $1.30702E^{\frac{1}{2}}$ | −0.180087 | −0.005244 |
| | $Q$ | $1.05602E^{-\frac{1}{2}}$ | 0.058449 | 0.002418 |
| | $\sigma_M$ | $0.33520E^{-2}$ | 0.007639 | −0.000065 |

The constants used were:

$$a=-7.66\times10^{-13}\text{ cm},\qquad r_0=2.62\times10^{-13}\text{ cm}. \tag{4.8}$$

Use of (1.1) and (1.2) with these parameters yields the following values of $\delta_0$ as a function of energy:

| $E$ | 2 | 3 | 4 | 5 | 6 | 7 | 8 | 9 | 10 |
|---|---|---|---|---|---|---|---|---|---|
| $\delta_0$ | 45.6 | 50.9 | 53.5 | 54.8 | 55.5 | 55.7 | 55.7 | 55.6 | 55.3 |

The values of $\delta_0$ above 4 Mev should be considered as approximate since they are based on an extrapolation of the linear fit of $\mathbf{K}$ to the low energy data. In the energy range up to 2.4 Mev, the values of $\delta_0$ used here agree closely with those employed by BTE. In Tables III and IV, the quantities $\sigma(\partial\delta_0/\partial\sigma)_E$ and $E(\partial\delta_0/\partial E)_\sigma$ in degrees are listed. Part of the tables are taken directly from BTE, and only quoted here for completeness. The rest of the tables are the extensions to smaller angles and higher energies.

It should be noted that $\sigma(\partial\delta_0/\partial\sigma)_E$ and $E(\partial\delta_0/\partial E)_\sigma$ are approximately equal for energies above 2 Mev, and are almost constant in angle at any one energy, except at small scattering angles. The latter corresponds to the fact that the scattering is predominantly nuclear except at small angles, and is therefore almost isotropic in the center-of-mass system. Typical curves of $\sigma(\partial\delta_0/\partial\sigma)_E$ and $E(\partial\delta_0/\partial E)_\sigma$ are shown in Fig. 6. A discussion of their implications will be deferred to the next section

TABLE III. Values of $\sigma(\partial\delta_0/\partial\sigma)_E$ in degrees. $E$ is in Mev in the laboratory system; $\theta$ is in the center-of-mass system (laboratory scattering angle is $\theta/2$).

| $E$ (Mev) \ $\theta$ | 16° | 20° | 30° | 40° | 50° | 60° | 70° | 80° | 90° |
|---|---|---|---|---|---|---|---|---|---|
| 0.175 | −1954. | −819. | −230. | −97. | −51. | −28. | −16. | −10. | −8.2 |
| 0.275 | −682. | −382. | −140. | −71. | −40. | −23. | −12. | −6.1 | −3.9 |
| 0.375 | −453. | −276. | −120. | −64. | −42. | −29. | −19. | −9.1 | −1.3 |
| 0.450 | −382. | −240. | −110. | −67. | −55. | −85. | +34. | +4.9 | +1.7 |
| 0.550 | −332. | −216. | −110. | −85. | −310. | +29. | +8.8 | +4.7 | +3.9 |
| 0.650 | −307. | −207. | −120. | −220. | +50. | 14. | 8.3 | 6.8 | 6.4 |
| 0.750 | −296. | −206. | −150. | +310. | 27. | 12. | 9.4 | 8.5 | 8.3 |
| 0.850 | −294. | −213. | −220. | +85. | 21. | 12. | 11. | 10.2 | 10.1 |
| 1.21 | −349. | −319. | +180. | 30. | 18. | 16. | 15. | 15. | 15. |
| 1.60 | −562. | −1650. | 66. | 25. | 20. | 19. | 19. | 19. | 20. |
| 2.0 | −2186. | +453. | 46. | 25. | 22. | 22. | 22. | 23. | 23. |
| 3.0 | +410. | 128. | 35.1 | 27.6 | | 28.2 | | 29.2 | 29.3 |
| 4.0 | 207. | 84.2 | 33.5 | 30.0 | | 31.7 | | 32.8 | 32.9 |
| 5.0 | 148. | 67.6 | 33.2 | 31.6 | | 33.8 | | 35.0 | 35.1 |
| 6.0 | 119. | 55.8 | 33.2 | 32.7 | | 35.1 | | 36.3 | 36.4 |
| 7.0 | 103. | 53.5 | 33.1 | 33.3 | | 35.8 | | 37.0 | 37.0 |
| 8.0 | 91.1 | 49.6 | 33.0 | 33.6 | | 36.2 | | 37.3 | 37.4 |
| 9.0 | 83.7 | 46.8 | 32.9 | 33.7 | | 36.4 | | 37.3 | 37.4 |
| 10.0 | 76.8 | 44.7 | 32.8 | 33.8 | | 36.2 | | 37.2 | 37.3 |

TABLE IV. Values of $E(\partial\delta_0/\partial E)_\sigma$ in degrees. $E$ is in Mev in the laboratory system; $\theta$ is in the center-of-mass system (laboratory scattering angle is $\theta/2$).

| $E$ \ $\theta$ | 16° | 20° | 30° | 40° | 50° | 60° | 70° | 80° | 90° |
|---|---|---|---|---|---|---|---|---|---|
| 0.175 | −3930. | −1650. | −460. | −200. | −105. | −60. | −36. | −23. | −19. |
| 0.275 | −1380. | −774. | −290. | −150. | −86. | −51. | −30. | −17. | −13. |
| 0.375 | −917. | −563. | −240. | −140. | −91. | −65. | −46. | −26. | −10. |
| 0.450 | −888. | −492. | −230. | −150. | −119. | −180. | +63. | +2.7 | −4.5 |
| 0.550 | −676. | −445. | −230. | −180. | −65. | +51. | 8.1 | −0.4 | −1.8 |
| 0.650 | −625. | −429. | −260. | −460. | +90. | 17. | 4.9 | +1.8 | +1.2 |
| 0.750 | −607. | −426. | −320. | +610. | 41. | 12. | 5.5 | 3.8 | 3.4 |
| 0.850 | −607. | −441. | −470. | 160. | 27. | 10. | 6.7 | 5.6 | 5.5 |
| 1.21 | −722. | −661. | +360. | 43. | 17. | 12. | 11.4 | 11.3 | 11.4 |
| 1.60 | −1160. | −3370. | 110. | 29. | 18. | 16. | 16. | 16. | 16. |
| 2.0 | −4480. | +911. | 71. | 26. | 20. | 19. | 19. | 20. | 20. |
| 3.0 | +825. | 242. | 45.4 | 26.9 | | 25.5 | | 26.7 | 26.9 |
| 4.0 | 406. | 151. | 39.3 | 28.7 | | 29.3 | | 30.6 | 30.8 |
| 5.0 | 285. | 115. | 37.0 | 30.1 | | 31.6 | | 33.1 | 33.2 |
| 6.0 | 225. | 90. | 35.6 | 31.0 | | 33.1 | | 34.5 | 34.6 |
| 7.0 | 190. | 84.2 | 35.4 | 31.6 | | 33.9 | | 35.3 | 35.4 |
| 8.0 | 166. | 75.6 | 34.1 | 31.9 | | 34.4 | | 35.8 | 35.8 |
| 9.0 | 150. | 69.3 | 33.5 | 32.0 | | 35.4 | | 35.8 | 36.0 |
| 10.0 | 136. | 64.7 | 33.1 | 32.0 | | 34.6 | | 35.8 | 35.9 |

where $P$-wave and $D$-wave effects will be considered as well.

## V. DETERMINATION OF PHASE SHIFTS FOR HIGHER ANGULAR MOMENTA—THEORY

Breit, Condon, and Present[1] have given formulas for proton-proton scattering including the effects of all angular momenta, and in particular for the case where the nuclear scattering is important in the $S$, $P$, and $D$ states, but unimportant for orbital angular momenta $l \geq 3$. The analysis of experimental cross sections for $P$-wave and $D$-wave phase shifts, using these formulas directly, is rather cumbersome. Under the assumption that the higher phase shifts $\delta_1$ ($P$-wave), $\delta_2$ ($D$-wave), etc., are very small, one can find a relatively easy method for such an analysis. The higher phase shifts are expected to be small for energies below 10 Mev, say. In that energy region, most of the nuclear scattering is in the $S$-state. We therefore introduce the concept of an "apparent $S$-wave phase shift" defined as follows: the experimental cross section at a given energy $E$ and angle $\theta$ depends upon the nuclear phase shifts $\delta_0, \delta_1, \delta_2 \cdots$.

$$\sigma = \sigma(E, \theta; \delta_0, \delta_1, \delta_2, \cdots). \tag{5.1}$$

*The apparent S-wave phase shift $\delta_a$ is defined by setting all the higher phase shifts equal to zero and solving (5.1) for the resulting "apparent" $\delta_0$; thus*

$$\sigma = \sigma(E, \theta; \delta_a, 0, 0, 0, \cdots). \tag{5.2}$$

If the higher phase shifts are actually zero, the apparent $S$-wave phase shift $\delta_a$ will be equal to the true $S$-wave phase shift $\delta_0$, and will therefore be independent of the scattering angle $\theta$ at a given energy. If the higher phase

TABLE V. Values of $p_1(E, \theta)$. $E$ is in Mev in the laboratory system; $\theta$ is in the center-of-mass system.

| $E$ \ $\theta$ | 16° | 20° | 24° | 30° | 40° | 50° | 60° | 70° | 80° | 90° |
|---|---|---|---|---|---|---|---|---|---|---|
| 2.0 | 137.0 | −45.29 | −17.31 | −7.831 | −3.196 | −1.504 | −0.6958 | −0.2734 | −0.06381 | 0 |
| 2.5 | −67.40 | −21.22 | −11.51 | −6.057 | −2.665 | −1.290 | −0.6047 | −0.2392 | −0.05603 | 0 |
| 3.0 | −31.52 | −15.07 | −9.140 | −5.127 | −2.356 | −1.159 | −0.5473 | −0.2174 | −0.05101 | 0 |
| 3.5 | −22.40 | −12.31 | −7.868 | −4.572 | −2.150 | −1.068 | −0.5067 | −0.2017 | −0.04740 | 0 |
| 4.0 | −18.24 | −10.73 | −7.062 | −4.191 | −2.000 | −0.999 | −0.4755 | −0.1896 | −0.04458 | 0 |
| 4.5 | −15.88 | −9.70 | −6.50 | −3.91 | −1.883 | −0.944 | −0.450 | −0.180 | −0.0423 | 0 |
| 5.0 | −14.32 | −8.97 | −6.08 | −3.69 | −1.787 | −0.898 | −0.429 | −0.171 | −0.0403 | 0 |
| 6.0 | −12.41 | −7.98 | −5.53 | −3.36 | −1.64 | −0.825 | −0.394 | −0.158 | −0.0371 | 0 |
| 7.0 | −11.26 | −7.32 | −5.13 | −3.11 | −1.52 | −0.767 | −0.367 | −0.147 | −0.0345 | 0 |
| 8.0 | −10.47 | −6.84 | −4.82 | −2.92 | −1.43 | −0.719 | −0.344 | −0.137 | −0.0323 | 0 |
| 9.0 | −9.89 | −6.47 | −4.56 | −2.76 | −1.35 | −0.679 | −0.324 | −0.130 | −0.0305 | 0 |
| 10.0 | −9.44 | −6.17 | −4.35 | −2.62 | −1.28 | −0.644 | −0.308 | −0.123 | −0.0289 | 0 |

TABLE VI. Values of $p_2(E, \theta)$. $E$ is in Mev in the laboratory system; $\theta$ is in the center-of-mass system.

| $E$ \ $\theta$ | 16° | 20° | 24° | 30° | 40° | 50° | 60° | 70° | 80° | 90° |
|---|---|---|---|---|---|---|---|---|---|---|
| 2.0 | 41.77 | −7.795 | −0.4221 | 1.580 | 1.577 | 0.5726 | −0.6374 | −1.711 | −2.437 | −2.693 |
| 2.5 | −18.61 | −2.767 | +0.3542 | 1.695 | 1.582 | 0.5733 | −0.6389 | −1.717 | −2.447 | −2.704 |
| 3.0 | −7.984 | −1.464 | 0.6918 | 1.756 | 1.587 | 0.5739 | −0.6398 | −1.719 | −2.451 | −2.709 |
| 3.5 | −5.252 | −0.8532 | 0.8918 | 1.805 | 1.594 | 0.5747 | −0.6402 | −1.720 | −2.452 | −2.711 |
| 4.0 | −3.974 | −0.4822 | 1.0339 | 1.848 | 1.601 | 0.5754 | −0.6403 | −1.720 | −2.451 | −2.709 |
| 4.5 | −3.224 | −0.2215 | 1.1476 | 1.889 | 1.609 | 0.5761 | −0.6400 | −1.718 | −2.448 | −2.706 |
| 5.0 | −2.71 | −0.0206 | 1.243 | 1.925 | 1.617 | 0.577 | −0.640 | −1.717 | −2.45 | −2.70 |
| 6.0 | −2.03 | +0.284 | 1.38 | 1.99 | 1.63 | 0.578 | −0.640 | −1.71 | −2.44 | −2.69 |
| 7.0 | −1.58 | 0.519 | 1.51 | 2.06 | 1.65 | 0.580 | −0.639 | −1.71 | −2.43 | −2.68 |
| 8.0 | −1.23 | 0.712 | 1.62 | 2.11 | 1.66 | 0.581 | −0.638 | −1.70 | −2.42 | −2.67 |
| 9.0 | −0.954 | 0.879 | 1.72 | 2.16 | 1.67 | 0.582 | −0.638 | −1.70 | −2.41 | −2.66 |
| 10.0 | −0.717 | 1.028 | 1.81 | 2.21 | 1.69 | 0.583 | −0.637 | −1.70 | −2.41 | −2.66 |

shift is not zero, $\delta_a$ will be a (slowly varying) function of $\theta$ at constant energy $E$. Thus the presence of higher phase shifts shows itself directly in a plot of the apparent $S$-wave phase shift *vs.* angle of scattering.

We now use the fact that the higher phase shifts are small in two ways: First (5.1) can be expanded in a Taylor series in the higher phase shifts and we can drop all but the leading (linear) terms; second, (5.2) can be expanded in a Taylor series in the difference between the apparent and true $S$-wave phase shifts, which difference is presumably a small number. Equating the two expansions, keeping only the linear terms, yields

$$\delta_a = \delta_0 + p_1\delta_1 + p_2\delta_2 + \cdots, \tag{5.3}$$

where

$$p_n(E, \theta, \delta_0) = (\partial\sigma/\partial\delta_n)/(\partial\sigma/\partial\delta_0). \tag{5.4}$$

The partial derivatives are to be taken at the correct value of $\delta_0$ but at $\delta_1 = \delta_2 = \cdots = 0$.

The crucial point here is that the functions $p_n$ do not depend very critically upon $\delta_0$. Hence an approximate value of $\delta_0$ substituted into (5.4) will not lead to a large error in the values of the higher phase shifts inferred by the use of the expansion (5.3). In particular, the expansion (1.2) can be used to interpolate or extrapolate $\delta_0$ as a function of energy from the measured values. We have used the linear fit of $\mathbf{K}$ *vs.* $k^2$ with the constants (4.8) to determine $\delta_0(E)$ and evaluate $p_1(E, \theta)$ and $p_2(E, \theta)$. The results are given in Tables V and VI for scattering angles from 16° to 90° in the center-of-mass system and energies from 2 to 10 Mev in the laboratory system. The results are shown graphically in Figs. 4 and 5. For a more detailed discussion of these functions and their explicit forms see Appendix I.

These functions are to be used as follows: One first determines the apparent $S$-wave phase shifts and their probable errors from the measured cross sections using formula (4.5) and Table I (or formula (4.7) and Table II for the smaller scattering angles) and Tables III and IV. If $\delta_a$ shows no variation with $\theta$ outside the experimental errors, one concludes that the nuclear scattering occurs only in the $S$-state within the accuracy of the measurements. If $\delta_a$ does show a systematic variation with $\theta$, one plots $\delta_a$ *vs.* $p_1(E, \theta)$. If $\delta_2$, $\delta_3$ etc., can still be neglected, formula (5.3) shows that this plot will turn out to be a straight line of intercept $\delta_0$ and slope $\delta_1$, so both phase shifts can be read off directly from the graph, and their errors can be determined by inspection.

If the plot of $\delta_a$ *vs.* $p_1(E, \theta)$ should show appreciable curvature, several causes may be responsible (1) $\delta_1$ may be large enough so that the linear term in a power series does not suffice; estimates show that with the best experimental accuracies attainable, the linear approximation used here will be adequate as long as $\delta_1$ is less than $\eta$ radians (less than 2 or 3 degrees at 10 Mev); (2) the $D$-wave phase shift $\delta_2$ may not be negligible. To test for this, one can select a trial value of $\delta_1$ and plot $(\delta_a - p_1\delta_1)$ *vs.* $p_2$. According to (5.3), this ought to be a straight line of intercept $\delta_0$ and slope $\delta_2$. The trial value of $\delta_1$ should

then be varied until the best straight line is obtained; (3) the tensor force in the $^3P$-state can lead to a curvature in the plot of $\delta_a$ *vs.* $p_1$, even though the apparent slope ($\delta_1$) is within the limits mentioned and the higher phase shifts are sufficiently small. Breit, Kittel, and Thaxton[16] have pointed out that the presence of the tensor force in the $^3P$-state complicates the analysis of the scattering data since three $P$-wave phase shifts are then required to fit the data, namely $\delta(^3P_0)$, $\delta(^3P_1)$ and $\delta(^3P_2)$. However, as Breit[17] has pointed out, their formulas show that to the extent that one can restrict one-self to the terms linear in the $P$-wave phase shifts, these enter only in the combination

$$\delta_1=(1/9)\delta(^3p_0)+(3/9)\delta(^3P_1)+(5/9)\delta(^3P_2)\cdots. \quad (5.5)$$

This is to be expected since the $^3P_0$-, $^3P_1$-, $^3P_2$-states have the statistical weights 1/9, 3/9, 5/9, respectively. The combination $\delta_1$ (5.5) enters the scattering cross section in exactly the same way as if no tensor force existed. However, let us now suppose that the three $P$-wave phase shifts are large enough numerically so that their squares cannot be neglected. It is still possible, indeed fairly likely, that their weighted average (5.5) will be small enough to fall within the limits given earlier. In that case, a plot of $\delta_a$ *vs.* $p_1$ will show appreciable curvature even though the implied $\delta_1$ is less than $\eta$ radians and the $D$-wave phase shifts etc., are negligible. Since the experimental data are not accurate enough at present there is no need to go into this possibility in more detail here.

We shall now discuss the effects of systematic errors in cross section and energy measurement upon the determination of the phase shifts. The apparent $S$-wave phase shift $\delta_a$ can vary with scattering angle as the result either of real effects, i.e., higher phase shifts, or of experimental errors. Let $\Delta_E(=0.01E(\partial\delta_a/\partial E)_\sigma)$ be the change in $\delta_a$ due to a one percent change in beam energy, $\Delta_\sigma(=0.01\sigma(\partial\delta_a/\partial\sigma)_E)$ the effect produced by a one percent change in scattering cross section; the effect on $\delta_a$ of a $P$-wave phase shift of one degree is given by $p_1(E,\theta)$ and of a $D$-wave phase shift of one degree by $p_2(E,\theta)$. All these quantities are plotted as functions of the scattering angle in Fig. 6, for a typical energy (5 Mev).

We first note the flat central part of the $\Delta_\sigma$ and $\Delta_E$ curves, between $\theta_1$ and $\pi-\theta_1$. In this region the nuclear scattering is predominant, and is by assumption mostly $S$-wave scattering, i.e., symmetrical in the center-of-mass system. Thus a systematic change in the cross section (or the energy) will lead to a systematic error in the $S$-wave phase shift, but it will *not* lead to spurious higher phase shifts. Cyclotrons at present do not have a very accurate voltage control, and it is difficult to get

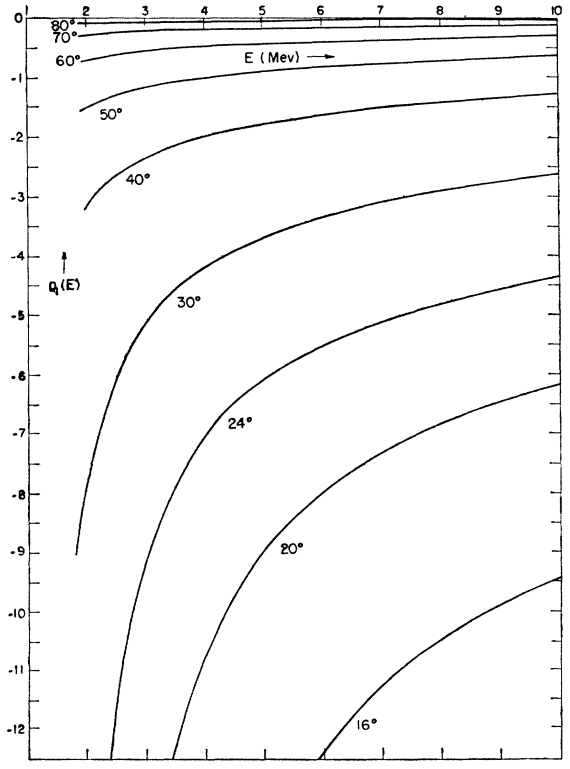


FIG. 4. Ordinate, $p_1(E,\theta)$; abscissa, $E$. $p_1(E)$ as a function of the energy in the laboratory (in Mev) for various scattering angles in the center-of-mass system.

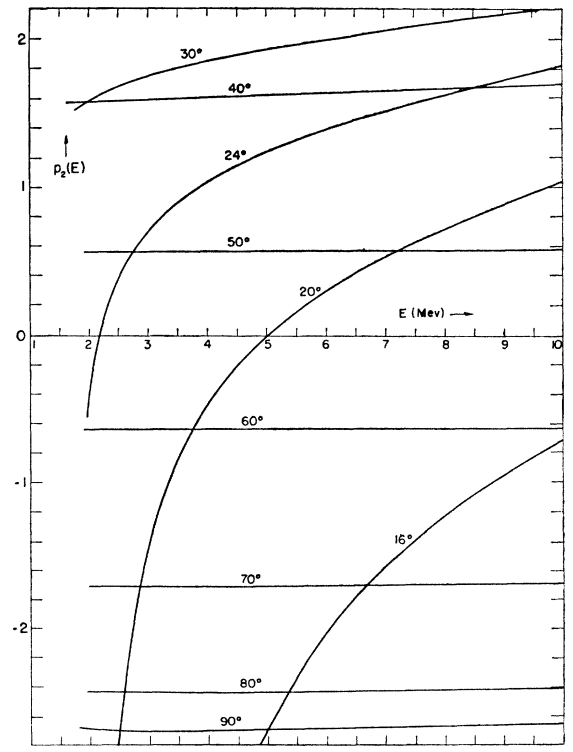


FIG. 5. Ordinate, $p_2(E,\theta)$; abscissa, $E$. $p_2(E)$ as a function of the energy in the laboratory (in Mev) for various scattering angles in the center-of-mass system.

[16] Breit, Kittel, and Thaxton, Phys. Rev. **57**, 255 (1940).
[17] G. Breit, University of Pennsylvania Bicentennial Conference, "Nuclear Physics" (1941), p. 10.

TABLE VII. Values of the $S$-wave phase shift, $\eta$, $h(\eta)$, **K** and $k^2$ for the experimental data. $k^2=1.20(5)\times10^{24}E$ (Mev) cm$^{-2}$; $E$ is the energy in the laboratory system.

(a). Data obtained with Van de Graaff generators

| Energy (Mev) | $S$-wave phase shift (degrees) | $\eta$ | $h(\eta)$ | **K** | $k^2$ ($\times10^{24}$ cm$^{-2}$) | Source |
|---|---|---|---|---|---|---|
| 0.1765 | 5.78±0.35 | 0.376 | 0.552 | 3.79±0.16 | 0.213 | RKT |
| 0.2002 | 6.80±0.32 | 0.353 | 0.600 | 3.82±0.14 | 0.241 | RKT |
| 0.2259 | 7.82±0.30 | 0.333 | 0.644 | 3.87±0.12 | 0.272 | RKT |
| 0.2495 | 9.03±0.30 | 0.316 | 0.686 | 3.83±0.11 | 0.301 | RKT |
| 0.2753 | 10.06±0.28 | 0.303 | 0.719 | 3.82±0.09 | 0.332 | RKT |
| 0.2983 | 10.96±0.26 | 0.289 | 0.758 | 3.91±0.09 | 0.359 | RKT |
| 0.3214 | 11.82±0.30 | 0.279 | 0.787 | 3.93±0.15 | 0.387 | RKT |
| 0.670 | 24.68±0.40 | 0.1931 | 1.111 | 4.00±0.10 | 0.807 | HHT |
| 0.776 | 27.12±0.40 | 0.1795 | 1.178 | 4.12±0.08 | 0.935 | HHT |
| 0.867 | 29.32±0.40 | 0.1697 | 1.230 | 4.17±0.07 | 1.045 | HHT |
| 0.860 | 29.28±0.40 | 0.1704 | 1.226 | 4.15±0.03 | 1.036 | HKPP |
| 1.200 | 35.94±0.40 | 0.1444 | 1.383 | 4.32±0.03 | 1.446 | HKPP |
| 1.390 | 38.76±0.40 | 0.1341 | 1.453 | 4.41±0.03 | 1.675 | HKPP |
| 1.830 | 44.02±0.40 | 0.1169 | 1.586 | 4.59±0.02 | 2.206 | HKPP |
| 2.105 | 46.18±0.40 | 0.1090 | 1.653 | 4.72±0.03 | 2.537 | HKPP |
| 2.392 | 48.08±0.40 | 0.1022 | 1.716 | 4.85±0.03 | 2.883 | HKPP |
| 2.42 | 48.24±0.50 | 0.1016 | 1.725 | 4.86±0.05 | 2.917 | BFLSW |
| 3.04 | 50.95±0.50 | 0.0906(5) | 1.834 | 5.15±0.06 | 3.664 | BFLSW |
| 3.27 | 51.89±0.50 | 0.0874 | 1.870 | 5.24±0.06 | 3.941 | BFLSW |
| 3.53 | 52.58±0.50 | 0.0841 | 1.907 | 5.36±0.07 | 4.254 | BFLSW |
| 2.42 | 47.91±0.40 | 0.1016 | 1.725 | 4.90±0.05 | 2.917 | RWH |
| 3.04 | 50.80±0.30 | 0.0906(5) | 1.834 | 5.17±0.05 | 3.664 | RWH |
| 3.28 | 51.77±0.40 | 0.0873 | 1.870 | 5.26±0.06 | 3.953 | RWH |
| 3.53 | 52.20±0.30 | 0.0841 | 1.907 | 5.41±0.06 | 4.254 | RWH |

(b). Data obtained with cyclotrons

| Energy (Mev) | $S$-wave phase shift (degrees) | $\eta$ | $h(\eta)$ | **K** | $k^2$ ($\times10^{24}$ cm$^{-2}$) | Source |
|---|---|---|---|---|---|---|
| 4.2 | 52.7±2.0 | 0.0771 | 1.995 | 5.83±0.30 | 5.06 | MP |
| 4.94±0.04 | 54.7±1.0 | 0.0714 | 2.070 | 6.02±0.18 | 5.95±0.06 | M |
| 7.03±0.06 | 52.0±0.6 | 0.0598 | 2.243 | 7.63±0.11 | 8.48±0.07 | DOP |
| 8.0 ±0.1 | 52.7±2.0 | 0.0559 | 2.31 | 8.00±0.40 | 9.64±0.12 | WC |
| 14.5 ±0.7 | 52.2±3.5 | 0.0415 | 2.61 | 10.78±0.80 | 17.5 ±0.8 | WLRWS |

very accurate absolute values for the cross sections no matter what high voltage generator is used. We now see, however, that *one does not need high absolute accuracy to detect the presence of higher phase shifts in the scattering, merely high relative accuracy, provided one restricts oneself to scattering angles between $\theta_1$ and $\pi-\theta_1$.* Thus it appears worth while to make very careful relative cross-section determinations with protons from cyclotrons. One must be sure, of course, that the systematic errors are the same for all angles of scattering.

The next point to observe in Fig. 6 is the behavior of $p_1$ and $p_2$ in this central region. Except for a change in sign they look very much alike, with a roughly parabolic shape. Hence *measurements in the central region cannot discriminate between P-wave and D-wave contributions to the scattering.*

We now investigate the region where the interference between nuclear and Coulomb scattering is important, i.e., between $\theta_2$ and $\theta_1$ in Fig. 6.|| || In this region systematic errors in energy and yield will lead to spurious higher phase shifts. However, Fig. 6 shows that the error in energy is much more serious in this regard than the error in yield, i.e., $\Delta_E$ begins to rise rapidly at somewhat larger angles than $\Delta_\sigma$. This is fortunate, since Van

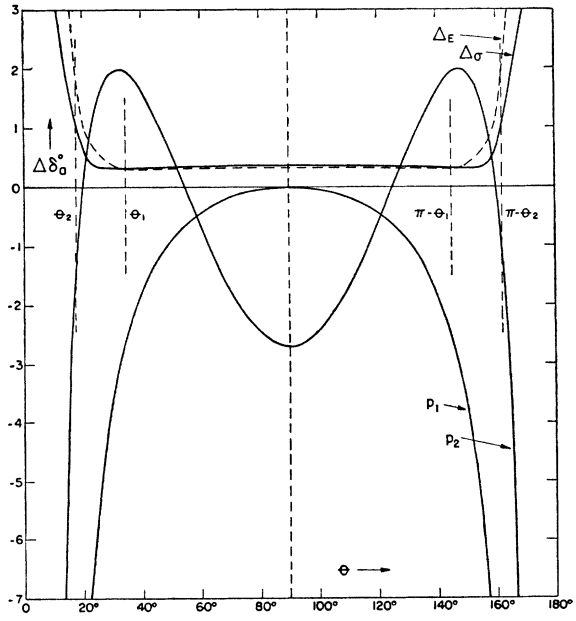


FIG. 6. Ordinate, $\Delta\delta_a$ in degrees; abscissa, $\theta$ in degrees. Effects of small changes in energy ($\Delta_E=0.01E(\partial\delta_a/\partial E)_\sigma$) and cross section ($\Delta_\sigma=0.01\sigma(\partial\delta_a/\partial\sigma)_E$) and the presence of $P$-wave ($p_1$) and $D$-wave ($p_2$) phase shifts of one degree on the apparent $S$-wave phase shift as a function of the scattering angle in the center-of-mass system at an energy of 5 Mev in the laboratory system.

|| || For $\theta\leq\theta_2$ the Coulomb scattering is dominant and the measurements are very insensitive to nuclear effects.

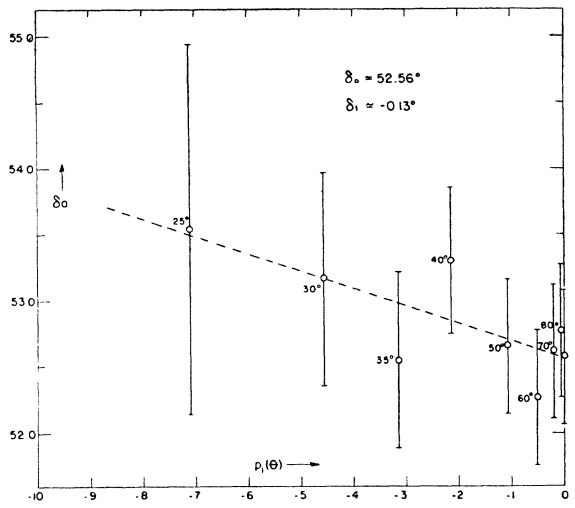


FIG. 7. Apparent $S$-wave phase shifts from BFLSW data at 3.53 Mev plotted *vs.* $p_1(\theta)$. A slight repulsive interaction in the $^3P$-state seems to be indicated, although the experimental uncertainties are relatively large.

de Graaff generators can give protons of very accurately known energy, while absolute cross-section measurements are considerably harder to make experimentally. Figure 6 shows that *there is sense in controlling the voltage to 0.1 percent, say, while measuring cross sections only to* $\frac{1}{2}$ *percent or even 1 percent.* The very different behavior of $p_1$ and $p_2$ in this region of scattering angles implies that one will be able to differentiate between $P$-wave and $D$-wave effects by measurements there.*

The angles $\theta_1$ and $\theta_2$ depend upon energy, of course. They can be inferred from Tables III and IV for any one energy. Reasonable interpolation formulas for energies from 2 to 10 Mev are

$$\theta_1 \simeq 25+50/E, \qquad \theta_2 \simeq 12+30/E, \tag{5.6}$$

where $E$ is the laboratory energy in Mev and $\theta_1$ and $\theta_2$ are in degrees, in the center of gravity system.

The experimental data available at present are discussed in Appendix II and the next section. Whenever the accuracy of the data allow, an analysis in terms of apparent $S$-wave phase shift is made there in order to obtain estimates of the higher phase shifts. The $S$-wave phase shifts implied by the experimental data are collected in Table VII, along with other quantities of interest for the further analysis.

## VI. PHASE SHIFT ANALYSIS OF EXPERIMENTAL DATA

The available experimental data are analyzed for the apparent $S$-wave phase shifts by means of formula (4.5) or (4.7). The data at higher energies are examined for $P$-wave (or $D$-wave) effects wherever the accuracy warrants it. For convenience the data are broken up into two groups—the data obtained with Van de Graaff generators, and that obtained with cyclotrons. The Van de Graaff data are, in general, more precise than the cyclotron data. The $S$-wave phase shifts implied by the data are given in Table VII with probable errors estimated from experiment. A detailed tabulation of the phase shifts is given in Appendix II; the values in Table VII represent averages over the scattering angles.

The following data are available at this time:

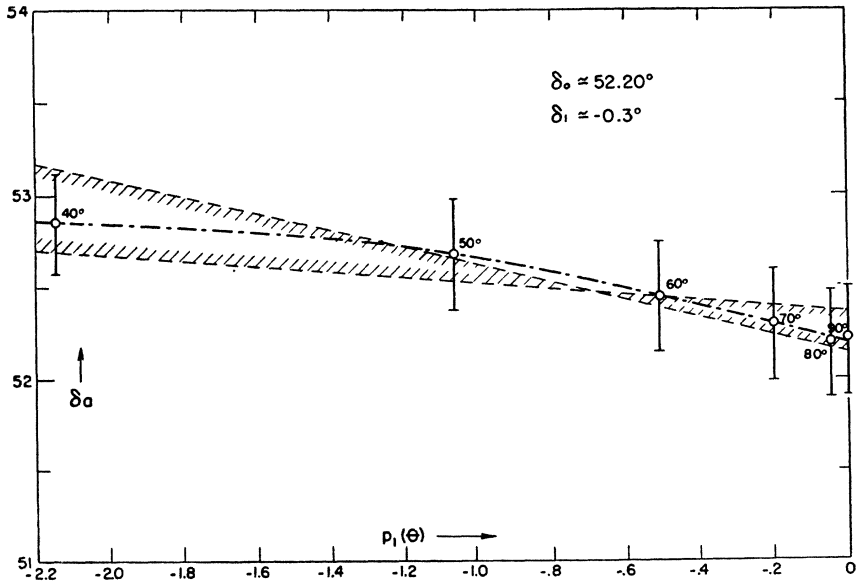


FIG. 8. Apparent $S$-wave phase shifts from RWH data at 3.53 Mev plotted *vs.* $p_1(\theta)$. A slight repulsion in the $^3P$-state is implied.

* Professor Breit has pointed out that if there are three $P$-wave phase shifts (due to the presence of a tensor force), their quadratic terms (which can be appreciable even though the linear term (3.5) is small) might give rise to a spurious $D$-wave contribution to the scattering that could not be distinguished from a true $D$-wave effect by this method of analysis.

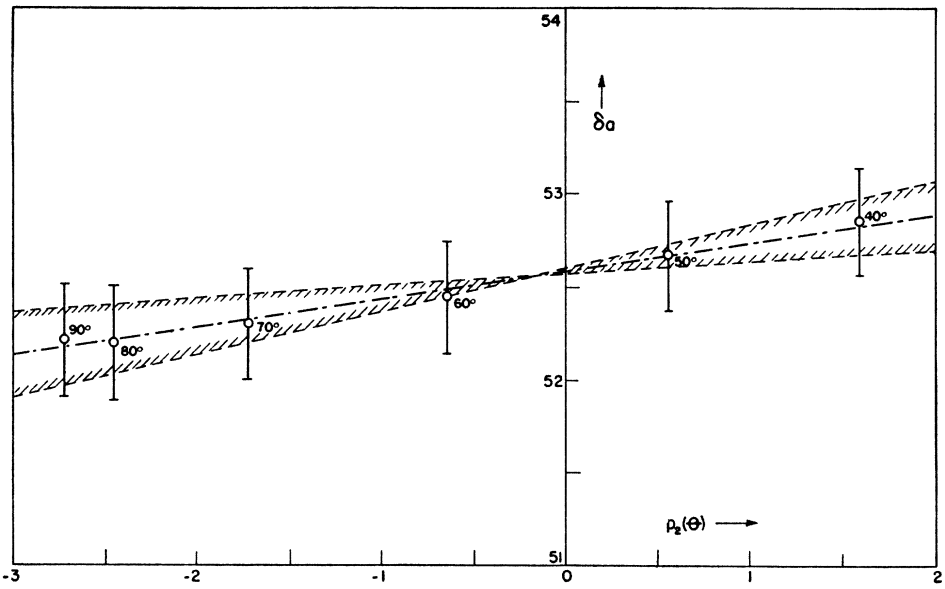


FIG. 9. Apparent $S$-wave phase shifts from RWH data at 3.53 Mev plotted *vs.* $p_2(\theta)$. The points imply an unreasonably strong attraction in the $^1D$-state, assuming no interaction in the $^3P$-state. The somewhat better fit of the RWH data to a $D$-wave effect rather than a $P$-wave effect (see Fig. 8) is not to be regarded as significant.

### 1. Data Obtained with Van de Graaff Generators (in Order of Increasing Energy)

RKT.—Ragan, Kanne, and Taschek[18] have made measurements in the 200–300 kev region. Their high voltage apparatus was actually a transformer-rectifier device, not a Van de Graaff generator. However, for simplicity their measurements have been grouped with those made with electrostatic generators as distinct from data obtained with cyclotrons. The measurements were mostly exploratory in character and do not claim very high accuracy. The points at 90 degrees were corrected most carefully for various sources of experimental error; therefore these points were used to determine the phase shifts.

HHT.—The data of Heydenburg, Hafstad, and Tuve[19] in the 670–870 kev region were analyzed by BTE. Later, Creutz[20] reanalyzed these data obtaining slightly different results for the phase shifts. Creutz looked for $P$-wave effects and found some; however, he interpreted them as being spurious. The $S$-wave phase shifts found by Creutz are given in Table VII.

HKPP.—The data of Herb, Kerst, Parkinson, and Plain[2] were taken with extreme care, and are still the most accurate data available today. BTE showed that these data, covering the energy region from 860 kev to 2.4 Mev, could be interpreted in terms of $S$-wave phase shifts only. The phase shifts found by BTE for these data will be used here.

BFLSW.—More recently, Blair, Freier, Lampi, Sleator, and Williams[21] have extended the measurements to higher energies (from 2.4 Mev to 3.5 Mev). An analysis of these data by Critchfield and Dodder[22] showed that they could not be fitted by $S$-wave phase shifts only. Furthermore, Critchfield and Dodder stated that a combination of $S$-wave and $P$-wave phase shifts still does not give good agreement with the experimental data. For comparison, a plot of the apparent $S$-wave phase shift $\delta_a$ *vs.* $p_1(\theta)$ for the data at 3.53 Mev is shown in Fig. 7. A slight downward trend of $\delta_a$ with increasing $p_1$ seems to exist, indicating a small $P$-wave phase shift of the order of 0.13 degree, with a negative sign (repulsive potential in the $^3P$-state). Critchfield and Dodder, by a rather different method of analysis, arrived at a value of $-2.3$ degrees for the $P$-wave phase shift at this energy. In view of Fig. 7 such a large negative value of $\delta_1$ is rather difficult to reconcile with the analysis given here.

It should be noted that the data represented in Fig. 7 do not appear to be incompatible with a zero or slightly positive value for the $P$-wave phase shift. The experimental errors are large, and it is felt that definite conclusions about $P$-wave effects cannot be drawn from these data. As far as determining $\delta_1$ is concerned, the experimental errors shown in Fig. 7 could be considered as over-estimates since they include all experimental errors, whether they affect all angles equally or not (see discussion in Section V). However, the scatter of the points themselves indicates that the errors shown are not gross over-estimates, and are probably quite reasonable. In consequence the possible $P$-wave effects indicated will be ignored; only the $S$-wave phase shifts will be utilized. These $S$-wave phase shifts were computed independently of Critchfield and Dodder (see Appendix II); the values found are in close agreement with theirs. They do not quote any error for the phase shifts. The

[18] Ragan, Kanne, and Taschek, Phys. Rev. **60**, 628 (1941), referred to as RKT.
[19] Heydenburg, Hafstad, and Tuve, Phys. Rev. **56**, 1078 (1939), referred to as HHT.
[20] E. C. Creutz, Phys. Rev. **56**, 893 (1939).
[21] Blair, Freier, Lampi, Sleator, and Williams, Phys. Rev. **74**, 553 (1948), referred to as BFLSW.
[22] C. L. Critchfield and D. C. Dodder, Phys. Rev. **75**, 419 (1949).

errors given in Table VII appear to be reasonable from an examination of the experimental data.

RWH.—The most recent Van de Graaff data are those of Ralph, Worthington, and Herb,[23] taken at the same energies as those of the Minnesota group. They state that the data cannot be fitted by a $S$-wave anomaly only. A plot of $\delta_a$ *vs.* $p_1(\theta)$ for their data at 3.53 Mev is shown in Fig. 8. The experimental errors shown *exclude* errors in pressure and current measurement (which affect all angles nearly equally), and are assumed to be reasonable errors as far as the slope determination is concerned. The two limiting straight lines drawn on the figure indicate that the $P$-wave phase shift lies between $-0.15$ and $-0.45$ degree (RWH put it at $-0.30$ degree), i.e., a repulsive potential in the $^3P$-state.

However, two additional views can be taken. If one suspects that the experimental errors have been underestimated, only a slight stretching of the errors would make the points in Fig. 8 not inconsistent with a horizontal line, i.e., pure $S$-wave scattering, with no $P$-wave effects at all. On the other hand, from the discussion based on Fig. 6, it is clear that the data could probably be fitted by a $D$-wave contribution just as well as by a $P$-wave contribution (or by a mixture of the two). The fact that the points in Fig. 8 lie on a smooth curve more closely than on any straight line might imply such a thing, disregarding for a moment the relatively large experimental uncertainties. The possibility of a $D$-wave effect instead of a $P$-wave effect is illustrated in Fig. 9 where $\delta_a$ is plotted *vs.* $p_2(\theta)$. The $D$-wave phase shift (assuming the $P$-wave phase shift is zero) is seen to lie between $+0.07$ and $+0.24$ degree, and the points fall along a straight line more closely than in the $P$-wave case. The data at 2.42, 3.04, and 3.28 Mev all give slightly better fits to the $D$-wave anomaly than to the $P$-wave. However, the $D$-wave phase shifts so determined are abnormally large. If one assumes that the potentials in the $^1S$ and $^1D$ are the same, the theoretical estimates (see Section XII) for $\delta_2$ are from 5 to 50 times smaller than the values implied by these data, depending upon the well shape assumed. In addition, the energy dependence for $\delta_2$ (or else for $\delta_1$) implied by the data is not at all reasonable. It is unlikely that the slightly better fit to the $D$-wave anomaly is significant in view of the relatively large experimental uncertainties and the possibility of unknown systematic errors. As was indicated earlier, measurements between 20 and 40 degrees (between $\theta_2$ and $\theta_1$ of Section V) would almost certainly settle this point.

There is even reason to question the existence of a $P$-wave effect. If one compares the pre-war values of apparent $S$-wave phase shift found by the Wisconsin group at 2.39 Mev (which were interpreted in terms of $S$-wave effects only) with the recent values at 2.42 Mev, one sees a marked difference in trend and a considerable difference in numerical values at the smaller angles. The over-all accuracy of the present measurements is not significantly greater than that of the earlier measurements. Because of this discrepancy at the one point of overlap of the two sets of data and all the other uncertainties involved, it seems unwise to draw any definite conclusions about $P$- or $D$-wave effects at this time. Only the values of the $S$-wave phase shift from these data are used in the analysis.

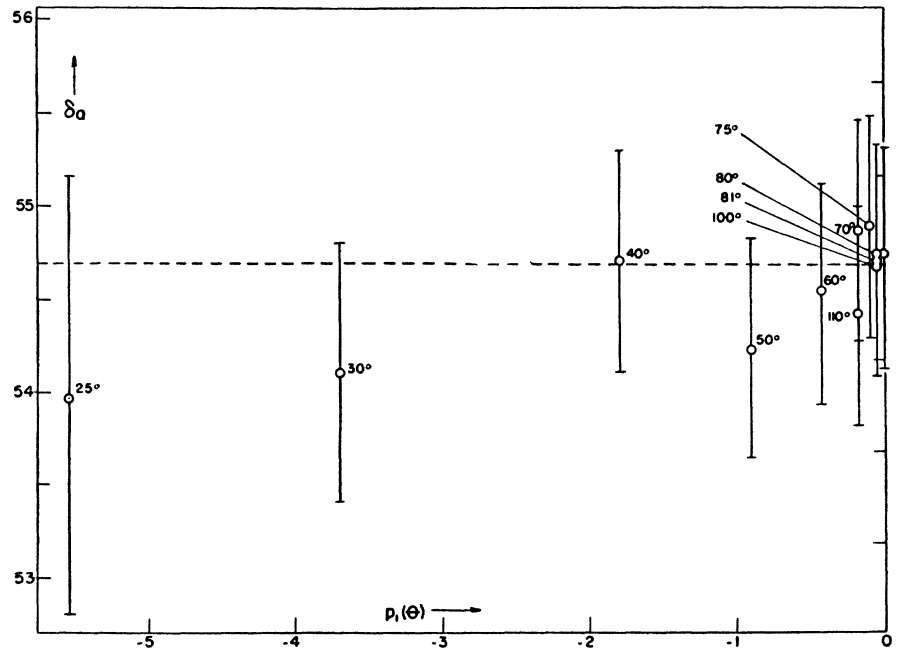


FIG. 10. Apparent $S$-wave phase shifts from the data of Meagher at 4.94 Mev plotted *vs.* $p_1(\theta)$. A small *attraction* in the $^3P$-state seems indicated. However, the experimental points are completely consistent with no interaction in the $^3P$-state.

[23] Ralph, Worthington, and Herb (private communication), referred to as RWH.

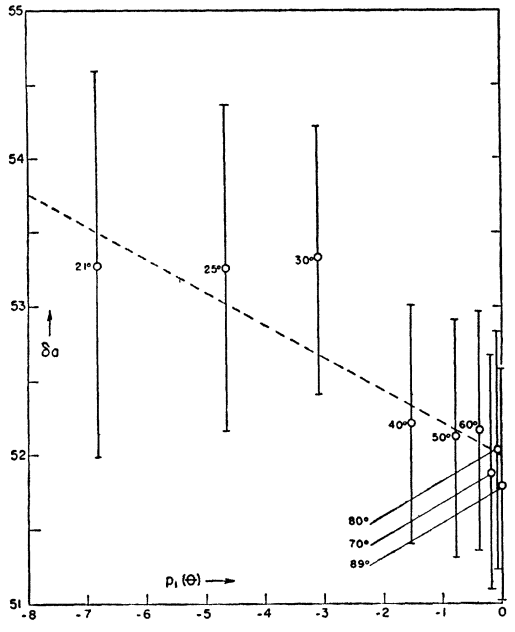


FIG. 11. Apparent $S$-wave phase shifts from the DOP data at 7 Mev plotted *vs.* $p_1(\theta)$. The dotted line is the fit given by DOP. A small repulsive interaction in the $^3P$-state seems indicated.

## 2. Data Obtained with Cyclotrons

MP.—May and Powell[24] determined the ratio of observed scattering to Mott scattering at 90 degrees with 4.2 Mev protons using photographic techniques. The ratio has an uncertainty of about 6 percent, and is therefore of negligible value to this analysis. The only reason for mentioning this experimental point is the fact that it was used incorrectly by Lubanski and de Jager.[25] These authors misstated the most probable value of the $S$-wave phase shift implied by these data (it is 52.7 degrees rather than 54.0). Since their analysis depends very critically on this particular point, their result cannot be considered as valid (although, by a combination of errors, it is rather close to the truth).

M.—Very recently, Meagher[26] has made measurements at 4.94 Mev using photographic plate detection. A plot of the apparent $S$-wave phase shift $\delta_a$ implied by these data *vs.* $p_1(\theta)$ is given in Fig. 10. The horizontal line is the best fit to the points near 90 degrees assuming $\delta_1=0$. It is seen that the data allow such a fit, but that a line of positive slope would provide somewhat better agreement. In view of the fact that the (more accurate) Van de Graaff data at 3.5 Mev indicate a zero or negative $P$-wave phase shift, the slight positive $P$-wave

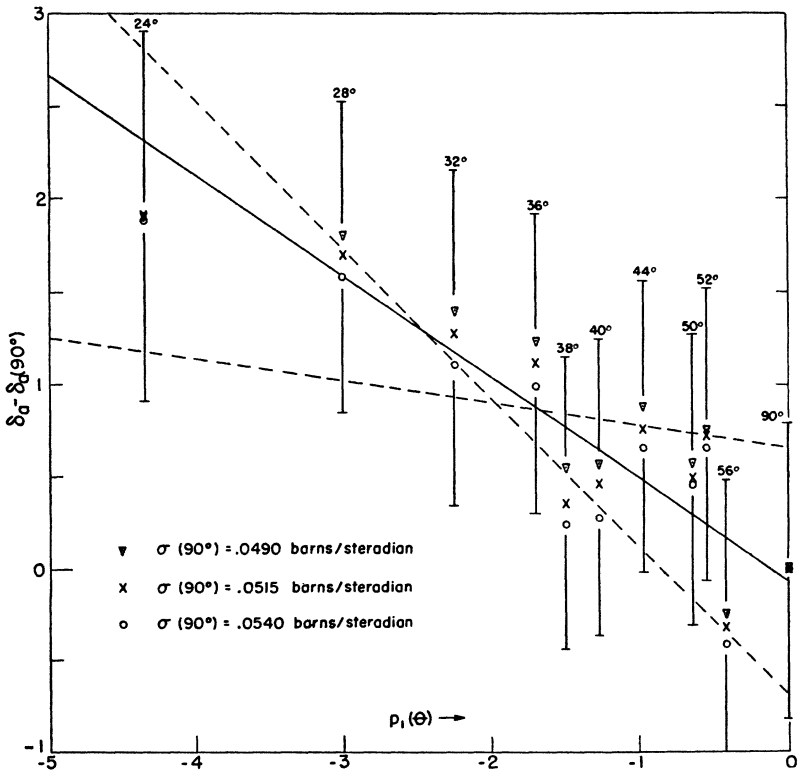


FIG. 12. Relative values of the apparent $S$-wave phase shifts from the data of Wilson (relative measurements on angular distribution of scattering) at 10 Mev plotted *vs.* $p_1(\theta)$ for various reasonable assumptions as to the absolute value of the cross section at 90 degrees. The slope of the line is seen to be insensitive to the choice of the normalization of cross section. The data are very inaccurate, but seem to imply a slight repulsion in the $^3P$-state.

[24] A. N. May and C. F. Powell, Proc. Roy. Soc. **A190**, 170 (1947), referred to as MP.
[25] J. K. Lubanski and C. de Jager, Physica **14**, 8 (1948).
[26] R. E. Meagher, Ph.D. thesis, University of Illinois (1949); see also papers submitted to Phys. Rev. with P. G. Kruger, H. A. Leiter, and F. A. Rodgers, referred to as M.

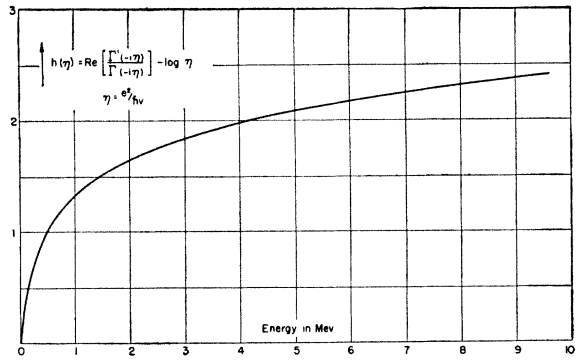


FIG. 13. $h(\eta)$ as a function of the energy in the laboratory.

phase shift indicated here should be taken very cautiously.

DOP.—Dearnley, Oxley, and Perry[12] have used the same technique at 7 Mev. They state that their data are in agreement with a slightly negative $P$-wave phase shift. Figure 11 shows a plot of $\delta_a$ *vs.* $p_1(\theta)$ which bears out this analysis. The dotted line represents their values of the $P$-wave phase shift ($-0.22$ degree) and $S$-wave phase shift. It is seen to give a reasonable fit to the experimental points although the large experimental uncertainties allow considerable leeway. The accuracy of the data is too low to draw definite conclusions about the $P$-wave phase shift. The $S$-wave phase shift implied by these data is very hard to reconcile with the lower energy measurements quoted above. (See Sections VII and XI.) A redetermination of the scattering at this energy would be very desirable.

WC.—Wilson and Creutz[27] have made measurements at 8 Mev in which they determined the absolute value of the cross section at 90 degrees, and made relative measurements at other angles. The accuracy of their absolute measurement was about $\pm 5$ percent. The data at other angles based on the point at 90 degrees are consistent with $S$-wave scattering only, but the accuracy is comparatively poor, and a detailed analysis is not warranted. The value of the $S$-wave phase shift determined from these data is given in Table VII.

W.—Wilson[28] has made relative measurements of the angular distribution of scattering at 10 Mev. A theoretical analysis of his data has been given by Peierls and Preston[29] and by Foldy[30] with somewhat different results. Preston and Peierls find that the $P$-wave phase shift is approximately $-0.8$ degree, and state that a repulsive square well potential of range $2.5\times10^{-13}$ cm and depth 10 Mev will give this value of $\delta_1$ at an energy of 10 Mev. Foldy claims that the data imply a $P$-wave phase shift of about $-0.4$ degree, in disagreement with Preston and Peierls. For comparison purposes, Fig. 12 shows a plot of $\delta_a$ *vs.* $p_1(\theta)$ under various reasonable assumptions as to the absolute value of the cross section at 90 degrees. The actual magnitude of $\delta_a$ has no meaning, only the change with scattering angle is important. Accordingly, the differences $\delta_a-\delta_a$ (90°) are

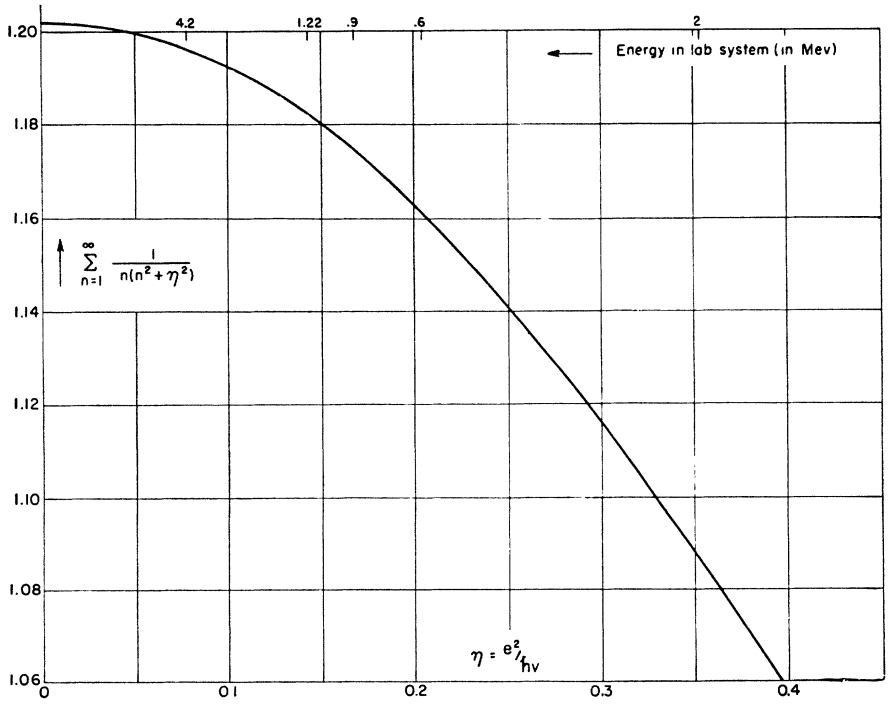


FIG. 14. Auxiliary summation occurring in $h(\eta)$ as a function of $\eta$. The limiting value of the summation as $\eta$ vanishes is $\Sigma_1^\infty n^{-3}=1.202$.

[27] R. R. Wilson and E. C. Creutz, Phys. Rev. **71**, 339 (1947), referred to as WC.
[28] R. R. Wilson, Phys. Rev. **71**, 384 (1947); see also reference 31.
[29] R. E. Peierls and M. A. Preston, Phys. Rev. **72**, 250 (1947).
[30] L. L. Foldy, Phys. Rev. **72**, 125, 731 (1947).

plotted. The errors indicated are due to statistics only (about 2 percent) and are therefore likely to be an underestimate. It is seen that the over-all variation of 10 percent in the normalizing values for the cross section at 90 degrees produces a change in the relative position of the points that is small compared to their statistical uncertainties. The two dotted lines indicate possible extremes ($-0.80$ and $-0.12$ degree) in the value of $\delta_1$, while the solid line, giving some sort of average fit, implies $\delta_1 \simeq -0.5$ degree. The analysis given here shows that (1) the data are sufficiently uncertain to make any detailed interpretation doubtful; (2) the data, assuming no unknown systematic errors, imply a small repulsive potential in the $^3P$-state (or else a small attractive $^1D$-potential, since for the angular region in question, a $D$-wave fit would give just as good agreement as a $P$-wave (see Section V)); (3) the value of the $P$-wave phase shift found here is more in accord with Foldy's value than that of Preston and Peierls; however, the difference is within the experimental errors.

WLRWS.—Wilson, Lofgren, Richardson, Wright, and Shankland[31] have made measurements at 14.5 Mev. Their measurements were absolute in nature, but relatively inaccurate. The point at 90 degrees was determined with more precision; accordingly it was used to evaluate the $S$-wave phase shift. It is seen from Table VII that the uncertainty in the phase shift is quite large.

## VII. THE DETERMINATION OF THE EXPANSION PARAMETERS FROM THE EXPERIMENTAL DATA

In the definition of **K** (1.1) the function $h(\eta)$ was not defined. The definition of $h(\eta)$ is:

$$h(\eta)=Re\frac{\Gamma'(-i\eta)}{\Gamma(-i\eta)}-\ln\eta. \tag{7.1}$$

Here $Re$ stands for the real part of the logarithmic derivative of the $\Gamma$-function. The function $h(\eta)$ is shown plotted against energy in the laboratory system in Fig. 13. For more accurate work $h(\eta)$ can be written in the form:

$$h(\eta)=-\ln\eta-0.5772\cdots+\eta^2\sum_{n=1}^{\infty}\frac{1}{n(n^2+\eta^2)}, \tag{7.2}$$

where $0.5772\cdots$ is Euler's constant. The sum in (7.2) is plotted as a function of $\eta$ in Fig. 14. This sum is a slowly varying function of energy, and for energies over 200 kev enters only as a small correction term. Thus formula (7.2) in conjunction with Fig. 14 gives considerably more accuracy than is necessary considering the uncertainties in the experimental data.

The values of **K** (1.1) determined from the experimental data were given in Table VII. These values are plotted against $k^2$ (i.e., against energy) in Fig. 15 (Van de Graaff data) and Fig. 16 (cyclotron data). It is obvi-

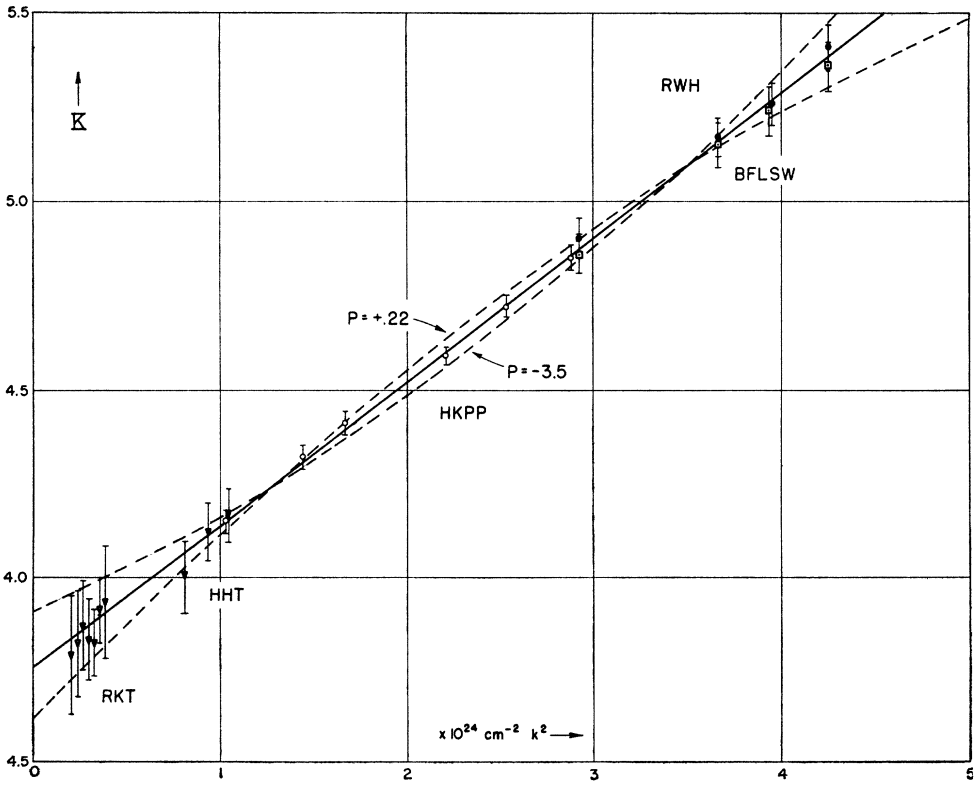


FIG. 15. The experimental values of **K** plotted *vs.* $k^2=1.20(5)\times10^{24}E$ (Mev) cm$^{-2}$ for the Van de Graaff data. The best linear approximation is shown, along with two parabolic fits to the data. The experimental points lie very closely along the straight line. ▽RKT, ▽HHT, ⊙HKPP, ⊡BFLSW, ●RWH.

[31] Wilson, Lofgren, Richardson, Wright, and Shankland, Phys. Rev. **72**, 1131 (1947), referred to as WLRWS.

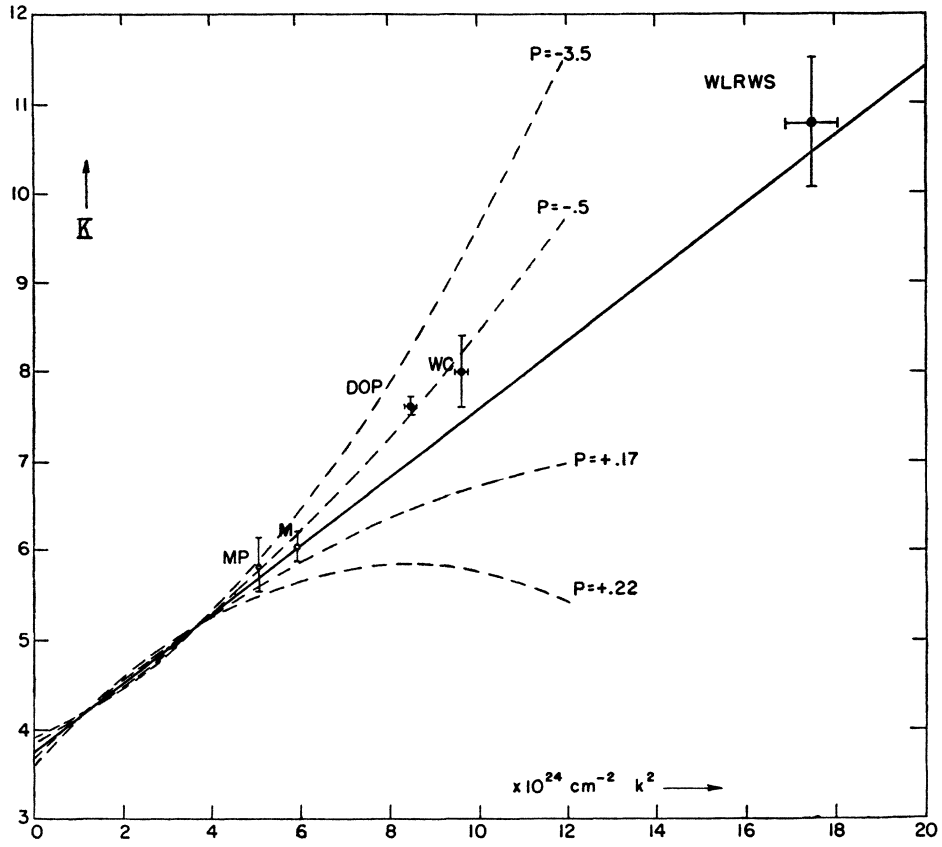


FIG. 16. The experimental values of **K** for the cyclotron data plotted *vs.* $k^2$, with the best linear and several parabolic fits to the Van de Graaff data extrapolated. The cyclotron data favor a negative value for the well shape parameter $P$.

ous from Fig. 15 that the Van de Graaff data allow an extremely good straight line fit. The best straight line is drawn in on the figure. Its parameters, as determined by a least squares analysis with proper weighting of the data according to the probable errors given in Table VIIa, are:

$$\begin{aligned} -R/a &= 3.755 \pm 0.024, \\ a &= -7.67 \pm 0.05 \times 10^{-13} \text{ cm}, \\ (\tfrac{1}{2})Rr_0 &= 0.382 \pm 0.010 \times 10^{-24} \text{ cm}^2, \\ r_0 &= 2.65 \pm 0.07 \times 10^{-13} \text{ cm}. \end{aligned} \tag{7.3}$$

Since the data of Heydenburg, Hafstad, and Tuve[19] show evidence of systematic deviation from the slope of the **K** *vs.* $k^2$ curve, it is of interest to determine the best linear fit to the data omitting the HHT points. When such a fit is made, the resulting values for the coefficients are:

$$\begin{aligned} -R/a &= 3.757, \\ \tfrac{1}{2}Rr_0 &= 0.381 \times 10^{-24} \text{ cm}^2. \end{aligned}$$

These values are seen to be almost exactly the same as those given in (7.3).

Having determined the best values of the coefficients in the expansion (1.2) for the shape-independent approximation, it is pertinent to ask just how much the data delimit the shape of the nuclear potential. The seemingly obvious method to answer this question is to make a least squares fit to the data with a polynomial of higher order in $k^2$ than the linear approximation, and thus determine higher coefficients in the expansion which are sensitive to potential shape. However, the probable errors of the data are so large that such a determination has doubtful significance. One must therefore resort to a somewhat less direct method of approach. For that purpose we assumed that the terms in $k^6$ and higher powers of $k$ in (1.2) do not contribute appreciably to the value of **K**. The one remaining shape-dependent parameter, $P$, was then assigned various values and least squares fits were made to the data. Two typical "best fit" parabolas are shown in Fig. 15. These two parabolas, with $P=+0.22$ and $-3.5$, appear to be excluded by the experimental data. The large asymmetry in the values of $P$ for curves which appear essentially as mirror images of each other in the $P=0$ curve (straight line) is due to the fact that the quantity in the expansion (1.2) which determines the curvature is $Pr_0^3R$, not $P$. For $P$ negative, the "best" value of $r_0$ is smaller than for $P=0$; for $P$ positive, it is larger than for $P=0$. Hence, to give the same value of $|Pr_0^3R|$, $|P|$ will be much larger for negative $P$ ($r_0$ is smaller) than for positive $P$ ($r_0$ larger).

The cyclotron data are plotted in Fig. 16. The point of Meagher at 4.9 Mev is reasonably accurate and is seen to lie on the extrapolated best linear fit to the Van de Graaff data; it might have been used in the least squares analysis above. However, the other points (ex-

cept the DOP point at 7 Mev) are rather inaccurate, and it was felt that until the accuracy of the data obtained with cyclotrons is improved, all cyclotron data should be consistently excluded from the least squares analysis. The peculiarities of the DOP point will be examined below.

In spite of its relatively poor accuracy, the cyclotron data can be used in a qualitative way to narrow the limits on $P$ somewhat. In Fig. 16, in addition to the best linear fit to the Van de Graaff data extrapolated to higher energies, several "best fit" (to the Van de Graaff data) parabolas are shown for comparison. The cyclotron data are seen to exclude any large positive value of $P$, and perhaps any positive value of $P$. They are also seen to exclude negative values of $P$ as large (negatively) as 3.5. In fact, except for the DOP point at 7 Mev, these data seem to exclude negative $P$'s appreciably greater than 0.5. The DOP point, on the contrary, implies that negative values of $P$ less (in absolute value) than 0.5 should be excluded. If we neglect the WLRWS point at 14.5 Mev for a moment, we see that the other cyclotron points are not inconsistent with the DOP point, although full use must be made of the probable errors on both the Meagher point and the DOP point to give agreement.

In this connection it should be remarked that the limits of uncertainty on the Meagher point are conservatively large. The charge measurement in this experiment was made in two ways (resistor method and capacitor method), the measurements differing by 1.3 percent. The capacitor value is believed to be more reliable; accordingly, we use that value here. However, the uncertainty given is sufficient to include both points and their extremes in uncertainty, and so can be considered as an overestimate of the error if anything. With this generous error estimate the Meagher point and the DOP point are just barely consistent with each other.

If the trend indicated by the DOP point (i.e., a rather large negative value for $P$) were correct, the nuclear interaction would be more compact (in some sense) than a square well potential (see Section XI for the variation of $P$ with potential shape)—a not completely unreasonable possibility with velocity-dependent forces. We prefer to wait for more experiments and to conclude meanwhile only that the value of $P$ is probably less negative than $-0.8$ or so, and probably not more positive than $+0.15$.

For each assumed value of $P$ within a reasonable range ($+0.2$ to $-1.0$, say) one gets "best" values for the scattering length $a$ and the effective range $r_0$ by a least squares fit. The values of $a$ and $r_0$ can deviate around their "best" values somewhat without destroying the fit to the data entirely. For example, for $P=0$ (shape-independent approximation) the possible deviations are given in (7.3) by the probable errors attached to $a$ and $r_0$. One therefore gets an allowed region on a plot of $a$ *vs.* $P$ and also on a plot of $r_0$ *vs.* $P$. These are shown in Fig. 17 and Fig. 18 respectively. The arrows indicate that the deviations from the most probable value are correlated, i.e., if one picks a scattering length somewhat smaller (more negative) than the best fit, the corresponding effective range is somewhat larger than the best fit.

It will be seen from Figs. 17 and 18 that the best values of $a$ and $r_0$ depend considerably on the value assumed for $P$. In that sense the linear (two term) approximation to the series (1.2) is not really shape independent (since $P=0$ in itself implies a certain shape of potential). The reason for this behavior is the fact that there are no data at all at zero energy (unlike neutron-proton scattering, where the best data are at zero energy and at the negative energy corresponding to the binding energy of the deuteron), and there are only very inade-

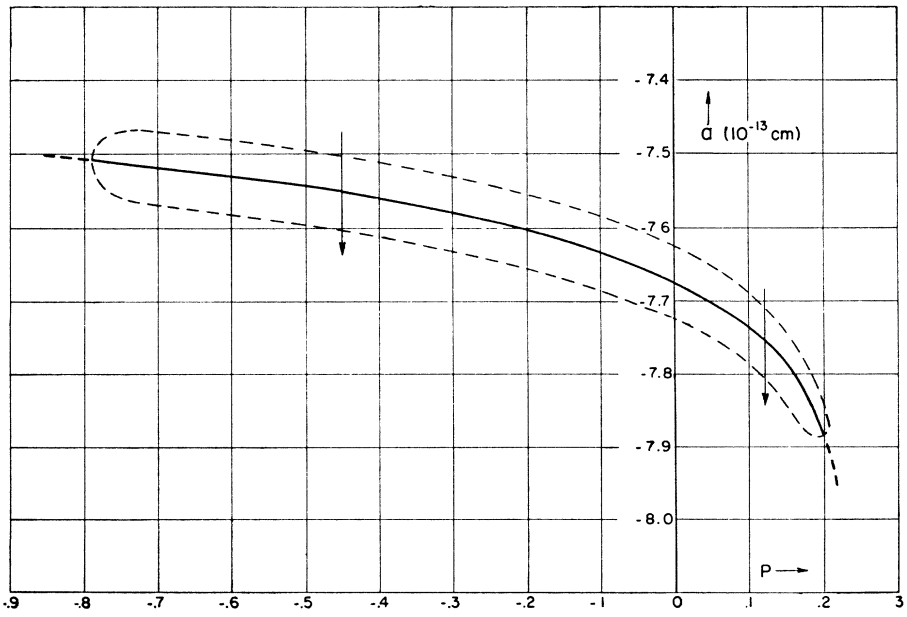


FIG. 17. Ordinate, $a$; abscissa, $P$. Values of the scattering length $a$ implied by experiment (Van de Graaff data) as a function of the well shape parameter $P$. The linear approximation to $\mathbf{K}(P=0)$ implies $a=-7.67 \pm 0.05\times10^{-13}$ cm.

quate data at energies lower than 800 kev. From that point of view it might have been advantageous to expand $\mathbf{K}$ in a power series in the energy centered around 2 Mev, say, rather than about zero energy. The two term approximation to a series centered around 2 Mev would really be shape-independent i.e., the coefficients of these two terms would then not depend upon the shape of the well (the value of $P$). However, even though at present the best data are in the region between one and three Mev, there is no reason why very good data cannot be taken at lower and higher energies. If and when this is done, the choice of 2 Mev as the center point in an expansion of $\mathbf{K}$ will be just as arbitrary (and more tedious from a computing point of view) than the zero energy center chosen here.

As an aid to planning future experiments it is of interest to know how sensitive the function $\mathbf{K}$ is to errors in cross section and energy measurements at various scattering angles and energies. For that purpose the quantities $E(\partial\mathbf{K}/\partial E)_\sigma$ and $\sigma(\partial\mathbf{K}/\partial\sigma)_E$ have been computed for the energy range up to 10 Mev. These derivatives, when multiplied by the relative error in $E$ and $\sigma$ respectively, give directly the resulting error in $\mathbf{K}$. The phase shift $\delta_0$ enters these derivatives. As was done for $p_1(\theta)$ etc., the linear approximation to $\mathbf{K}$ given by (4.8) was used to determine $\delta_0(E)$ over the energy range in question. This will not lead to appreciable error in the results. The quantities $E(\partial\mathbf{K}/\partial E)_\sigma$ and $\sigma(\partial\mathbf{K}/\partial\sigma)_E$ are shown in Figs. 19 and 20 for various scattering angles as functions of the energy.

The curves in both figures all show a characteristic behavior with energy. The curves of $E(\partial\mathbf{K}/\partial E)_\sigma$ are very similar to those of $\sigma(\partial\mathbf{K}/\partial\sigma)_E$, but with a constant displacement upward. At a given angle, $\sigma(\partial\mathbf{K}/\partial\sigma)_E$ decreases with energy to a minimum, then increases rapidly to infinity at a certain energy. Above that energy the function decreases in absolute value from minus infinity, has another minimum, and then increases (negatively) in a regular fashion.

The infinite value of $\sigma(\partial\mathbf{K}/\partial\sigma)_E$ (or of $E(\partial\mathbf{K}/\partial E)_\sigma$) at a certain energy does not mean that the value of $\mathbf{K}$ is infinitely sensitive to errors in cross section (or energy) at that energy. Rather, it means that the error in $\mathbf{K}$ will be of the order of the *square root* of the relative error in cross section (or energy). This can be seen readily when one considers the cross section as a function of energy and phase shift. At the singularities in $\sigma(\partial\mathbf{K}/\partial\sigma)_E$ the cross section can be shown to be insensitive to first-order changes in the phase shift, depending only upon second-order variations i.e., $\Delta\sigma\sim(\Delta\delta_0)^2$. This means that $\sigma$ is insensitive to first-order variations in $\mathbf{K}$ (since $\mathbf{K}$ is a function of $\delta$ and $E$), and hence $\Delta\sigma\sim(\Delta\mathbf{K})^2$. In consequence, the curves cease to have more than qualitative meaning in the immediate neighborhood of their singularities. Investigation shows that for the $\theta=90°$ curve the region of non-validity is confined to an energy range of $\pm 15$ kev about the singularity if the relative error in cross section is less than 10 percent, or $\pm 10$ kev, if the relative error is less than 5 percent. Measurements are not likely to be made at exactly the energies and angles corresponding to these singularities because of the very high accuracy necessary to get useful data. Hence the fact that the curves are not valid in the immediate neighborhood of these points is no serious drawback.

One interesting point is the behavior of $\sigma(\partial\mathbf{K}/\partial\sigma)_E$ at scattering angles near 90° at energies around 400 kev.

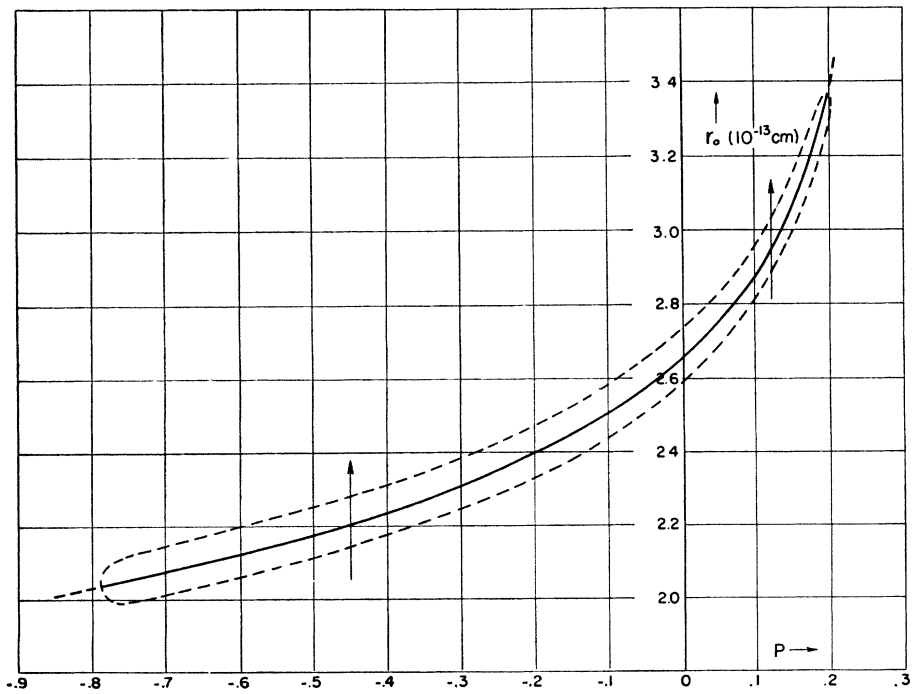


FIG. 18. Ordinate, $r_0$; abscissa, $P$. Values of the effective range $r_0$ implied by experiment (Van de Graaff data) as a function of the well shape parameter $P$. The linear approximation to $\mathbf{K}(P=0)$ implies $r_0=2.65\pm0.07\times10^{-13}$ cm.

This energy range is where the interference between Coulomb and nuclear scattering produces the pronounced minimum in the scattering. Exactly at the minimum ($\sim$400 kev) the value $\sigma(\partial\mathbf{K}/\partial\sigma)_E$ at 90° becomes infinite. But on either side of the minimum it has a very small absolute value. This means that on either side of the interference minimum a very precise value of $\mathbf{K}$ could be determined with reasonable experimental uncertainties. Long ago, Breit, Thaxton, and Eisenbud[1] arrived at what amounts to the same conclusion from a different point of view. Measurements exactly at the minimum (or within five or ten kev of it) are not useful because of the fact that (1) the errors in $\mathbf{K}$ will be proportional to the square root of the relative error in $\sigma$ (2) the differential cross section itself is extremely small (a few millibarns per steradian) so that accuracy of any sort is very difficult to attain.

Since a very accurate determination of $\mathbf{K}$ in the low energy region seems both possible and desirable, it is worth while to discuss some of the considerations which enter into the planning of such an experiment. First of all, with present day machines with very good voltage control, it is not too difficult to keep the error in the voltage of the beam low enough so that it does not influence the value of $\mathbf{K}$ appreciably. A voltage controlled to $\pm$0.1 percent is adequate for that purpose (Fig. 19 shows that the resultant uncertainty in $\mathbf{K}$ is about $\pm$0.005 which is quite small compared to the errors on the values in Table VII). Second, it is not possible to eliminate certain systematic errors in the calibration of the yield of the apparatus; in particular, the calibration of the current to much better than $\pm$1 percent seems to present great experimental difficulties. This implies that one should take measurements at energies $E$ not too far removed from the energy $E_{\min}$ of the interference minimum, in order to take full advantage of the small values of $\sigma(\partial\mathbf{K}/\partial\sigma)_E$ in that region. Third, the scattering cross section near the minimum energy is very small so that one encounters difficulties due to the low counting rate and due to in-scattering from angles of scattering different from 90° (since the scattering cross section is much larger at these other angles). This implies that one should stay away from $E_{\min}$ as much as possible. Clearly, the second and third points narrow down the useful energy region to two strips at somewhat lower and somewhat higher energy than the interference minimum. There remains the choice of going either higher or lower in energy than $E_{\min}$. It appears that the behavior of the cross section as a function of angle implies that one should go to energies somewhat *above* $E_{\min}$, since there the differential cross section is rather flat around $\theta=90°$, whereas it rises rapidly on both sides of 90° at energies below $E_{\min}$. Hence in-scattering ought to be a much less serious effect at the higher energies, allowing one to use wider slits and correspondingly greater counting rates. In view of all these considerations, we would like to recommend measurements of 90° scattering in the energy region 420–450 kev with an energy definition of $\pm$0.1 percent and an over-all error in cross section around $\pm$1 percent. In view of the fact that no effects due to waves of higher angular momentum have been found at considerably larger energies, an angular distribution measurement seems to be an unnecessary luxury here.

Figure 15 shows that a very accurate point around 400 kev would narrow down the possible values of the shape-parameter $P$ considerably. Furthermore, it would make the variation of $a$ and $r$ with the choice of $P$ much less pronounced, i.e. the two-term approximation to the series (1.2) would become much more shape-independent.

Breit, Broyles, and Hull[11] have given arguments for accurate measurements in that same energy region. They claim that such a measurement, in conjunction with the data at higher energies, will allow one to say something quite definite about the shape of the well. In their paper they present the picture that the repulsive Coulomb field shields the central part of the attractive nuclear potential for low energies, and the observed scattering should be sensitive to the strength of the "tail" of the potential.

To examine this idea, let us consider the quantity of interest in this regard, namely the ratio of the range $b$ of the nuclear forces to the characteristic distance $R$ for the electrostatic repulsion. If $(b/R)$ is very small, the nuclear potential acts only in the region where the Coulomb potential varies too rapidly to have a large effect on the detailed behavior of the wave function (i.e., the WKB approximation for the wave functions in a pure Coulomb potential fails in the significant region). For distances much smaller than $R$, the Coulomb wave functions behave very similarly to the wave functions without the Coulomb field except for the constant penetration factors in front (see Appendix III). Consequently, one cannot speak of the Coulomb potential "shielding" all but the tail of the nuclear potential at low enough energies *unless* the tail of the potential is appreciable at distances of order $R$. The usual potential shapes simply do not have tails extending that far out. Hence the Coulomb field "shields" all the potential, or none of it.

For example, Breit, Broyles, and Hull find that with an experimental accuracy of one percent in scattering one could detect a lump of potential $(e^2/mc^2)$ wide of strength 1 kev at a distance of 5 $(e^2/mc^2)$, and of strength 10 kev at 3 $(e^2/mc^2)$. For comparison, we examine the corresponding strength of a Yukawa potential (the longest-tailed of the conventional well shapes) at these distances. At $5(e^2/mc^2)$, the Yukawa potential giving the best fit to the experimental data has a value of about $2\times10^{-2}$ kev; at $3(e^2/mc^2)$ it has a value of about 4 kev. The ratios of actual to detectable potential in this case are approximately 1/50 and $\frac{1}{2}$ at the two distances quoted. Actually, one should compare differences of potentials for various shapes. This would make the comparison even worse.

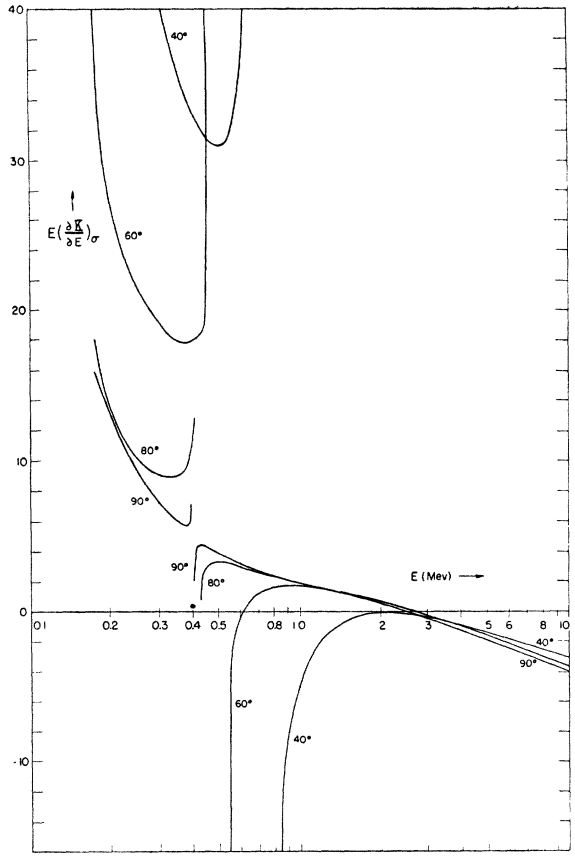


FIG. 19. Ordinate, $E(\partial \mathbf{K}/\partial E)_\sigma$; abscissa, $E$. The function $E(\partial \mathbf{K}/\partial E)_\sigma$ plotted as a function of the energy in the laboratory (in Mev) for various scattering angles in the center-of-mass system. Multiplication by the relative uncertainty in energy gives directly the uncertainty implied in $\mathbf{K}$, assuming the cross section is known exactly.

Breit, Broyles, and Hull do point out that the presence of the interference minimum is also a factor contributing to the increased sensitivity of the low energy region. From the analysis given here, this is the only effect which can (and does) make it advantageous to perform measurements near 400 kev.

If, and when, such measurements are made, the value of $\mathbf{K}$ at 400 kev should be known to much higher accuracy than at one or two Mev. Then the measurement at 400 kev will provide a fulcrum, so to speak, around which a $\mathbf{K}$ *vs.* $k^2$ plot will turn; but this measurement will not determine the shape of the well to any appreciable extent. Rather, one will need to have measurements over a wider range of energies, at least up to 7 or 8 Mev, before the curvature of the $\mathbf{K}$ *vs.* $k^2$ plot (i.e., the value of $Pr_0^3$) can be determined with sufficient accuracy to say something about the shape of the potential well. The main advantage of accurate measurements at very low energies e.g., near 400 kev is that they will allow a more accurate determination of the effective range, so that a determination of the curvature ($Pr_0^3$) by means of all the data will imply a closer evaluation of the shape-parameter $P$ itself.

Breit *et al.* point out that in order to determine four parameters from the data it is necessary to have two regions of sensitivity, and recommend measurements near 400 kev plus measurements above 10 Mev for this purpose. However, the analysis presented here indicates that to determine even three parameters with any accuracy measurements must be made over an energy range wide enough to bring out the curvature (or lack of it) in the $\mathbf{K}$ *vs.* $k^2$ plot. In any event, the recommendations to the experimentalists made here are in full agreement with those made by Breit, Broyles, and Hull, even though the opinions as to detailed interpretation differ somewhat.

## VIII. LANDAU-SMORODINSKY RESULT AND AN APPROXIMATE RELATION BETWEEN THE NEUTRON-PROTON AND THE PROTON-PROTON SCATTERING LENGTHS

Before describing the variational derivation of the expansion of $\mathbf{K}$ (1.2), it is worth while, because of the qualitative understanding gained, to examine the Landau-Smorodinsky result for the energy independent approximation to (1.2) and to make a simple extension of their result in order to relate the neutron-proton singlet scattering length to the proton-proton scattering length for the same nuclear potential.

Outside the range of nuclear forces, the wave function of the system of two protons satisfies the Schrödinger equation for a pure Coulomb potential. The partial wave of zero angular momentum satisfies:

$$[-(d^2/dr^2)+(1/Rr)]\varphi(r)=k^2\varphi(r), \tag{8.1}$$

where $\varphi(r)=r\psi_0(r)$; $R$ was defined in connection with the expansion (1.2); and $k^2=2mE/\hbar^2$ is the square of the relative wave number. The wave function $\varphi(r)$ for the region outside the range of the nuclear force can be written as

$$\varphi(r)=G(r)+\cot\delta F(r), \tag{8.2}$$

where $G(r)$ and $F(r)$ are the irregular and regular solutions of the equation (8.1) describing two charged particles in an $S$-state under electrostatic interaction only. They go over into sines and cosines in the absence of the Coulomb field (i.e., as $R\rightarrow\infty$). These solutions have been treated by Yost, Wheeler, and Breit[32] and others, and are considered in some detail in Appendix III where an expansion in powers of the energy is obtained for $G(r)$ analogous to that deduced by Beckerley[33] for $F(r)$. $\delta$ is interpreted as the phase shift in $\varphi(r)$ caused by the specifically nuclear force, i.e., the $S$-wave phase shift used in the preceding sections.

For small values of $r$ and low energies ($kr\ll 1$ and

[32] Yost, Wheeler, and Breit, Phys. Rev. **49**, 174 (1936).
[33] J. G. Beckerley, Phys. Rev. **67**, 11 (1945).

$r \ll R$), $F(r)$ and $G(r)$ become (see Appendix III):

$$F(r)=Ckr(1+r/2R+\cdots),$$
$$G(r)=1/C[1+(r/R)(\ln(r/R)+2\gamma-1+h(\eta))+\cdots], \quad (8.3)$$

where

$$C^2=\frac{2\pi\eta}{e^{2\pi\eta}-1} \quad (8.4)$$

is the Coulomb penetration factor and can be interpreted as the relative probability of finding two protons together compared with the probability of finding two uncharged particles together, other things being equal. $h(\eta)$ is given by (7.1), and $\gamma=0.5772\cdots$ is Euler's constant. In the absence of the Coulomb field $C^2=1$, $R=\infty$; and $F(r)$ and $G(r)$ in (8.3) go over into the first terms in the expansions of $\sin(kr)$ and $\cos(kr)$, namely $kr$ and 1 respectively.

Landau and Smorodinsky proceed to match the logarithmic derivative of the wave function inside the nuclear potential with the logarithmic derivative of $\varphi(r)$ (8.2) at the boundary of the nuclear potential. $r$ times the logarithmic derivative of $\varphi(r)$ at $r=r_0$ (range of the nuclear force) is:

$$f(r_0)\equiv r_0\frac{\varphi'(r_0)}{\varphi(r_0)}\simeq(kr_0)C^2\cot\delta + (r_0/R)(\ln(r_0/R)+2\gamma+h(\eta)), \quad (8.5)$$

where terms of order $(kr_0)^2$ and $(r_0/R)^2$, etc., have been neglected. The logarithmic derivative of the wave function inside $r=r_0$ is nearly independent of energy for low energies at least, since the strength of the nuclear potential is much greater than the kinetic energy outside the range of nuclear forces. Therefore, $f(r_0)$ inside is approximated by its value $f_0$ at $E=0$. Putting (8.5) equal to $f_0$ and dividing by $r_0$ leads to:

$$kC^2\cot\delta+1/R[\ln(r_0/R)+2\gamma+h(\eta)]\simeq f_0/r_0. \quad (8.6)$$

Use is made of the relation $2k\eta R=1$, and the singlet proton-proton scattering length $a_P$ is defined by:

$$a_P^{-1}\equiv -f_0/r_0+1/R[\ln(r_0/R)+2\gamma]. \quad (8.7)$$

The result (8.6) can then be written as:

$$\mathbf{K}\equiv(\pi\cot\delta)/(e^{2\pi\eta}-1)+h(\eta)\simeq -R/a_P. \quad (8.8)$$

(8.8) is the result obtained by Landau and Smorodinsky, and served as the basis of their analysis of the experimental data. The form (8.8) is seen to be the same as the expansion (1.2) in the limit of zero energy.

As was mentioned in Section I, Landau and Smorodinsky found that the "constant" $a_P^{-1}$ was experimentally very nearly a linear function of the energy (see Fig. 15), and interpreted this correctly as meaning that a range correction was necessary. They also showed that *there will be a stable di-proton if and only if the proton-proton scattering length is positive.* The fact that $a$ is actually negative implies that there cannot be any stable $He^2$ in nature. The beauty of this argument lies in the fact that nothing need be assumed about the nuclear forces except the experimentally known parameter $a$.

The neutron-proton formula equivalent to (8.6) is:

$$f/r_0=k\cot\delta\simeq -a_N^{-1}+\tfrac{1}{2}rk^2+\cdots$$

so that the neutron-proton scattering length $a_N$ is defined by:

$$a_N^{-1}\equiv -f_N/r_0, \quad (8.9)$$

where $f_N/r_0$ is the logarithmic derivative of the zero energy neutron-proton wave function at $r=r_0$ (formally (8.9) can be obtained from (8.7) by letting $R\to\infty$). As a very crude approximation one would expect that the Coulomb field would have a negligible effect on the wave function so that one could substitute $f_N$ for $f_0$ in (8.7) to get an approximate relation between the two scattering lengths. However, the terms in $R^{-1}$ in (8.7) are first-order effects due to the Coulomb field so that it is necessary to include the first-order change in the logarithmic derivative as well.

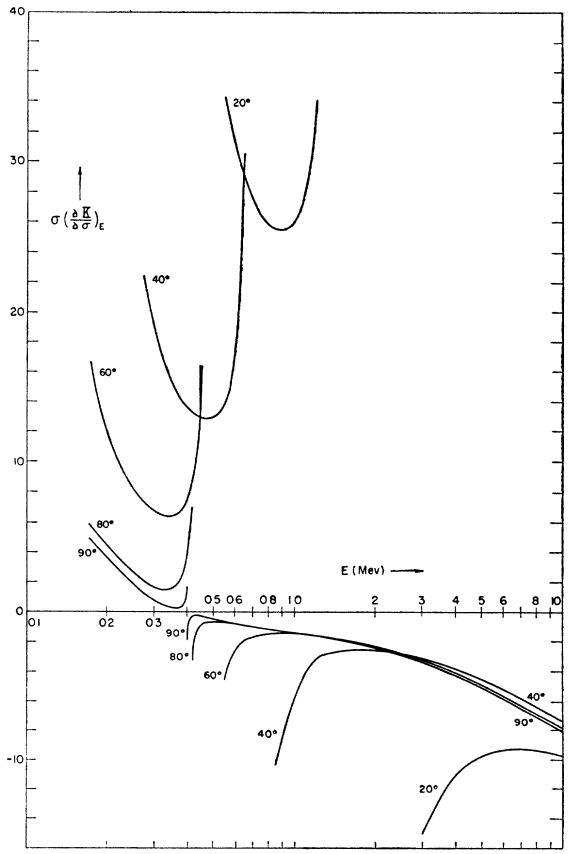


FIG. 20. Ordinate, $\sigma(\partial\mathbf{K}/\partial\sigma)_E$; abscissa, $E$. The function $\sigma(\partial\mathbf{K}/\partial\sigma)_E$ as a function of the energy in the laboratory (in Mev) for various scattering angles in the center-of-mass system. Multiplication by the relative uncertainty in cross section gives directly the uncertainty implied in $\mathbf{K}$, assuming the energy is known exactly.

The first-order change in the logarithmic derivative at $r=r_0$ due to a change in potential is (see Section X):

$$u^2(r_0)\frac{\partial}{\partial\epsilon}\left[\frac{f(r_0)}{r_0}\right]=-\int_0^{r_0}W'(r)u^2(r)dr,$$

where $u(r)$ is the wave function inside the range of nuclear forces in the absence of the Coulomb field, and the (attractive) potential is changed from $W(r)\rightarrow W(r)+\epsilon W'(r)$. $W(r)=(-2m/\hbar^2)V(r)$. If the Coulomb potential is switched on, in addition to the nuclear potential, then $W(r)\rightarrow W(r)-1/Rr$, that is, $\epsilon=1/R$ and $W'(r)=-1/r$. It is assumed that the nuclear potential stays the same, i.e., the comparison is between scattering lengths for a given nuclear potential in the absence and presence of the Coulomb potential. Consequently, the logarithmic derivative in the proton-proton case is approximately:

$$\frac{f_0(r_0)}{r_0}\simeq\frac{f_N(r_0)}{r_0}+\frac{1}{R}\frac{\partial}{\partial\epsilon}\left[\frac{f(r_0)}{r_0}\right]+\cdots,$$

where the quantities on the right-hand side involve the neutron-proton wave function. To evaluate $\partial/\partial\epsilon[f(r_0)/r_0]$ exactly one must know the wave function for the neutron-proton system inside the range of nuclear forces. However, one can obtain a reasonable approximation by using $u\simeq\sin(\pi r/2r_0)$ (this expression is exact for a square well potential with a depth such that $a_N^{-1}=0$; i.e., resonance at zero energy). The result is:

$$\partial/\partial\epsilon[f(r_0)/r_0]\simeq\tfrac{1}{2}[\ln\pi+\gamma-Ci(\pi)]=0.824,$$

where $Ci(x)$ is the cosine integral. Thus the logarithmic derivative is given by:

$$\frac{f_0(r_0)}{r_0}\simeq-a_N^{-1}+\frac{1}{R}(0.824).$$

The proton-proton scattering length $a_P$ (8.7) is:

$$\begin{aligned}a_P^{-1}&\simeq a_N^{-1}+1/R[\ln(r_0/R)+2\gamma-0.824]\\&\simeq a_N^{-1}+1/R[\ln(r_0/R)+0.330],\end{aligned}\qquad(8.10)$$

where $a_N$ is the corresponding neutron-proton scattering length for the same nuclear potential, and $r_0$ is the "range" of the nuclear force. Estimates show that this relation (8.10) is valid to within about 2.5 percent for the commonly assumed potentials which fit the proton-proton scattering data (see Section XI). The values obtained for $a_P$ are low in absolute value by about 2.5 percent for the square well, and high in absolute value by the same amount for the Yukawa well. For these numerical estimates the value of $r_0$ was taken to be equal to the effective range of the potential as defined in Eq. (9.6).

Bethe[8] has obtained a relation quite similar to (8.10) from somewhat different considerations, based on the fact that at some distance of the order $\frac{1}{2}b$ the logarithmic derivatives of the proton-proton wave function and the neutron-proton wave function are equal.

Chew and Goldberger[8] have given a more exact relation than (8.10) taking into account higher order changes due to the Coulomb field. When more accurate estimates of the scattering lengths are needed, one must resort to their formula, or to the results of Section XI. However, (8.10) allows a rapid comparison of scattering lengths and is useful as a first approximation.

The fact that an approximation for $a_P$ accurate to only a few percent is at all useful is connected with the closeness of the scattering to a "resonance at zero energy" ($a_P^{-1}=0$). The value of $a_P$ is large compared to the range of the forces. In consequence, a small change in the force strength implies a large change in the scattering length. Conversely, an error of a few percent in the comparison of scattering lengths for proton-proton and neutron-proton (singlet) scattering implies an error of only a few tenths of a percent in the comparison of the force-strengths.

## IX. DERIVATION OF THE EXPANSION (1.2)†

Since a detailed derivation of the Schwinger variational method for scattering problems has been given in our earlier paper on neutron-proton scattering,[6] it will suffice to restrict the presentation to the special features which show up when the method is applied to proton-proton scattering. We assume only $S$-wave nuclear scattering in addition to the Coulomb interaction. The quantity of interest is the nuclear scattering. Accordingly, the asymptotic wave function $\varphi(r)$ (outside the range of the nuclear force) will be a linear combination of the Coulomb wave functions $F(r)$ and $G(r)$ given by Eq. (8.2), where $\delta=\delta_0$ is the $S$-wave *nuclear* phase shift.

Equation (8.2) is valid only outside the range of the nuclear force. Actually, $u(r)$ ($r$ times the $S$-state radial wave function) satisfies the equation:

$$(-d^2/dr^2-k^2+1/Rr)u(r)=W(r)u(r),\qquad(9.1)$$

where $k^2=(2mE)/\hbar^2$ is the square of the relative wave number in the center-of-mass system, $R=\hbar^2/(Me^2)=2.88(15)\times10^{-12}$ cm, and $W(r)$ is related to the nuclear potential $V(r)$ through

$$W(r)=-(2m/\hbar^2)V(r)=-(M/\hbar^2)V(r),\qquad(9.2)$$

$M$ being the proton mass. $W(r)$ is assumed to approach zero rapidly outside the range $b$ of the nuclear force. In that limit, the right-hand side of (9.1) is zero, and the solution takes on the form (8.2).

In analogy with the derivation of formula (2.11) in reference 6, one introduces a Green's function $K(r,r')$ for the left-hand side of Eq. (9.1). $K(r,r')$ satisfies the equation

$$(-d^2/dr^2-k^2+1/Rr)K(r,r')=\delta(r-r')$$

† A simpler non-variational derivation is presented in Appendix IV. See an earlier footnote.

and is given by:

$$K(r, r') = (1/k)F(r_<)G(r_>),$$

where $r_<$ means the smaller of $r$ and $r'$, $r_>$ means the greater of $r$ and $r'$. The derivation then proceeds just as for neutron-proton scattering with sines and cosines replaced by $F(r)$ and $G(r)$, respectively. The resulting variational principle is:

$$k\cot\delta = \frac{\int_0^\infty W(r)u^2(r)dr - \int_0^\infty dr \int_0^\infty dr' W(r)u(r)K(r,r')W(r')u(r')}{\left[(1/k)\int_0^\infty W(r)u(r)F(r)dr\right]^2}. \tag{9.3}$$

Equation (9.3) is stationary with respect to first-order changes in $u(r)$, as can be shown by direct substitution.

It will be necessary to have expansions of the Coulomb wave functions in powers of $k^2$. The necessary definitions and formulas are given in Appendix III. The convention adopted is that all auxiliary functions defined in Appendix III approach unity as $r\to 0$. Furthermore, in the limit $R\to\infty$ and $\eta\to 0$ (i.e., in the limit of neutron-proton scattering) all these functions can be replaced by unity. Since the expansions for $F(r)$ and $G(r)$ must reduce in that limit to the well-known power series expansions for $\sin(kr)$ and $\cos(kr)$, respectively, this gives a simple way of checking these more complicated expressions.

The variational principle (9.3) can be used to obtain a simple expression such as (1.2) for the energy dependence of the phase shift, $\delta$. To do this, the wave function $u(r)$ in (9.3) is replaced by a trial wave function $u_0(r)$ which is the correct expression for $u(r)$ at some particular energy, say $k_0^2$. Then the error in $k\cot\delta$ will be in the terms proportional to the square of the difference in the energies (i.e., in the coefficient of $(k^2-k_0^2)^2$) because of the stationary property of (9.3). It is most convenient to choose $u_0(r)$ appropriate to zero energy, and to expand (9.3) in powers of $k^2$, retaining the first two terms (since the terms in $k^4$ and higher are in error). This will be the linear (shape-independent) approximation discussed above.

The two independent solutions of the equation for a free particle at zero energy are 1 and $r$. The corresponding solutions for a particle of zero energy in a pure Coulomb field (i.e., solutions of Eq. (9.1) with $k^2=0$ and $W(r)=0$) are $H_1(r)$ and $rL_1(r)$ (see Appendix III). Hence the correct wave function (including the effect of the nuclear potential) at zero energy will behave in the "outside" region (beyond the range of the nuclear forces) like

$$u_0(r)\sim H_1(r)-(r/a)L_1(r)\equiv\varphi_0(r) \text{ for } r\gg b. \tag{9.4}$$

The quantity $a$ defined by this equation is the *proton-proton scattering length* which enters into the expansion (1.2). The solution $u_0(r)$ is substituted into (9.3), and the integrals are manipulated in a manner completely analogous to the derivation in reference 6. The resulting *two-term (shape-independent) approximation* is:

$$C^2k\cot\delta = -\frac{h(\eta)}{R}\frac{1}{a}+\tfrac{1}{2}r_0k^2+0(k^4), \tag{9.5}$$

where the *effective range* $r_0$ for proton-proton scattering is:

$$r_0\equiv 2\int_0^\infty [\varphi_0^2(r)-u_0^2(r)]dr, \tag{9.6}$$

in complete analogy with formula (3.9) of reference 6. Equation (9.5) clearly reduces to the first two terms of the expansion (1.2) ($2k\eta R=1$!). This result was first derived by Schwinger.[4]

The next step is to derive the expressions for the next two terms in the power series (1.2). Since (9.3) is a variational expression for $k\cot\delta$, an error of order $k^4$ in the trial wave function implies an error of order $k^8$ in the result. Hence we can obtain the terms to $k^6$ inclusive by the use of a trial wave function correct to order $k^2$ only. The non-variational derivation (see Appendix IV) of the expansion (1.2) would lead one to suspect that a knowledge of the wave function to order $k^{2n}$ gives the coefficients in (1.2) only up to the order $k^{2n+2}$, whereas actually it gives the coefficients up to order $k^{4n+2}$. This statement does not imply that these coefficients cannot be derived directly from the differential equation without variation principles. However, the derivation then involves integrations by parts which are not always obvious. The variational approach makes it perfectly evident that coefficients of order $k^{4n+2}$ and lower are expressible in terms of the wave function correct only to order $k^{2n}$, even though the detailed derivation is slightly more lengthy.

Unlike the work of reference 6, we shall not use the integral equation to iterate on the wave function. Rather, we will use the differential equation directly. The wave function $u(r)$ is written as an expansion in $k^2$:

$$u(r)=u_0(r)+k^2v_1(r)+k^4v_2(r)+\cdots, \tag{9.7}$$

where only the first two terms need be considered in order to obtain terms up to $k^6$ in the expansion (1.2). Substitution of (9.7) into the differential Eq. (9.1) and the equating of coefficients in $k^2$ leads to the differential equation for $v_1(r)$:

$$[-d^2/dr^2+1/Rr-W(r)]v_1(r)=u_0(r). \tag{9.8}$$

This equation must be solved (usually numerically) sub-

ject to the initial condition $v_1(0)=0$. The solution is then defined up to the addition of an arbitrary constant multiple of $u_0(r)$ which can be easily shown[6] to be equivalent to a change of normalization of the trial wave function and hence without influence on the final result. It is convenient to normalize $u(r)$ (i.e., $v_1(r)$ in this case) and it asymptotic form $\varphi(r)$ so that:

$$\varphi(r)=CG(r)+C\cot\delta F(r). \tag{9.9}$$

If we write:

$$\varphi(r)=\varphi_0(r)+k^2\chi_1(r)+k^4\chi_2(r)+\cdots, \tag{9.10}$$

then $\varphi_0(r)$ is given by (9.4) as before, while the asymptotic form of $v_1(r)$ is:

$$v_1(r)\sim\chi_1(r)\equiv\tfrac{1}{2}r_0rL_1(r)-\tfrac{1}{2}r^2M(r)+(r^3/6a)L_2(r). \tag{9.11}$$

In numerical integration of (9.8) the solution obtained will, in general, be of the form, asymptotically:

$$\chi_1(r)+A\varphi_0(r)=DH_1(r)+ErL_1(r) -\tfrac{1}{2}r^2M(r)+(r^3/6a)L_2(r).$$

From (9.4) and (9.11) it is apparent that the following relations hold:

$$A=D,\quad r_0/2=E+D/a. \tag{9.12}$$

Since $r_0$ has previously been determined by use of $u_0(r)$ in (9.6) and $a$ is known if $u_0(r)$ is known, the second relation (9.12) provides a valuable check on the results of the numerical integration for $v_1(r)$. The convenient normalization for $v_1(r)$ given by (9.9) and (9.11) is readily obtained by subtracting $A\varphi_0(r)$ from the result of the numerical integration.

In analogy to the derivation of the shape-independent approximation, the first two terms of (9.7) are substituted into (9.3) as an approximation to $u(r)$. Again use is made of the differential equations involved, integrations by parts are performed, and the numerator and denominator of (9.3) are expanded in powers of $k^2$ to terms of order $k^6$ inclusive. The result for the expansion is:

$$\mathbf{K}/R=C^2k\cot\delta+\frac{h(\eta)}{R} =-\frac{1}{a}+\tfrac{1}{2}r_0k^2-Pr_0^3k^4+Qr_0^5k^6, \tag{9.13}$$

where $a$ is defined by (9.4), $r_0$ is given by (9.6), and

$$Pr_0^3=-\int_0^\infty[\varphi_0(r)\chi_1(r)-u_0(r)v_1(r)]dr \tag{9.14}$$

and

$$Qr_0^5=\int_0^\infty[\chi_1^2(r)-v_1^2(r)]dr. \tag{9.15}$$

Equation (9.13) is seen to be just the expansion (1.2) for $\mathbf{K}$ (1.1) correct to terms in $k^6$ inclusive.

In reference 6 the expansion for $k\cot\delta$ and the variational parameters $a$ and $r_0$ were used to define an "intrinsic range" and a "well depth parameter" for the nuclear potential. A similar specification could be made here for the proton-proton system. However, the need for two sets of parameters to describe the same nuclear potential, depending upon whether the Coulomb field is switched on or off, is unnecessary and superfluous. In addition, a proton-proton range defined in analogy with the neutron-proton intrinsic range would not be an intrinsic property of the nuclear potential since another length would enter in, namely the characteristic length $R$ of the Coulomb field. Accordingly, we will use the conventions of reference 6 as to the specification of the nuclear potentials. It should be remembered that a well with well depth parameter $s=1$ does not lead to a zero energy resonance in proton-proton scattering (i.e., the proton-proton scattering length is not infinite). Rather, a well with $s=1$ would lead to a resonance at zero energy only in the absence of the Coulomb field.

## X. THE EFFECT OF SMALL CHANGES IN THE POTENTIAL ON THE EXPANSION PARAMETERS

Unlike neutron-proton scattering, the data in proton-proton scattering are sufficiently accurate and sufficiently easy to interpret (only one phase shift at low energies) so that the effective range and scattering length are known to a reasonable accuracy (see Section VII). Hence it is advantageous to make calculations with each potential well shape for only one choice of the intrinsic range $b$ and well depth parameter $s$, and to find $a$ and $r_0$ for slightly different choices of $b$ and $s$ by a perturbation calculation.

The variational principle (9.3) provides an easy means of getting the answer. Assume we know the wave function $u(r)$ appropriate to a potential $W(r)$. Now consider scattering due to the modified potential $W(r)+\epsilon W'(r)$ where $\epsilon$ is a small number. The correct wave function for this modified potential will differ from $u(r)$ by terms of order $\epsilon$. Since (9.3) is a variational expression for $k\cot\delta$, we will obtain $k\cot\delta$ correct to terms of order $\epsilon$ inclusive by substituting the unperturbed wave function $u(r)$ instead of the correct wave function. Hence we can get the first-order change of $k\cot\delta$ with a small change in the potential directly from the unperturbed wave function, by a process of quadratures only.

There is one caution to be observed here. The trial wave function which we are going to substitute in (9.3) differs from the true wave function for two reasons: (1) It is not correct for the energy in question, i.e., it will differ from the true $u(r)$ in the unperturbed potential by terms of order $k^{2n+2}$; (2) it is a wave function appropriate to the unperturbed potential rather than the perturbed potential, i.e., it differs from the true $u(r)$ by terms of order $\epsilon$. The error in $k\cot\delta$ will be of the order of the square of the error in the trial wave function, i.e., it will be of order

$$(k^{2n+2}+\epsilon)^2=k^{4n+4}+2\epsilon k^{2n+2}+\epsilon^2.$$

The occurrence of errors of order $\epsilon k^{2n+2}$ shows that a

wave function correct to order $k^{2n}$ will give the *change* of the variational parameters with small changes in the potential only up to the coefficients of $k^{2n}$, whereas it will give the parameters in the unperturbed potential ($\epsilon=0$) up to the coefficients of $k^{4n+2}$.

In particular, we have calculated numerical wave functions up to order $k^2$ inclusive (i.e., we know $u_0(r)$ and $v_1(r)$ in each case). Hence we can get $a$, $r_0$, $P$, $Q$ for the unperturbed potential, and $\partial a/\partial\epsilon$, $\partial r_0/\partial\epsilon$ for small changes in the potential. Since the terms with $P$ and $Q$ already are quite small corrections to the value of $\mathbf{K}$, this is not a serious shortcoming. The calculations of reference 6 have shown that $P$, at any rate, is a slowly varying function of the well parameters $s$ and $b$. Hence it is perfectly permissible to use the unperturbed values of $P$ and $Q$ for the perturbed potentials. This procedure will give much better accuracy than necessary for the interpretation of the experimental data.

It should be pointed out that the first-order changes in $a$ and $r_0$ due to a change in potential can be obtained directly from the differential equation, without variational methods, by considering the change in the logarithmic derivative of the wave function at large distances.[1]

By either of these methods we obtain the first-order variation in $\mathbf{K}$ (1.1) due to a change of potential $W(r)\rightarrow W(r)+\epsilon W'(r)$:

$$\partial\mathbf{K}/\partial\epsilon=-R\int_0^\infty W'(r)u^2(r)dr. \tag{10.1}$$

Using the expansion (9.7) of $u(r)$ in powers of $k^2$ and the expansion (1.2) for $\mathbf{K}$, we find that the changed coefficients $a'$ and $r_0'$ can be written as:

$$\begin{aligned} a'&=a-\epsilon a^2\int_0^\infty W'(r)u_0^2(r)dr,\\ r_0'&=r_0-4\epsilon\int_0^\infty W'(r)u_0(r)v_1(r)dr. \end{aligned} \tag{10.2}$$

We note that, in accord with the predictions based on the variational principle, to obtain the first-order changes in higher coefficients than $a$ and $r_0$ ($P$, $Q$, etc.) it would be necessary to have knowledge of higher terms in the expansion of $u(r)$ in powers of $k^2$.

Of particular interest are the variations in $a$ and $r_0$ due to changes in the well depth parameter $s$ and in the intrinsic range $b$ of the nuclear potential. $W(r)$ can be written for each well shape in the standard form:

$$W(r)=sb^{-2}f(r/b) \tag{10.3}$$

where $f(x)$ specifies the well *shape*. A change in the well depth parameter $s$ by an amount $\Delta s$ leads to a perturbed potential of the form:

$$W(r)+\epsilon W'(r)=W(r)+(\Delta s/s)W(r). \tag{10.4}$$

If the small change consists of a change in the intrinsic range $b$ by an amount $\Delta b$, the perturbed potential is:

$$\begin{aligned} W(r)+\epsilon W'(r)=W(r)\\ -(\Delta b/b)[2W(r)+sb^{-2}(r/b)f'(r/b)] \end{aligned} \tag{10.5}$$

where $f'(x)$ is the derivative of $f(x)$. With Eqs. (10.2)–(10.5) the quantities $(\partial a/\partial s)$, $(\partial r_0/\partial s)$, $(\partial a/\partial b)$, $(\partial r_0/\partial b)$ can be readily calculated.

## XI. NUMERICAL RESULTS FOR VARIOUS POTENTIAL SHAPES AND COMPARISON WITH EXPERIMENT

We have calculated the variational parameters and their derivatives with respect to small changes in the potential for the four usual choices of potential (square, Gaussian, exponential, and Yukawa wells). As was pointed out in reference 6, although the calculations have been performed only for static potentials, the expansion (1.2) is valid for more general interactions described by Wheeler's velocity-dependent forces.[13] This is apparent in view of the fact that the expressions (9.6), (9.14), (9.15) for the coefficients involve integrals over the wave functions only; the potential $W(r)$ does not appear explicitly.

For the sake of convenience, the specification of $W(r)$ and $V(r)$ given in reference 6 will be repeated here:

*Square well*
$$W(r)=s(\pi/2)^2b^{-2}(r<b);\quad W(r)=0(r>b),$$
*Gaussian well*
$$W(r)=sb^{-2}(5.5296)\exp[-2.0604(r/b)^2],$$
*Exponential*
$$W(r)=sb^{-2}(18.1308)\exp(-3.5412r/b),$$
*Yukawa well*
$$W(r)=sb^{-2}(3.5605)(b/r)\exp(-2.1196r/b). \tag{11.1}$$

Here $W(r)$ is in $\text{cm}^{-2}$ if $b$ is given in cm. The conversion to energy units is slightly different from the neutron-proton case because the reduced mass in the neutron-proton case differs slightly from the reduced mass in the proton-proton case (i.e., from $\frac{1}{2}M_p$). Since the neutron-proton mass-difference is very small, this change in the conversion to energy units has no practical significance in the interpretation of scattering experiments. Below we give the expressions for the potential $V(r)$ in Mev under the assumption that $b$ is measured in units of $10^{-13}$ cm, correct for proton-proton scattering:

*Square well*
$$V(r)=-sb^{-2}(102.35)(r<b);\quad V(r)=0(r>b),$$
*Gaussian well*
$$V(r)=-sb^{-2}(229.37)\exp[-2.0604(r/b)^2],$$
*Exponential well*
$$V(r)=-sb^{-2}(752.06)\exp(-3.5412r/b),$$
*Yukawa well*
$$V(r)=-sb^{-2}(147.69)(b/r)\exp(-2.1196r/b), \tag{11.2}$$

The conversion factor used was

$$\hbar^2/M_P=41.480\times10^{-26}\ \text{Mev}\times\text{cm}^2.$$

For the Yukawa well, the equivalent meson mass is $\mu=818.57b^{-1}m_e$.

TABLE VIII. Calculated values of the variational parameters and their derivatives for various potential well shapes. All lengths are in units of $10^{-13}$ cm.

| Well shape | $s$ | $b$ | $a$ | $r_0$ | $P$ | $Q$ |
|---|---|---|---|---|---|---|
| Square | 0.890 | 2.626 | −7.7930 | 2.6388 | −0.03313 | 0.00179 |
| Gaussian | 0.900 | 2.540 | −7.7797 | 2.6055 | −0.01936 | −0.00073 |
| Exponential | 0.900 | 2.500 | −7.4235 | 2.6776 | 0.00907 | 0.00089 |
| Yukawa | 0.924 | 2.400 | −7.6512 | 2.6756 | 0.05540 | 0.019 |

| Well shape | $\partial a/\partial s$ | $\partial r_0/\partial s$ | $\partial a/\partial b$ | $\partial r_0/\partial b$ |
|---|---|---|---|---|
| Square | −33.521 | −1.5300 | −2.0824 | 0.94975 |
| Gaussian | −34.654 | −1.8553 | −2.0966 | 0.98193 |
| Exponential | −33.813 | −2.5690 | −2.0510 | 1.0439 |
| Yukawa | −39.399 | −3.6387 | −2.1002 | 1.1157 |

In the calculations the Coulomb potential was assumed to be valid right down to $r=0$ *ie* Eq. (9.1) was used, with $W(r)$ given by (11.1). Present concepts about the nature of the nucleons themselves makes such an assumption questionable. Deviations from the purely Coulomb form of the electromagnetic interaction most probably occur at distances of the order of, or smaller than, the range of nuclear forces. However, the Coulomb field itself produces little change in the variational parameters[8] except the scattering length $a$ (see Section VIII). Consequently, deviations from the Coulomb law at small distances can be assumed to produce no significant changes in the higher coefficients in (1.2), and only slight modification in $a$. In any event, when the actual form of these deviations is known, the parameters can be corrected accordingly by the methods of Section X.

The results of the calculation are collected in Table VIII. The first column of the table specifies the potential shape. The second and third columns give the values of the well parameters $s$ and $b$ for which the calculation was carried out. The next four columns give the variational parameters $a$, $r_0$, $P$, $Q$. Finally the last four columns give the derivatives $\partial a/\partial s$, $\partial r_0/\partial s$, $\partial a/\partial b$, $\partial r_0/\partial b$ which one needs to compute the effects of small changes in the well parameters.

These numbers can be compared with those obtained by Hatcher, Arfken, and Breit[34] for the Gaussian and Yukawa well shapes. These authors computed $S$-wave phase shifts, then evaluated $\mathbf{K}$ (1.1), and made a least squares fit with a second-degree polynomial over the energy range up to 10 Mev. The comparison is satisfactory.

They can also be compared with the corresponding parameters for neutron-proton scattering.[6] The scattering lengths differ appreciably, as expected from Section VIII. However, the higher coefficients agree quite well. For the same values of $s$ and $b$ as given in Table VIII, a comparison with the curves of reference 6 shows that the effective ranges differ by 6 percent at most (the difference is 0.2 percent for the Yukawa well, and 5.6 percent for the square well). Similarly, the values of $P$ in the two cases differ by 10 percent at most for all the well shapes considered. This gives a clear indication that the Coulomb potential can be treated as a small perturbation on the higher parameters in (1.2).

The first thing to note in the comparison with experiment is the very small value of $P$ for all four well shapes. In view of the fact that the present experimental data are not in disagreement with values of $P$ anywhere in the range $+0.15$ to $-0.8$, one can conclude that *all four commonly assumed well shapes give equally good fits to the Van de Graaff data,* the fits being quite excellent compared to the experimental errors. Conversely, the disagreement of the DOP point at 7 Mev cannot be used as an indication of well shape since this point is in disagreement no matter which well shape is assumed.

The present results are in essential agreement with the results of Breit, Thaxton, and Eisenbud.[1] However, they disagree with the results of Hoisington, Share, and Breit[35] concerning the exponential well shape. These authors claim that the exponential well provides a significantly poorer fit to the then available data than the Yukawa well. They attribute this difference to the longer tail of the exponential well, claiming that the $1/r$ singularity at the origin in the Yukawa well compensates for its tail. Their fit to the data with the exponential well was made using the well parameters determined by Rarita and Present[36] ($s=0.885$, $b=3.08\times10^{-13}$ cm). These well parameters give too large (absolute) values for both $a(\sim-8.10\times10^{-13}$ cm) and $r_0(\sim3.32\times10^{-13}$ cm) so that a plot of $\mathbf{K}$ *vs.* $k^2$ would lie across the best linear fit shown in Fig. 15, passing below the lower energy points and above the higher energy points of HKPP. But it just happens that the Rarita-Present well predicts the same value for the phase shift as determined from the HHT data at 670 kev. This point will be seen to lie considerably below the best fit in Fig. 15. Hoisington, Share, and Breit remark that their comparison may be unfair since they choose to fit their theoretical curve exactly to the HHT point at 670 kev. However, they go on to argue that this really should make no difference since the curvature of the $\delta_0$ *vs.* $E$ curve for the exponential well is too great to be in agreement with all the experimental data no matter at what energy it was fitted, and that a change in the range of the potential primarily affects the slope, not the curvature of such a plot. It is clear that, since the present data do not discriminate between well shapes, the earlier data (which covered a narrower energy range) certainly discriminate even less. With the proper choice of range and depth (see Table IX) the exponential well gives as good a fit to the data (either as it was then or as it is now) as any of the other usually assumed shapes. The conclusion to be drawn from the work of Hoisington, Share, and Breit is that the Rarita-Present exponential well gives a poor fit to the data, but not that the exponential well per se gives a poorer fit than any other well shape. This situation illustrates the difficulties involved in deciding what is a "good fit" if one

[34] Hatcher, Arfken, and Breit, Phys. Rev. **75**, 1389 (1949).

[35] Hoisington, Share, and Breit, Phys. Rev. **56**, 884 (1939).

[36] W. Rarita and R. D. Present, Phys. Rev. **51**, 793 (1937).

TABLE IX. The variational parameters and well parameters which give the best weighted least-squares fit to the experimental data below 3.6 Mev.

| Well shape | $P$ | $a(10^{-13}$ cm) | $r_0(10^{-13}$ cm) | $s$ | $b(10^{-13}$ cm) |
|---|---|---|---|---|---|
| Square | −0.033 | −7.66±0.05 | 2.60±0.07 | 0.889±0.003 | 2.58±0.06 |
| Gaussian | −0.019 | −7.66(5)±0.05 | 2.62±0.07 | 0.896±0.003 | 2.55±0.06 |
| Exponential | +0.009 | −7.68±0.05 | 2.67±0.07 | 0.907±0.003 | 2.51±0.06 |
| Yukawa | +0.055 | −7.70±0.05 | 2.76±0.07 | 0.922±0.003 | 2.47±0.06 |

does not have a simple functional form such as (1.2) with which to fit the data.

The results in Table VIII are not in the most convenient form for comparison with experiment since we want to find $s$ and $b$ from the measured $a$ and $r_0$, rather than the other way around. The quantities in Table VIII are used as follows:

$$a \simeq a_0+(\partial a/\partial s)(s-s_0)+(\partial a/\partial b)(b-b_0),$$
$$r \simeq r_0+(\partial r/\partial s)(s-s_0)+(\partial r/\partial b)(b-b_0).$$

These equations can be treated as a pair of linear simultaneous equations in two unknowns ($s$ and $b$), and can be solved for these unknowns in terms of $(a-a_0)$ and $(r-r_0)$. The resulting expressions, given below, correspond to the linear terms in a Taylor series around the computed points.

*Square well*

$$s=0.890-0.02712(a+7.793)-0.05946(r_0-2.639), \quad (11.3S)$$
$$b=2.626-0.04369(a+7.793)+0.95716(r_0-2.639).$$

*Gaussian well*

$$s=0.900-0.02590(a+7.780)-0.05529(r_0-2.606), \quad (11.3G)$$
$$b=2.540-0.04893(a+7.780)+0.91395(r_0-2.606).$$

*Exponential well*

$$s=0.900-0.02573(a+7.424)-0.05056(r_0-2.678), \quad (11.3E)$$
$$b=2.500-0.06333(a+7.424)+0.83354(r_0-2.678).$$

*Yukawa well*

$$s=0.924-0.02162(a+7.651)-0.04070(r_0-2.676), \quad (11.3Y)$$
$$b=2.400-0.07051(a+7.651)+0.76353(r_0-2.676).$$

All lengths in these formulas are in $10^{-13}$ cm.

Using the results of the weighted least squares fitting to the Van de Graaff data for arbitrary values of $P$ which are summarized in Figs. 17 and 18 we can determine the best values of $a$ and $r_0$ for each well shape. Then we use Eqs. (11.3) to determine the best well parameters $s$ and $b$ in each case. These results are given in Table IX. The first column of the table gives the well shape, the second column the value of $P$ for that well. The third and fourth columns give the corresponding values of $a$ and $r_0$ with their probable errors, while the next two columns give the implied values of the well parameters $s$ and $b$ with their probable errors. The potentials corresponding to these values of $s$ and $b$ can be found by reference to Eqs. (11.2). For the Yukawa well the "meson" mass turns out to be 332±8 electron masses. The values of $b$ are seen to be determined to within 2.5 percent, while the values of $s$ are determined to within 0.3 percent.

The results summarized in Table IX are in essential agreement with the results of Breit, Thaxton, and Eisenbud[1] for the square and Gaussian well shapes (they obtained $s=0.872$, $b=2.81$ for the square well; $s=0.887$, $b=2.78$ for the Gaussian well), and those of Hoisington, Share, and Breit[35] for the Yukawa well (they got $s=0.920$, $b=2.51$). The differences can be accounted for by the fact that Breit *et al.* had only the data of HHT and HKPP available for their analysis at that time. As pointed out by Bethe,[8] the errors can now be narrowed down somewhat, both because the data extend to higher energies and because the simple functional form (1.2) allows one to make a reasonable estimate of error by simple inspection rather than by complicated computations.

Bethe[8] has given a discussion of the assumption of charge independence of the specifically nuclear forces. He has shown that the recent data for the epithermal neutron-proton cross section definitely imply a neutron-

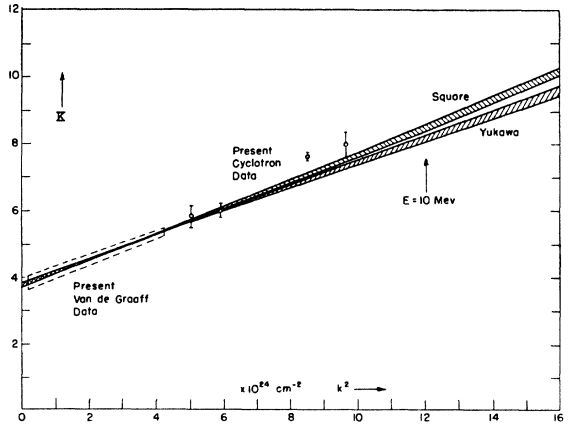


FIG. 21. The function **K** plotted *vs.* $k^2$ for the square and Yukawa wells giving equivalently good fits to the Van de Graaff data (see Table IX). The shaded regions are those allowed by the uncertainty in the least-squares fitting to the data at the lower energies. The allowed regions overlap below 7 Mev, preventing effective discrimination between the two well shapes at lower energies (except insofar as the curves will be spread farther apart in the high energy region by a precise measurement near 400 kev). Similar plots for the Gaussian and exponential wells would lie between those shown.

proton potential in the singlet state with a bigger value of $s$ than the proton-proton force, assuming the same intrinsic range and shape for the potentials. To obtain quantitative information on this difference, we take the values of $b$ given in Table IX for each potential shape, and assume that the neutron-proton singlet potential has the same value of intrinsic range. Then the value $-(2.376\pm0.010)\times10^{-12}$ cm for the singlet neutron-proton scattering length (obtained from the coherent and incoherent $n$-$p$ scattering cross sections)[6] and these values of $b$ determine corresponding values of $(\alpha b)$ for the singlet $n$-$p$ state. From Fig. 4 of reference 6 we find the implied values of the well depth parameter $s$ for the singlet $n$-$p$ potential. Comparison of these $n$-$p$ values with the corresponding $p$-$p$ values of $s$ in Table IX shows that the $n$-$p$ interaction in the singlet $S$-state is stronger than the $p$-$p$ interaction (assuming the same intrinsic range and shape) by 3.3 percent for the square well, 1.6 percent for the Yukawa well, and in between for the other two well shapes.

The same results can be obtained by means of the approximate relation (8.10) between scattering lengths together with the values of $r_0$ and $\partial a/\partial s$ from Table IX and Table VIII. This (less accurate) method of comparison leads to the conclusion that the $n$-$p$ interaction is stronger than the $p$-$p$ interaction by about 3 percent for the square well and about 2 percent for the Yukawa well, in good agreement with the more precise comparison.

The differences in strength of the $n$-$p$ and $p$-$p$ potentials in the singlet state are small, but seem definitely outside the limits of experimental error, so that the hypothesis of the charge-independence of nuclear forces is not exactly satisfied.* However, while the disagreement seems to be definite enough, one should perhaps emphasize that it is quite small numerically. Hence the general conclusions of Wigner[37] regarding the spectroscopic classification of nuclear energy levels are not affected by this result. One might argue that the presence of the nuclear force distorts the Coulomb field for values of $r$ less than the nuclear range. If so, the distortion has to be in such a way that the effective Coulomb potential is increased. One of the other aspects of charge-independence, namely the charge independence of the intrinsic range of the nuclear potential, has no direct experimental verification at present. The present neutron-proton scattering data are not accurate enough to settle this point (see reference 6). And, of course, the question of potential shape is completely unanswered by present experimental data of any sort. The closer equality of the neutron-proton and proton-proton forces found by Breit and collaborators[38] was due to the use of Simon's[39] value of the epithermal neutron-proton scattering cross section, which has since been shown to be considerably too low. Their calculations with $\sigma_0=20$ barns are in accord with the results given here.

In conclusion we will give some indication of the accuracy necessary for a hypothetical experiment at 10 Mev to discriminate between the Yukawa and square well shapes (these being the two extremes in well shapes usually employed). The parameters specifying the Yukawa and square wells giving the best fits to the Van de Graaff data are given in Table IX. The curves of $\mathbf{K}$ *vs.* $k^2$ implied by the variational parameters $a$, $r_0$, $P$ and $Q$ for these two potentials are plotted in Fig. 21. For each potential there is an allowed region (shaded area) for the values of $\mathbf{K}$ due to the leeway in the values of $a$ and $r_0$ as determined from the fitting of the Van de Graaff data. We see that below 7 Mev ($k^2\sim8\times10^{24}$ cm$^{-2}$) the allowed regions overlap making it virtually impossible to discriminate between the well shapes (assuming that the experimental point falls within the shaded zone). At 10 Mev the difference between the values of $\mathbf{K}$ for the best fits (the center line of the shaded areas in each case) for these two potentials is $\Delta\mathbf{K}\simeq0.3$, while the gap between the shaded regions (the most pessimistic choice) is about $\Delta\mathbf{K}\simeq0.16$.

To determine the accuracy in cross section and energy measurements necessary to discriminate between values of $\mathbf{K}$ differing by an amount $\Delta\mathbf{K}$ we turn to Figs. 19 and 20 to find the values of $E(\partial\mathbf{K}/\partial E)_\sigma$ and $\sigma(\partial\mathbf{K}/\partial\sigma)_E$. At 10 Mev (and at moderate scattering angles) we find that $E(\partial\mathbf{K}/\partial E)_\sigma\simeq-4$, while $\sigma(\partial\mathbf{K}/\partial\sigma)_E\simeq-8$ i.e., the uncertainty in cross section is twice as important as the uncertainty in beam energy as far as errors in $\mathbf{K}$ are concerned. Since the signs of the experimental errors are presumably unknown, it is necessary to consider the worst possible case namely,

$$4|\Delta E/E|+8|\Delta\sigma/\sigma|=\Delta\mathbf{K}.$$

* *Note added in proof.*—Schwinger (private communication) has pointed out that if, in addition to the electrostatic Coulomb interaction, we consider electromagnetic interactions between the nucleons of a magnetic nature, such as the interaction between two magnetic dipoles, we find that the charge-independence (in the narrow sense used here) of the specifically nuclear force is improved. In an $S$-state, the dipole-dipole interaction is: $V_{\text{int}}=-(8\pi/3)(\mu_1\mu_2)\boldsymbol{\sigma}_1\cdot\boldsymbol{\sigma}_2\delta(\mathbf{r}_1-\mathbf{r}_2)$ (see, for example, L. Rosenfeld, *Nuclear Forces* (Interscience Publishers, New York, 1948), p. 95). Due to the difference in sign between the magnetic moments of the neutron and the proton, $V_{\text{int}}$ is attractive in the neutron-proton singlet state, and repulsive in the proton-proton singlet state ($\boldsymbol{\sigma}_1\cdot\boldsymbol{\sigma}_2=-3$ in the singlet state). Thus, with the *same* nuclear force, the effective neutron-proton interaction will appear slightly more attractive than the effective proton-proton interaction (after correction for the Coulomb field). We can readily estimate the effect of the dipole-dipole interaction on $a$ and $r_0$ (and hence on the strength of the nuclear force) by means of the formulas (10.2). The result is that the inclusion of the dipole-dipole interaction produces a change of the order of one percent in the strength of the nuclear force, and improves its charge-independence. There is a negligible change in the range of the nuclear interaction. Schwinger has made detailed calculations (to be published) of the effects on charge-independence of the magnetic dipole-dipole interaction, and other related effects (such as the interaction of the proton current with the magnetic moment of the other nucleon). He finds that the inclusion of these magnetic effects improves the charge-independence of the nuclear force for all the conventional potential shapes, but that the improvement is least for a square well, and most for a Yukawa well, this latter shape giving exact charge-independence within the experimental uncertainty of $\pm\frac{1}{2}$ percent.

[37] E. Wigner, Phys. Rev. **51**, 106, 947 (1937).
[38] Breit, Hoisington, Share, and Thaxton, Phys. Rev. **55**, 1103 (1939).
[39] L. Simons, Phys. Rev. **55**, 792 (1939).

If $\Delta\mathbf{K}$ is taken to be equal to the gap (*ie* $\Delta\mathbf{K}=0.16$) between the shaded areas for the two potential shapes, a reasonable estimate will be found for the accuracy needed to discriminate between the two shapes. The chart below shows how the allowable uncertainties go.

| | | | |
|---|---|---|---|
| $(\Delta\sigma)/\sigma$ | 0 | 0.01 | 0.02 |
| $(\Delta E)/E$ | 0.04 | 0.02 | 0 |

We see that to differentiate between extremes in potential shapes it is necessary to have an over-all uncertainty in cross section measurement of two percent or less, assuming no accompanying uncertainty in beam energy. However, in view of the cyclotron measurements at 7 and 8 Mev an energy accuracy of around one percent seems to be the lower practical limit, so that the cross section measurement must be accurate to about one and a half percent, or better—a not impossible requirement with careful work. It appears, then, that a measurement in the neighborhood of 10 Mev that would discriminate between extremes in well shapes is possible with existing equipment and techniques, but only if considerable care is taken to reduce all possible errors to an absolute minimum.

In these considerations we have tacitly assumed that the hypothetical experimental point falls on, or between, the shaded regions in Fig. 21. There is, of course, no theoretical reason why it should do so. A good measurement (of the accuracy estimated above) at 10 Mev, wherever it falls on the $\mathbf{K}$ *vs.* $k^2$ plot, will at least exclude some potential shapes from the array of possibilities (it being far easier to exclude some interactions than to determine the correct one). For that reason, as well as reasons cited earlier, we recommend that careful measurements be made at energies considerably above 3.5 Mev, and that particular attention be paid to the elimination of systematic errors (which might, for example, account for the peculiar DOP point at 7 Mev).

## XII. A ROUGH ESTIMATE OF THE PHASE SHIFTS FOR HIGHER ANGULAR MOMENTA FOR *P-P* AND *N-P* SCATTERING

It is an easy matter to write the generalization of the variation principle for orbital angular momenta $l$ different from zero. Indeed, all one has to do is to replace $F(r)=F_0(r)$ and $G(r)=G_0(r)$ by the appropriate Coulomb wave function for orbital angular momentum $l$, i.e. by the $F_l(r)$ and $G_l(r)$ given in Yost, Wheeler, and Breit.[32] (The replacement must be made also in the definition of the Green's function $K_l(r, r')$, of course.) The derivation of an expansion similar to (1.2) presents no difficulties. Indeed, the result has been derived by Chew and Goldberger[8] for $l=1$. The generalization of (1.2) to arbitrary $l$ was given by Landau and Smorodinsky[3] for the zero-range approximation.

However, such a detailed treatment for higher angular momenta is unnecessary at this time. As can be seen from Section VI, the experimental evidence for *P*- or *D*-wave contributions to the scattering is only of a qualitative nature. All that is necessary at present is a rough, order of magnitude, estimate of these higher phase shifts. Breit, Thaxton, and Eisenbud[1] have given estimates for the Gaussian and exponential well shapes. We give here estimates for the four usual well shapes in terms of the well depth parameter $s$ and the intrinsic range $b$ for both *P-P* and *N-P* scattering. We consider the *P-P* case first.

TABLE X. Values of $f_{2l+2}$ for the usually assumed potential shapes and $l=1, 2, 3$.

| | Square well | Gaussian well | Exponential well | Yukawa well |
|---|---|---|---|---|
| $l=1$ | 0.4935 | 0.6031 | 0.7814 | 1.058 |
| $l=2$ | 0.3525 | 0.7318 | 1.869 | 4.712 |
| $l=3$ | 0.2742 | 1.243 | 8.348 | 44.05 |

For a first orientation, it is sufficient to use the Born approximation for the phase shifts[40]

$$\delta_l^{PP}=k^{-1}\int_0^\infty F_l^2(r)W(r)dr. \tag{12.1}$$

Furthermore, we shall approximate the regular Coulomb wave function by its behavior near the origin (see reference 32):

$$F_l(r)\simeq C_l(kr)^{l+1}. \tag{12.2}$$

Here $C_l$ is the penetration factor for the combined centrifugal and Coulomb barriers, given by

$$C_l^2=\frac{2^{2l}}{(2l+1)!^2}(l^2+\eta^2)\times((l-1)^2+\eta^2)\cdots(1+\eta^2)\frac{2\pi\eta}{e^{2\pi\eta}-1}. \tag{12.3}$$

The potential $W(r)$ is written in the standard form (10.3). Then the estimate for the phase shift $\delta_l$ becomes:

$$\delta_l^{PP}\simeq C_l^2 s(kb)^{2l+1}f_{2l+2}, \tag{12.4}$$

where $f_n$ is the $n$th moment of the shape function $f(r/b)$ defined in (10.3):

$$f_n=\int_0^\infty x^n f(x)dx. \tag{12.5}$$

Formula (12.4) shows that $\delta_l^{PP}$ is proportional to (1) the barrier penetration factor (which for *P-P* scattering is a function of energy), (2) the well depth parameter $s$, (3) the $(l+\frac{1}{2})$ power of the energy, (4) the $(2l+1)$ power of the intrinsic range, (5) a pure number depending only upon the shape of the well and increasing rapidly as the well gets to be more "long-tailed." $\delta_l$ will be positive for attractive potentials (positive $s$) and negative for repulsive potentials (negative $s$).

In Table X we have collected the values of $f_{2l+2}$ for

[40] Reference 14, pp. 28, 90.

TABLE XI. Estimates of $\delta_l$. The sets of three numbers at each energy are the estimated values of $\delta_1$, $\delta_2$, and $\delta_3$ in degrees for $P$-$P$ scattering with $s=1$ and $b$ given in Table IX. The ratio of $\delta_l(NP)$ to $\delta_l(PP)$ is given in the last column. This ratio is just the reciprocal of the $S$-state Coulomb penetration factor (i.e., $C^{-2}$). The values of the energy are in the laboratory system.

| Energy (Mev) | Square well | Gaussian well | Exponential well | Yukawa well | $C^{-2}=\delta_l(NP)/\delta_l(PP)$ |
|---|---|---|---|---|---|
| | 0.14 | 0.17 | 0.21 | 0.27 | |
| 2 | 0.00065 | 0.0013 | 0.0030 | 0.0070 | 1.45 |
| | 0.0000017 | 0.0000069 | 0.000042 | 0.00020 | |
| | 0.44 | 0.52 | 0.65 | 0.84 | |
| 4 | 0.0041 | 0.0080 | 0.019 | 0.044 | 1.30 |
| | 0.000021 | 0.000087 | 0.00052 | 0.0025 | |
| | 0.85 | 1.01 | 1.25 | 1.61 | |
| 6 | 0.012 | 0.023 | 0.054 | 0.13 | 1.23 |
| | 0.000090 | 0.00038 | 0.0023 | 0.011 | |
| | 1.35 | 1.60 | 1.97 | 2.54 | |
| 8 | 0.025 | 0.049 | 0.12 | 0.27 | 1.20 |
| | 0.00025 | 0.0011 | 0.0064 | 0.030 | |
| | 1.93 | 2.27 | 2.81 | 3.62 | |
| 10 | 0.044 | 0.087 | 0.20 | 0.48 | 1.17 |
| | 0.00056 | 0.0024 | 0.014 | 0.067 | |

the four commonly assumed well shapes and for the first few values of $l$.

The values of $\delta_l$ for $P$-$P$ scattering at a few representative energies are given in Table XI under the assumption that $W(r)$ for the higher angular momenta has the same intrinsic range $b$ as the best fit (see Table IX) for the $S$-wave phase shifts, and a well depth parameter $s=1$. In order to get $\delta_l{}^{PP}$ for different assumptions about $s$ or $b$, it is only necessary to remember the proportionality of $\delta_l{}^{PP}$ to $s$ and $b^{2l+1}$.

To evaluate the $N$-$P$ phase shifts for higher angular momenta we just use the $N$-$P$ equivalent of formula (12.1). Instead of the regular Coulomb wave function we now have the regular spherical Bessel function $j_l(kr)$ times $(kr)$. In the approximation equivalent to Eq. (12.2),

$$krj_l(kr)\sim B_l(kr)^{l+1} \tag{12.6}$$

where $B_l$ is the centrifugal barrier penetration factor

$$B_l\equiv\frac{2^l l!}{(2l+1)!}=\frac{1}{1\times3\times5\cdots(2l+1)}. \tag{12.7}$$

The $N$-$P$ phase shifts $\delta_l{}^{NP}$ are then given by:

$$\delta_l{}^{NP}\simeq B_l{}^2 s(kb)^{2l+1}f_{2l+2}. \tag{12.8}$$

One can easily see that $C_l$ (12.3) reduces to $B_l$ in the limit $\eta\to0$, as required. Furthermore, $\eta^2<0.01$ for energies above 2 Mev. For such energies the combined Coulomb and centrifugal barrier penetration factor is given to a good approximation by the product of the $S$-state Coulomb factor $C$ (defined by Eq. (8.4)) and the centrifugal factor $B_l$:

$$C_l\simeq\frac{2^l l!}{(2l+1)!}\left(\frac{2\pi\eta}{e^{2\pi\eta}-1}\right)^{\frac{1}{2}}=B_l\times C. \tag{12.9}$$

In this approximation the ratio of the $N$-$P$ phase shifts $\delta_l{}^{NP}$ given by (12.8) to the $P$-$P$ phase shifts $\delta_l{}^{PP}$ given by (12.4) is just

$$\delta_l{}^{NP}/\delta_l{}^{PP}=B_l{}^2/C_l{}^2\sim1/C^2 \tag{12.10}$$

so that the ratio is dependent upon energy, but approximately independent of $l$ (the approximation being better the larger the values of the energy and $l$). The sixth column in Table XI gives the value of the ratio (12.10) for the energies quoted there. With this ratio the values of $\delta_l(P$-$P)$ can be readily converted to estimates for the corresponding $N$-$P$ phase shifts. As before, estimates for any other values of $s$, $b$, or energy can be easily obtained by means of the proportionality of $\delta_l{}^{NP}$ to $s$, $b^{2l+1}$, and $E^{l+\frac{1}{2}}$.

It should be emphasized that the numbers in Table XI are very rough estimates, and are to be used only in that sense. The possibility of a tensor force contribution in the states of odd angular momentum has not been included, since detailed considerations of this type seem premature. The absolute value of $\delta_l$ in higher approximation for a given potential depends on whether the force is attractive or repulsive. The values in Table XI are approximately the mean of the absolute values for attractive and repulsive potentials, the attractive potential giving a somewhat larger value for $\delta_l$, and the repulsive potential a smaller (absolute) value.

The following preliminary conclusions can be drawn from the estimates summarized in Table XI: (1) A $P$-wave phase shift of the order of half a degree at an energy around 3 Mev is not unreasonable. (2) A $D$-wave phase shift of the order of magnitude 0.1 degree at that same energy is considerably higher (by a factor of 5 to 50) than the expected values. (3) At energies of the order of 8 or 10 Mev the $P$-wave phase-shifts (assuming that they exist at all) are likely to become large enough so that the linear approximation of Section V will be invalid. If this turns out to be the case, one will also have to include tensor force effects more carefully at those energies (i.e., the replacement (5.5) will no longer be valid). (4) It is clear from (12.4) that the phase shift estimates depend quite strongly upon the shape of the well; hence one can always get larger estimates by using longer-tailed wells. However, the evidence summarized in Section VII limits the value of $P$ (the amount of tailing of the well) that one can permit for the force in the $^1S$-state. At present, it is a matter of taste whether one is willing to assume a potential with a very long tail in the states of higher angular momentum. In this connection, it should be noted that the analysis of the experiments given in Section VI indicates that the $P$-wave phase shifts, if real, are of the order of, or less than, one degree even up to 10 Mev. Hence there is no need at present to postulate long-tailed potentials in the states of higher angular momentum.

## ACKNOWLEDGMENTS

This paper could never have been written without constant reference to the excellent previous work on

proton-proton scattering by Breit and collaborators. The authors are happy to record their indebtedness to this pioneer work. We have greatly profited from discussions with Professors J. Schwinger at Harvard, G. Breit of Yale, V. F. Weisskopf, and D. H. Frisch of M.I.T. and H. A. Bethe of Cornell University. We have also been helped greatly by receiving pre-publication copies of the papers by H. A. Bethe,[8] G. Breit and Bouricius,[9] Chew and Goldberger,[8] Hatcher, Arfken, and G. Breit,[34] R. A. Meagher,[26] and Ralph, Worthington and R. G. Herb.[23] Last but not least, we would like to acknowledge the excellent computing work of Mrs. Barbara (Siegle) Levine.

## APPENDIX I. FORMULAS FOR THE DETERMINATION OF HIGHER PHASE SHIFTS

The functions $p_n(E, \theta, \delta_0)$ defined by:

$$p_n(E, \theta, \delta_0)=\frac{(\partial\sigma/\partial\delta_n)}{(\partial\sigma/\partial\delta_0)} \tag{5.4}$$

can be readily found by means of the formulas of Breit, Condon, and Present[1] for $n=1, 2$. Thus

$$\left(\frac{Mv^2}{e^2}\right)^2\frac{\partial\sigma}{\partial\delta_0}=\left[\frac{-2\mathbf{X}}{\eta}\cos(2\delta_0)+\left(\frac{4}{\eta^2}+\frac{2\mathbf{Y}}{\eta}\right)\sin(2\delta_0)\right] \tag{AI.1}$$

where $\mathbf{X}$ and $\mathbf{Y}$ are defined by Eqs. (4.4). Similarly

$$\left(\frac{Mv^2}{e^2}\right)^2\frac{\partial\sigma}{\partial\delta_1}=-\frac{18}{\eta}\left(\frac{\cos\alpha_1}{\sin^2\theta/2}-\frac{\cos\beta_1}{\cos^2\theta/2}\right)P_1(\cos\theta) \tag{AI.2}$$

and

$$\left(\frac{Mv^2}{e^2}\right)^2\frac{\partial\sigma}{\partial\delta_2}=\left[\frac{40}{\eta^2}\sin\delta_0\cos(\delta_0-2\sigma_2+2\sigma_0)-\frac{10}{\eta}\left(\frac{\cos\alpha_2}{\sin^2\theta/2}+\frac{\cos\beta_2}{\cos^2\theta/2}\right)\right]P_2(\cos\theta), \tag{AI.3}$$

where $\alpha_i$ and $\beta_i$ are defined in BCP. It should be noted that while (AI.1) and (AI.3) involve $\delta_0$, they are relatively insensitive to variations in $\delta_0$ over the energy range of interest. The higher phase shifts are certainly negligible for energies below 2 Mev while the assumption that $\delta_1$ and $\delta_2$ are small probably is not valid above 8 or 10 Mev. In this energy range of 2–10 Mev where the functions $p_n$ are presumably useful, the value of $\delta_0$ is in the neighborhood of 50 degrees. Thus $\sin(2\delta_0)$ is near unity, and a slowly varying function of $\delta_0$, while $\cos(2\delta_0)$ is small. From this it is seen that (AI.1) and (AI.3) are insensitive to $\delta_0$. Of course, (AI.2) does not involve $\delta_0$ at all.

Of some interest, as far as the general behavior of $p_1(\theta)$ and $p_2(\theta)$ is concerned, are the limiting forms for $p_1$ and $p_2$ as $E$ becomes very large. It is easily seen from examination of (AI.1) and (AI.2) that:

$$\lim_{E\to\infty} p_1(\theta)=[-18\eta/\sin(2\delta_0)]\cot^2\theta. \tag{AI.4}$$

Similarly, the limiting form of $p_2(\theta)$, from (AI.1) and (AI.3) is:

$$\lim_{E\to\infty} p_2(\theta)=5P_2(\cos\theta). \tag{AI.5}$$

It is interesting to note that the limiting form of $p_1(\theta)$ is proportional to $\eta$, so that $p_1(\theta)$ vanishes in the limit of very high energy (or when the electric charge is made to vanish). This is because $p_1(\theta)$ arises from an interference between the $^3P$-nuclear scattering and the Coulomb scattering in all the higher odd angular momentum states (the Pauli principle prevents interference effects between states of even and odd angular momentum). In the transition to neutron-neutron scattering (electric charge to zero) such a term must vanish if it is assumed that higher odd angular momentum states do not contribute to the nuclear scattering. In consequence, the $P$-wave phase shift first appears quadratically in neutron-neutron scattering, but appears linearly in proton-proton scattering if all $\delta$'s above $\delta_2$ vanish in both cases. On the other hand, the limiting form of $p_2(\theta)$ does not depend on the Coulomb scattering in the even angular momentum states, but involves only an interference effect between $^1S$- and $^1D$-nuclear scattering. Hence, the $D$-wave phase shift appears linearly in both neutron-neutron and proton-proton scattering.

The values of $p_1(E, \theta)$ and $p_2(E, \theta)$ which were computed using (AI.1), (AI.2), and (AI.3) are given in Tables V and VI for energies from 2 to 10 Mev in the laboratory and angles from 16 to 90 degrees in the center of gravity system (the functions are symmetrical about $\theta=90$ degrees).

Since the need for interpolation in energy occurs more often than the need for interpolation in angle, plots of $p_1(E, \theta)$ and $p_2(E, \theta)$ as functions of the energy $E$ for various scattering angles $\theta$ are quite useful. Such plots are shown in Figs. 4 and 5. It is seen from Fig. 5 that $p_2(E)$ is almost constant at any given value of $\theta$ over the whole energy range, for $\theta$'s between 40 and 90 degrees; in this angular range the asymptotic form (AI.5) yields very good values of $p_2$ independent of energy.

It should be pointed out that numerical interpolation in angle for $p_1(\theta)$ from Table V can be made quite accurate if the asymptotic behavior (AI.4) is divided out before interpolation; that is, the interpolation should be carried out between values of $p_1(\theta)\tan^2\theta$, rather than between values of $p_1(\theta)$, because $p_1(\theta)\tan^2\theta$ is a much more slowly varying function of angle than is $p_1(\theta)$ itself.

## APPENDIX II. APPARENT $S$-WAVE PHASE SHIFTS FROM EXPERIMENT

The values of the apparent $S$-wave phase shifts for the experimental data are tabulated below. The manner in which the $S$-wave phase shift given in Table VII was determined is also stated.

(1) RKT.[18]—The values quoted in Table VII were computed from the experimental cross sections at $\theta=90$ degrees (center of mass).

(2) HHT.[19]—The numbers given in Table VII were determined from the data by Creutz.[20]

(3) HKPP.[2]—These data were analyzed by Breit, Thaxton, and Eisenbud.[1] The values of $\delta_a$ from $\theta=40$ degrees to $\theta=90$ degrees are given by them. The $S$-wave phase shifts in Table VII are averages of the four values of $\delta_a$ from $\theta=60$ degrees to $\theta=90$ degrees in each case.

(4) BFLSW.[21]—Critchfield and Dodder[22] have published values of $\delta_a$ for $\theta=50$ degrees to 90 degrees from these data. Values of $\delta_a$ have been computed for a wider range of scattering angles than given by them. These numbers are tabulated below. They have been corrected for the second-order geometry effect discussed by Critchfield. The $S$-wave phase shifts given in Table VII are averages over the five values of $\delta_a$ from $\theta=50$ degrees to $\theta=90$ degrees.

BFLSW

| $\theta$ | $E$ (Mev) | | | |
|---|---|---|---|---|
| (degrees) | 2.42 | 3.04 | 3.27 | 3.53 |
| 25 | | 51.28 | 53.30 | 53.54 |
| 30 | 48.75 | 51.18 | 52.91 | 53.16 |
| 35 | 48.78 | 51.63 | 52.50 | 52.54 |
| 40 | 48.47 | 50.96 | 52.11 | 53.30 |
| 50 | 48.22 | 51.26 | 52.59 | 52.66 |
| 60 | 48.65 | 50.91 | 51.67 | 52.27 |
| 70 | 48.20 | 50.70 | 52.08 | 52.62 |
| 80 | 47.95 | 50.62 | 51.57 | 52.77 |
| 90 | 48.20 | 51.25 | 51.55 | 52.58 |

(5) RWH.[23]—The apparent $S$-wave phase shifts implied by these data have been computed and are tabulated below. The values of the $S$-wave phase shift quoted in Table VII were found by making a reasonable linear fit to the points on a $\delta_a$ *vs.* $p_1(\theta)$ diagram, and taking the intercept to be the $S$-wave phase shift. An example of this procedure for the 3.53 Mev data is shown in Fig. 8.

RWH

| $\theta$ | $E$ (Mev) | | | |
|---|---|---|---|---|
| (degrees) | 2.42 | 3.04 | 3.28 | 3.53 |
| 40 | 48.76 | 51.32 | 52.07 | 52.86 |
| 50 | 48.54 | 51.24 | 52.00 | 52.68 |
| 60 | 48.31 | 51.01 | 51.90 | 52.45 |
| 70 | 48.09 | 51.01 | 51.85 | 52.30 |
| 80 | 47.99 | 50.88 | 51.79 | 52.20 |
| 90 | 47.64 | 50.74 | 51.74 | 52.21 |

(6) MP.[24]—May and Powell determined the ratio of proton-proton scattering to Mott scattering at $\theta=90$ degrees to be $94\pm6$ at $E=4.2$ Mev by photographic plate techniques. This ratio leads to the value of $S$-wave phase shift given in Table VII. May and Powell incorrectly state $\delta_0=54.0\pm2.5°$.

(7) M.[26]—Meagher made measurements at an energy $E=4.94\pm0.04$ Mev with the Illinois cyclotron, using photographic plate techniques. The apparent $S$-wave phase shifts from these data are given below.

M

| $\theta$ | 25 | 30 | 40 | 50 | 60 | 70 |
|---|---|---|---|---|---|---|
| $\delta_a$ | 53.29 | 53.43 | 54.04 | 53.56 | 53.87 | 54.20 |

M

| $\theta$ | 75 | 80 | 81 | 90 | 100 | 110 |
|---|---|---|---|---|---|---|
| $\delta_a$ | 54.22 | 54.06 | 54.04 | 54.06 | 54.02 | 53.75 |

The value in Table VII is an average of the eight values of $\delta_a$ from 60 to 110 degrees.

(8) DOP.[12]—The apparent $S$-wave phase shifts implied by these data are tabulated below. $E=7.03\pm0.06$ Mev.

DOP

| $\theta$ | 21.02 | 25.18 | 30.12 | 39.90 | 49.98 |
|---|---|---|---|---|---|
| $\delta_a$ | 53.28 | 53.26 | 53.33 | 52.21 | 52.12 |

| $\theta$ | 60.00 | 69.66 | 79.74 | 89.24 |
|---|---|---|---|---|
| $\delta_a$ | 52.17 | 51.87 | 52.03 | 51.79 |

The $S$-wave phase shift given in Table VII was determined by Oxley from a least squares fit to the cross section, assuming $S$- and $P$-wave anomalies. Figure 11 (where $\delta_a$ is plotted *vs.* $p_1(\theta)$) shows that this is a reasonable value of the $S$-wave phase shift.

(9) WC.[27]—These data, taken at $E=8$ Mev, involved a series of comparative measurements at different angles based on the average of two absolute measurements at $\theta=90$ degrees. The apparent $S$-wave phase shifts computed from these data are:

WC

| $\theta$ | 30 | 40 | 50 | 60 | 70 |
|---|---|---|---|---|---|
| $\delta_a$ | 51.51 | 53.13 | 53.61 | 54.00 | 53.61 |

| $\theta$ | 80 | 90 | 96 | 100 |
|---|---|---|---|---|
| $\delta_a$ | 53.13 | 52.72 | 54.09 | 51.79 |

The $S$-wave phase shift in Table VII is just the value of $\delta_a$ at $\theta=90$ degrees (from the absolute measurement).

(10) Wilson.[28]—These data consist of relative measurements on angular distribution at $E=10$ Mev. In order to examine the data for $P$-wave effects and to determine the sensitivity of such effects to changes in the absolute value of the cross section, three values of the differential cross section (center of mass system) at $\theta=90$ degrees were assumed, and the apparent $S$-wave phase shifts determined in each case. The three normalizing values of $\sigma$ (90°) were (1) 0.0490 barn, (2) 0.0515 barn, and (3) 0.0540 barn. These lead to reasonable values of the function $\mathbf{K}$, namely (1) $\mathbf{K}=8.87$,

(2) $\mathbf{K}=8.47$, and (3) $\mathbf{K}=8.08$ (see Fig. 16). The values of the apparent $S$-wave phase shifts for each case are given in the chart below.

| | Wilson | | |
|---|---|---|---|
| $\theta°$ | $\sigma(90°)=0.0490$ | $\sigma(90°)=0.0515$ | $\sigma(90°)=0.0540$ |
| 24 | 54.74 | 56.48 | 58.27 |
| 28 | 54.63 | 56.28 | 57.93 |
| 32 | 54.23 | 55.85 | 57.46 |
| 36 | 54.06 | 55.69 | 57.34 |
| 38 | 53.37 | 54.94 | 56.59 |
| 40 | 53.40 | 55.04 | 56.63 |
| 44 | 53.69 | 55.34 | 57.01 |
| 50 | 53.41 | 55.07 | 56.82 |
| 52 | 53.58 | 55.32 | 57.01 |
| 56 | 52.59 | 54.26 | 55.94 |
| 90 | 52.83 | 54.58 | 56.35 |

(11) WLRWS.[31]—These data consist of absolute measurements taken at $E=14.5$ Mev$\pm$"a few percent." The apparent $S$-wave phase shifts implied by these data are:

| | WLRWS | | | | |
|---|---|---|---|---|---|
| $\theta$ | 20 | 24 | 28 | 36 | 90 |
| $\delta_a$ | 58.64 | 50.90 | 57.42 | 51.42 | 52.16 |

The uncertainties in these measurements are rather large. The value of the cross section at $\theta=90$ degrees was determined with the greatest precision. Accordingly, the $S$-wave phase shift quoted in Table VII is the value of $\delta_a$ for $\theta=90$ degrees.

The probable errors for the phase shifts shown on the points in the various figures in Section VI and given in Table VII were determined from the experimental uncertainties in cross section and in energy as they were evaluated in the original experimental papers.

## APPENDIX III. S-STATE COULOMB WAVE FUNCTIONS

The wave equation for the partial wave of zero angular momentum in a repulsive Coulomb field is:

$$[-d^2/dr^2+1/Rr]\varphi(r)=k^2\varphi(r), \tag{A3.1}$$

where $R=\hbar^2/2me^2$, $k^2=2mE/\hbar^2$, $m$ is the mass of the particle (the reduced mass), and $E$ is the kinetic energy of relative motion. $\varphi(r)$ is $r$ times the radial factor of the wave function.

This equation is a special case of the confluent hypergeometric equation,[41] the solutions of which are well known. The regular solution (bounded at the origin) can be shown to be:[42]

$$F(r)=Ckre^{ikr}F(1+i\eta;2;-2ikr), \tag{A3.2}$$

where $\eta=e^2/\hbar v=(2kR)^{-1}$, and

$$C^2\equiv e^{-\pi\eta}|\Gamma(1+i\eta)|^2=\frac{2\pi\eta}{e^{2\pi\eta}-1} \tag{A3.3}$$

and

$$F(a;b;z)=1+\frac{a}{b\times 1}z+\frac{a(a+1)}{b(b+1)\times 1\times 2}z^2+\cdots.$$

[41] E. M. Whittaker and G. N. Watson, *Modern Analysis* (Cambridge University Press, London, 1945), Chapter 16.
[42] Reference 14, p. 39.

$F(r)$ is normalized asymptotically ($k^2Rr\gg 1$) to the form:

$$F(r)\sim\sin(kr-\eta\ln(2kr)+\sigma_0) \tag{A3.4}$$

where $\sigma_0=\arg\Gamma(1+i\eta)$. The irregular solutions are known[43] to differ from $F(r)$ asymptotically only by the insertion of an arbitrary phase in the argument of the sine. The usual choice for the irregular solution $G(r)$ is that solution which asymptotically ($k^2Rr\gg 1$) has the form:

$$G(r)\sim\cos(kr-\eta\ln(2kr)+\sigma_0). \tag{A3.5}$$

Sexl[44] has examined the behavior of the irregular solution near the origin. He found that $G(r)$ can be written as:

$$G(r)=Re[y(r)], \tag{A3.6}$$

where

$$y(r)=\frac{1}{C}e^{-ikr}\Big[1+\sum_{n=1}^{\infty}(2ikr)^n c_n\{\ln(2ikr)+d_n\}\Big],$$

$$c_n=\frac{\Gamma(n-i\eta)}{\Gamma(n)\Gamma(n+1)\Gamma(-i\eta)},$$

$$d_n=\frac{1}{-i\eta}+\frac{1}{1-i\eta}+\cdots+\frac{1}{n-1-i\eta}+\frac{\Gamma'(-i\eta)}{\Gamma(-i\eta)}+\frac{1}{n}-2\left(1+\tfrac{1}{2}+\cdots+\frac{1}{n}\right)+2\gamma,$$

$\gamma=0.5772\cdots$ is Euler's constant. The function $y(r)=-Cy_k^{(2)}(kr)$ in Sexl's notation.

The behavior of $F(r)$ and $G(r)$ for $kr\ll 1$ and $r\ll R$ can be found by expanding (A3.2) and (A3.6). The results are:

$$\begin{aligned}F(r)&=Ckr[1+(r/2R)+\cdots],\\ G(r)&=(1/C)[1+(r/R)[\ln(r/R)+2\gamma-1+h(\eta)]+\cdots],\end{aligned} \tag{A3.7}$$

where

$$\begin{aligned}h(\eta)&=Re\frac{\Gamma'(-i\eta)}{\Gamma(-i\eta)}-\ln\eta\\ &=\eta^2\sum_{v=1}^{\infty}\frac{1}{v(v^2+\eta^2)}-\ln\eta-\gamma.\end{aligned} \tag{A3.8}$$

$h(\eta)$ was also defined in (7.1) and (7.2), with a graph of $h(\eta)$ given in Fig. 13 and a graph of the summation,

$$\sum_{v=1}^{\infty}\frac{1}{v(v^2+\eta^2)},$$

given in Fig. 14.

[43] W. Gordon, Zeits. f. Physik **48**, 180 (1928).
[44] T. Sexl, Zeits. f. Physik **56**, 72 (1929).

The expansions (A3.2) and (A3.6) are inconvenient since they involve real and imaginary quantities while the result is real. Yost, Wheeler, and Breit[32] have given power series expansions of $F(r)$ and $G(r)$ in terms of real quantities only. They also give an expansion for the regular solution $F(r)$ in powers of the energy, involving Bessel functions of argument $2(r/R)^{\frac{1}{2}}$. The expansion of $F(r)$ in powers of $k^2$ has been treated in more detail by Beckerley.[33]

Several combinations of Bessel functions arise in the expansions of $F(r)$ and $G(r)$. To be consistent, the following convention will be adopted: all the auxiliary functions defined below approach unity at $r=0$. Furthermore, in the limit $R\to\infty$ and $\eta\to 0$ (i.e., in the limit of vanishing Coulomb field), all these functions can be replaced by unity. Since the expansions for $F(r)$ and $G(r)$ go over in that limit to the well-known power series expansions for $\sin(kr)$ and $\cos(kr)$, this gives a simple method of checking these more complicated expansions. The following auxiliary functions are needed:

$$L_n(r)=n!\left(\frac{r}{R}\right)^{-\frac{1}{2}n} I_n[2(r/R)^{\frac{1}{2}}], \tag{A3.9}$$

$$H_n(r)=\frac{2}{(n-1)!}\left(\frac{r}{R}\right)^{\frac{1}{2}n} K_n[2(r/R)^{\frac{1}{2}}], \tag{A3.10}$$

where $I_n(z)$ and $K_n(z)$ are the modified Bessel functions defined in Watson.[45] The expansions of $L_n(r)$ and $H_n(r)$ for the first few values of $n$ are:

$$\begin{aligned}
L_1(r)&=1+\frac{r}{2R}+\frac{r^2}{12R^2}+\frac{r^3}{144R^3}+\frac{r^4}{2880R^4}+\cdots,\\
L_2(r)&=1+\frac{r}{3R}+\frac{r^2}{24R^2}+\frac{r^3}{360R^3}+\cdots,\\
L_3(r)&=1+\frac{r}{4R}+\frac{r^2}{40R^2}+\frac{r^3}{720R^3}+\cdots,
\end{aligned} \tag{A3.11}$$

$$\begin{aligned}
H_1(r)&=1+(r/R)[\ln(r/R)+2\gamma-1]+(r^2/2R^2)\\
&\quad\times[\ln(r/R)+2\gamma-(5/2)]+(r^3/12R^3)\\
&\quad\times[\ln(r/R)+2\gamma-(10/3)]+\cdots,\\
H_2(r)&=1-(r/R)-(r^2/2R^2)\\
&\quad\times[\ln(r/R+2\gamma-(3/2)]-(r^3/6R^3)\\
&\quad\times[\ln(r/R)+2\gamma-(17/6)]-\cdots,\\
H_3(r)&=1-(r/2R)+(r^2/4R^2)+(r^3/12R^3)\\
&\quad\times[\ln(r/R)+2\gamma-(11/6)]+(r^4/48R^4)\\
&\quad\times[\ln(r/R)+2\gamma-(37/12)]+\cdots.
\end{aligned} \tag{A3.12}$$

[45] G. N. Watson, *Theory of Bessel Functions* (Cambridge University Press, London, 1944).

In terms of the auxiliary functions (A3.9), Beckerley's (Yost, Wheeler, and Breit's) expansion for $F(r)$ can be written as:

$$\begin{aligned}
F(r)&=Ckr[L_1(r)-((kr)^2/6)L_2(r)\\
&+((kr)^4/120)[(10/9)L_3(r)-(1/9)L_4(r)]-\cdots].
\end{aligned} \tag{A3.13}$$

In the limit of vanishing Coulomb field, (A3.13) obviously reduces to the expansion of $\sin(kr)$.

The expansion for the irregular function $G(r)$ can be written as:

$$\begin{aligned}
G(r)=\frac{1}{C}\Big[&H_1(r)-\frac{(kr)^2}{2}M(r)+\frac{(kr)^4}{24}N(r)-\cdots\Big]\\
&+\frac{1}{C}h(\eta)\frac{r}{R}\Big[L_1(r)-\frac{(kr)^2}{6}L_2(r)\\
&+\frac{(kr)^4}{120}\left(\frac{10}{9}L_3(r)-\frac{1}{9}L_4(r)\right)-\cdots\Big],
\end{aligned} \tag{A3.14}$$

where

$$M(r)=\frac{2}{3}\frac{R}{r}[L_1(r)-H_2(r)]. \tag{A3.15}$$

From the expansions (A3.11) and (A3.12) it is readily seen that $M(r)$ has the expansion:

$$\begin{aligned}
M(r)&=1-\frac{4r}{9R}-\frac{67r^2}{216R^2}-\frac{107r^3}{2160R^3}-\cdots\\
&+\left(\ln\frac{r}{R}+2\gamma\right)\left(\frac{r}{3R}+\frac{r^2}{9R^2}+\frac{r^3}{72R^3}+\cdots\right).
\end{aligned} \tag{A3.16}$$

The function $N(r)$ is:

$$\begin{aligned}
N(r)&=(4/3)(R/r)[L_2(r)+(2R/r)H_3(r)\\
&+(12/5)(R^2/r^2)(H_4(r)-L_1(r))].
\end{aligned} \tag{A3.17}$$

$N(r)$ can be expanded in a power series, similarly to $M(r)$, i.e.,

$$N(r)=1+(r/5R)(\ln(r/R)+2\gamma-(23/15))+\cdots. \tag{A3.18}$$

The expansion (A3.14) for $G(r)$ reduces properly to the expansion of $\cos(kr)$ in the limit of vanishing Coulomb field; the first line becomes the expansion of $\cos(kr)$, while the coefficient $h(\eta)/R$ of the second line vanishes in that limit.

An alternative expansion for $G(r)$ has been stated recently by Breit and Bouricius.[9] Their result can be obtained from (A3.14) by the additional (more restrictive) assumption that $\eta\gg 1$. For $\eta\gg 1$, $h(\eta)$ (A3.8) can be approximated by:

$$h(\eta)\simeq(1/3)k^2R^2+(2/15)k^4R^4+\cdots. \tag{A3.19}$$

With this substitution in (A3.14), the result is:

$$G(r)=\frac{1}{C}\Big[H_1(r)+\tfrac{1}{3}k^2RrH_2(r)+\frac{k^4R^2r^2}{9}\Big(H_3(r)+\frac{6R}{5r}H_4(r)\Big)+\cdots\Big], \quad \text{(A3.20)}$$

which is equivalent to Eq. (7.26) of Breit and Bouricius.[9]

The expansion (A3.14) for $G(r)$ can be obtained in a straightforward (although tedious) manner from the power series expansions given by Sexl[44] or Yost, Wheeler, and Breit.[32] Alternatively, it may be obtained by examining the representation of $G(r)$ as a contour integral.[46] The expansion (A3.13) for $F(r)$ can also be derived readily in this manner. Still another method (the one actually used) is the use of a Green's function iteration scheme to obtain succeeding terms in the expansion of $G(r)$ in powers of $k^2$ in terms of the lower order coefficients. For the details of the derivation the reader is referred to a previously mentioned thesis by J. D. Jackson.

## APPENDIX IV. THE BETHE DERIVATION OF THE EXPANSION (1.2)

The simplicity of the final formulas (9.6), (9.14), (9.15) for the coefficients $r_0$, $P$, and $Q$ in the expansion (1.2) for $\mathbf{K}$ leads one to suspect that such an expansion can be derived from the fundamental properties of the differential equation involved, without recourse to the less obvious variational principle (9.3). Indeed, the rudiments of such a derivation lie in the work of Landau and Smorodinsky,[3] described in Section VIII. Recently, Chew and Goldberger[8] and Bethe,[8] as well as Barker and Peierls,[10] have given simple derivations using non-variational methods. We will follow the work of Bethe here.

If $u_a(r)$ is the radial wave function of the proton-proton system in the $S$-state (multiplied by $r$) at an energy $E_a$, then $u_a(r)$ satisfies Eq. (9.1):

$$\Big[-\frac{d^2}{dr^2}+\frac{1}{Rr}-W(r)\Big]u_a=k_a^2u_a. \quad (9.1)$$

For another energy $E_b$, the wave function $u_b(r)$ satisfies:

$$\Big[-\frac{d^2}{dr^2}+\frac{1}{Rr}-W(r)\Big]u_b=k_b^2u_b. \quad (9.1a)$$

Multiply Eq. (9.1) by $u_b$ and Eq. (9.1a) by $u_a$, subtract and integrate from some (small) lower limit $r$ to an arbitrary upper limit $R$. The result is:

$$u_bu_a'-u_au_b'\Big|_r^R=(k_b^2-k_a^2)\int_r^R u_au_b dr. \quad \text{(A4.1)}$$

[46] Reference 14, p. 38.

Now consider the asymptotic form $\varphi(r)$ of $u(r)$. $\varphi(r)$ satisfies the Eq. (8.1). For $\varphi_a(r)$ and $\varphi_b(r)$ a relation analogous to Eq. (A4.1) holds, namely:

$$\varphi_b\varphi_a'-\varphi_a\varphi_b'\Big|_r^R=(k_b^2-k_a^2)\int_r^R \varphi_a\varphi_b dr. \quad \text{(A4.2)}$$

The next step is to subtract (A4.1) from (A4.2) to get:

$$\varphi_b\varphi_a'-\varphi_a\varphi_b'-u_bu_a'+u_au_b'\Big|_r^R=(k_b^2-k_a^2)\int_r^R(\varphi_a\varphi_b-u_au_b)dr. \quad \text{(A4.3)}$$

Now if the upper limit $R$ is chosen large compared to the range of the nuclear force, there is no contribution to the integrated term (left-hand side) from the upper limit because each function $u_i$ will be equal to its asymptotic form $\varphi_i$. For the same reason, the integral on the right can now be extended to infinity. If the lower limit $r$ is chosen very small (in the limit going to zero), then $u_a=u_b=0$, and we are left with:

$$\varphi_b(r)\varphi_a'(r)-\varphi_a(r)\varphi_b'(r)=(k_b^2-k_a^2)\int_r^\infty(\varphi_a\varphi_b-u_au_b)dr. \quad \text{(A4.4)}$$

We must now examine the form of $\varphi(r)$ and its first derivative at small distances. The normalization of $\varphi(r)$ will be chosen to be that of Eq. (9.9):

$$\varphi(r)=CG(r)+C\cot\delta F(r). \quad (9.9)$$

From Eq. (8.3) or (A3.7) we see that in the limit of very small $r$ the $\varphi$'s are equal to unity; and from Eq. (8.5) we see that in that same limit:

$$\varphi_i'(r)=C_i^2k_i\cot\delta_i+(1/R)[\ln(r/R)+2\gamma]+(1/R)h(\eta_i) \quad \text{(A4.5)}$$

where $R$ now means the Bohr orbit of a proton as defined in Section I. Using the definition (8.4) of the Coulomb penetration factor $C^2$, we can write (A4.4) in the form:

$$\frac{\pi\cot\delta_b}{e^{2\pi\eta_b}-1}+h(\eta_b)-\frac{\pi\cot\delta_a}{e^{2\pi\eta_a}-1}-h(\eta_a)=R\int_0^\infty(\varphi_a\varphi_b-u_au_b)dr \quad \text{(A4.6)}$$

where we see that the troublesome logarithm term has disappeared because it was independent of energy. This equation is exact, and relates the function $\mathbf{K}$ at one energy to that at another energy through a simple integral over the wave functions at the two energies in question.

It is convenient to choose the energy $E_a$ to be zero, and to express things relative to zero energy. If we write $E$ and $\eta$ for $E_b$ and $\eta_b$ then (A4.6) becomes:

$$\mathbf{K}\equiv\frac{\pi\cot\delta}{e^{2\pi\eta}-1}+h(\eta)$$

$$=R\left[-\frac{1}{a}+k^2\int_0^\infty(\varphi_0\varphi-u_0u)dr\right], \quad \text{(A4.7)}$$

where the constant $a$ is the same one defined in the text. Equation (A4.7) is seen to be essentially the expansion (1.2) of $\mathbf{K}$.

If one now substitutes the expansions of $u(r)$ and $\varphi(r)$ in powers of $k^2$ (Eqs. (9.7) and (9.10)), then the first term in the expansion of the integral is exactly the expression (9.6) for one-half the effective range $r_0$. Similarly the term in $k^2$ in the expansion of the integral is equal to $-Pr_0^3$ given by Eq. (9.14). It would appear that all succeeding terms in the expansion of $\mathbf{K}$ would follow directly from this substitution of the expansions of $u(r)$ and $\varphi(r)$ in powers of $k^2$ into (A4.7). In fact they do, of course. However, as was mentioned in Section IX, the forms thus obtained lead one to believe that he needs to know higher terms in the expansion of $u(r)$ than are actually necessary to calculate a given coefficient. As an illustration consider the $k^4$ term in the expansion of the integral in (A.4.7), that is, the expression (9.15) for $Qr_0^5$. The variational principle told us that we need only have knowledge of the first two terms in the expansion of $u(r)$ in order to find $Qr_0^5$, as is borne out by the form of (9.15). However, let us look at the $k^4$ term obtained from the above integral; it is:

$$\int_0^\infty(\varphi_0\chi_2-u_0v_2)dr.$$

We see that it apparently involves $v_2$ and $\chi_2$, the third terms in the expansions of $u(r)$ and $\varphi(r)$, in contradiction to (9.15) and the general conclusion following from the variational principle. This contradiction is only apparent, and can be removed as follows: The set of functions $v_n(r)$ satisfy the following equations:

$$\left[-\frac{d^2}{dr^2}+\frac{1}{Rr}-W(r)\right]v_n(r)=v_{n-1}(r) \quad \text{(A4.8)}$$

of which Eq. (9.8) is the first. Similarly, $\chi_n(r)$ satisfies (A4.8) with $W(r)$ put equal to zero. By means of these equations and those satisfied by $u_0(r)$ and $\varphi_0(r)$, one can perform an integration by parts on the above integral for $Qr_0^5$ to put it into the form (9.15).

In a similar manner all higher terms in the expansion of the integral in (A4.7) can be reduced so that the minimum number of terms in the expansions of $u(r)$ and $\varphi(r)$ are needed to evaluate them. The advantage of the variational principle method is that it tells one immediately what the minimum number of terms is, and gives the coefficients directly in their reduced forms. Perhaps the most profitable compromise is to know that the expansion of $\mathbf{K}$ can be deduced from a variational principle, and to use that fact to guide the manipulations and the not-always-obvious integrations by parts that are necessary to reduce the expressions to their most convenient form.